International Scientific-Theoretical and Production Journal

ADVANCES IN ELECTROMETALLURGY

1, 2008

Quarterly

English translation of the quarterly «Sovremennaya Elektrometallurgiya» journal published in Russian since January 1985

Founders: *E.O. Paton Electric Welding Institute of the NASU*
International Association «Welding»

Publisher: *International Association «Welding»*

Editorial and advertising offices are located at PWI:
International Association «Welding»,
E.O. Paton Electric
Welding Institute of the NASU,
11, Bozhenko str., 03680,
Kiev, Ukraine
Tel.: (38044) 287 67 57,
529 26 23,
Fax: (38044) 528 04 86
E-mail: journal@paton.kiev.ua
http://www.nas.gov.ua/pwj

Subscriptions:
4 issue per year;
184$** — regular, **150$ — for subscription agencies, **100$** — for students;
postage and packaging included.
Back issues available.

CONTENTS

PHYSICAL MODELING OF SLAG POOL HYDRODYNAMICS IN SLAB CURRENT-CARRYING MOULD
Part 1. Ingot melting

K.A. TSYKULENKO
E.O. Paton Electric Welding Institute, NASU, Kiev, Ukraine

Investigations of hydrodynamics of slag pool in slab current-carrying mould were carried out. Assessment of effect of different schemes of connection of electrodes of a current-carrying section on nature of hydrodynamic flows was made by changing current value in the electrode–bottom plate circuit, distance from the bottom plate to the current-carrying section and depth of immersion of the electrodes. Qualitative pattern of distribution of hydrodynamic flows in the slag pool of the slab current-carrying mould was obtained. Results of the investigations will be used in designing of these moulds and determination of dimensions of the intermediate section and current-carrying areas.

Keywords: slab current-carrying mould, schemes of power supply source connection, modeling of hydrodynamic flows

Hydrodynamic flows in slag and metal pools in canonical process of electroslag remelting (ESR) are investigated sufficiently well. Balance of hydrodynamic forces and main directions of slag and metal flows were determined both for single-electrode and multi-electrode schemes of remelting at different circuit designs of the power supply source connection [1–5]. The ESR process was investigated in a slag mould [6, 7] and with application of magnetic fields [8, 9].

Perfection of the ESR technology caused development of a new equipment — a current-carrying mould, which ensures additional rotation of the slag pool in horizontal plane [10]. However, hydrodynamics of a slag pool in such mould is not completely clear. Modeling of the ESR process in the current-carrying mould did not give answer to the question if directions of the flows change in vertical plane (and if they change, then how), described for the canonical scheme [11]. Presented in this work scheme of the experiment corresponds more to the ingot melting process than to the process of electroslag cladding. It also remains unclear how pattern of hydrodynamic flows changes in case of transition from moulds of round section to moulds of rectangular section.

The purpose of this work is determination of optimal scheme of the current-carrying mould connection for melting of slabs from the viewpoint of the melt mixing and uniform distribution of flows.

For investigation of the slag pool hydrodynamics in a slab current-carrying mould a model from organic glass was made, which simulated such mould with 150×55 mm section (Figure 1). The current-carrying section represented copper plates-electrodes, installed flush with internal surfaces of the model. Between adjacent electrodes a 5 mm clearance was left, which simulated insulating elements of a real current-carrying mould. If necessary, adjacent electrodes were connected by copper jumpers for ensuring different schemes of connection. Middle separation section represented a belt of electrically interconnected copper

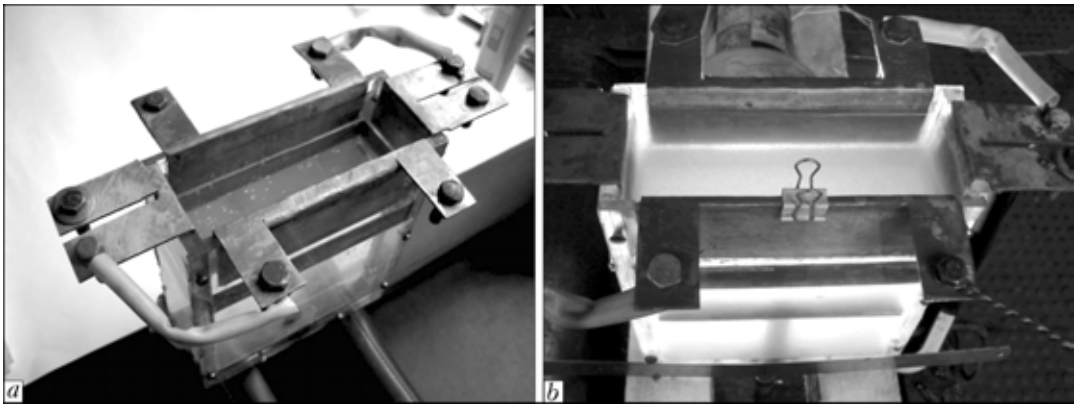

Figure 1. General view of model before (*a*) and in course (*b*) of experiment

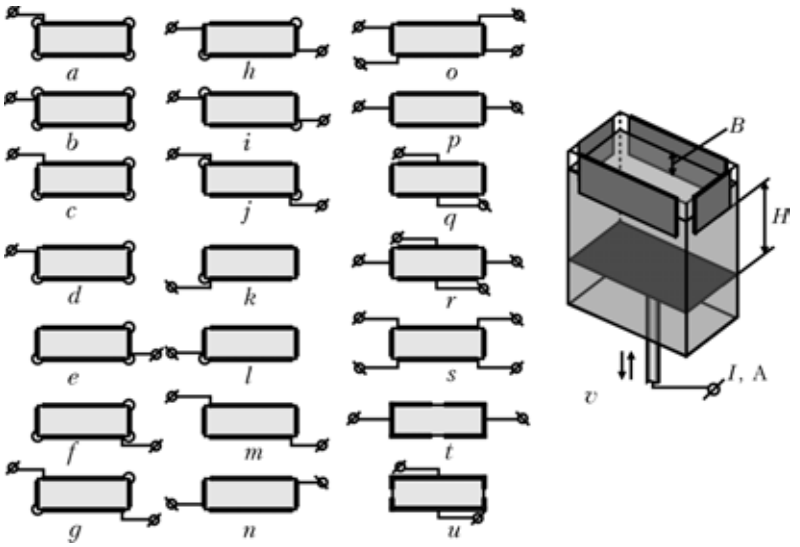

Figure 2. Investigated schemes of connection of current-carrying section electrodes (*a*–*u*) and model with parameters *H*, *B* and *I* changeable in course experiments (*v*): *a*–*u* — see explanations in the text

plates, installed with the same clearance below the current-carrying section. The lower copper plate, which simulated the bottom plate (the ingot), could move from the level of the separation section to the model bottom at the distance up to 110 mm (see Figure 1). Taking into account the fact that it was planned to investigate only distribution of current and directions of hydrodynamic flows, concentrated solution of calcium chloride, which was used in some models for canonical scheme of ESR and in modeling of this process in a current-carrying mould of round section, was selected as a medium for simulation of the slag melt [11]. Electrodes of the current-carrying section were connected to one pole of the power source, and bottom plate ---- to the other. Alternating current welding transformer with 60 V open-circuit voltage was used as a power source. Value of current in the experiments was regulated by means of a ballast rheostat within I = 20–110 A. In process of the experiments influence of different schemes of connection of electrodes of the current-carrying section on character of distribution of hydrodynamic flows was investigated, whereby not just value of current I in the electrodes–bottom plate circuit, but also distance H from the bottom plate to the current-carrying section and depth B of immersion of the electrodes were changed (Figure 2).

The whole big volume of the obtained actual material can not be, unfortunately, presented within the framework of this article, that's why here only main characteristic peculiarities of distribution of current and hydrodynamic flows are presented.

The experiments have confirmed evident assumption about spreading of current along the current-carrying section, consisting of several electrodes: the greater is the distance from the current lead area, the lower is current in the circuit of the current-carrying electrodes (Figure 3, *a*, *b*). Increase of the number of breaks in this circuit causes proportional reduction of value of current in each area of the current lead (Figure 3, *b*, *c*), whereby to the electrode of a bigger width corresponds current of a higher value (Figure 3, *d*). Such distribution of current will, undoubtedly, affect character of flows in the slag pool.

Main hydrodynamic flows in a slab current-carrying mould in majority of investigated cases represent flows, directed from the electrodes downwards along walls of the mould to the bottom plate and ascending in its central part. Similar character of flow movement was registered in ESR in a conventional mould with small depth of a slag pool between two bifilar connected electrodes [3] and in a slab mould with a current-conducting wall [7] (Figure 4). Such flows are also characteristic of free convection, occurring in the canonical ESR scheme in case of temperature differential [5]. But while in the canonical ESR scheme forces of free convection counteract electromagnetic

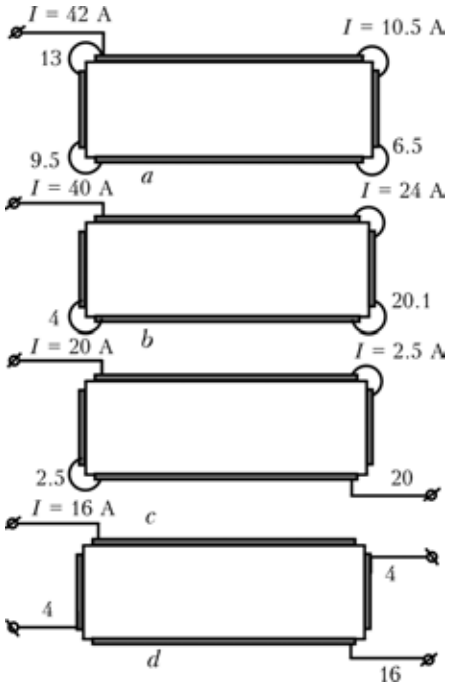

Figure 3. Distribution of current in circuit of current-carrying section of electrodes without breaks (*a*) and with one (*b*), two (*c*) and four (*d*) breaks

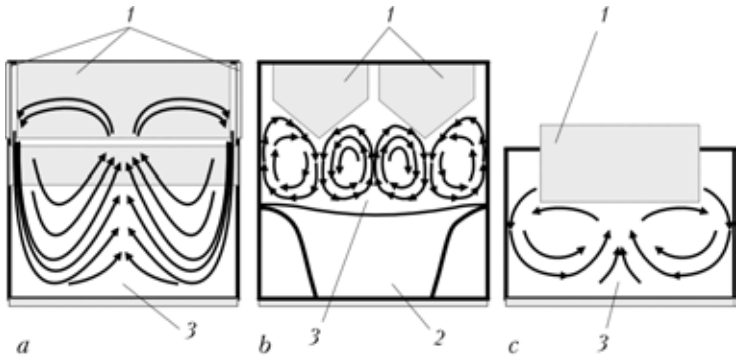

Figure 4. Main hydrodynamic flows in slab current-carrying mould (*a*), conventional mould with bifilar scheme of connection and small depth of slag pool (*b*) [3] and slab mould with current-carrying wall (*c*) [7]: *1* — electrodes; *2* — metal pool; *3* — slag pool

forces, in ESR in the current-carrying mould they, in all evidence, coincide. In order to give answer to the question if the observed flows are consequence of manifestation of the electromagnetic forces, a number of experiments were carried out, in which the model was positioned horizontally, like for example in study [1]. In horizontal position of the model character of the flows does not change, just small reduction of their speed is observed. In addition to the flows observed in the direction electrodes–bottom plate, it was also necessary to register flows caused by flowing of current along the current-carrying section over circuit of the electrodes. That's why all subsequent experiments with different schemes of connection, presented in Figure 2, were carried out in vertical position of the model.

If the current-carrying section has no breaks in circuit of the electrodes (see Figure 2, *a, b*), main influence of character of the flows will be exerted by the place of the current-carrying cable connection, whereby ascending flows somewhat shift from the mould center in the direction opposite to the place of connection. Growth of current value causes increase of the shift and speed of the flows. The same effect is achieved by reduction of distance *H* from the bottom plate to the current-carrying section. Connection of a cable to one of narrow electrodes of a current-leading section of the slab mould enables formation along surface of the model, on which this electrode is located, of more intensive flows than at its opposite surface. When value *H* is determined, it may happen that flows at the opposite surface of the model will not achieve the bottom plate, and in this place will be a quite area. In addition, a small eddying in horizontal plane of the mould model, shifted from the center to the connected electrode, is observed. Speed of rotation of this flow is small, but it may increase as depth *B* of immersion of the electrodes reduces.

Presence of a break in circuit of electrodes of the slab mould current-carrying section causes formation of horizontal flows, directed from the place of the cable connection along circuit of the electrodes over perimeter of the section to the break. In case of connection of a current-carrying cable to a wide electrode, shift of the ascending flow from center of the mould significantly exceeds that for a close current-carrying section, other conditions being the same. In addition, this flow is also shifted in direction of the connected wide electrode. Near a narrow, located adjacent to the break electrode, a flow is formed, which rotates in horizontal plane. Its intensity increases by means of value *H* reduction or increase of current in the electrode–bottom plate circuit, whereby current itself shifts in the direction opposite to the place of the cable connection.

It should be noted that formation of flows and their highest intensity in all investigated cases took place not near surface of the solution, which simulated slag, but in the area of transition from the current-carrying section to the middle separation section located near lower boundary of the electrodes. In this area flows, ascending from the bottom plate, collide with horizontal flows and shift in the direction corresponding to the scheme of the current-carrying section connection. In case of big deepening of the electrodes (Figure 5, *a*), it may happen that the ascending flows will not reach surface of the slag pool or their manifestation will be less pronounced.

As a whole, if the current-carrying section has one break (see Figure 2, *c*), character of distribution of hydrodynamic flows in a slab mould is asymmetrical. In case of connection of a cable to a narrow electrode, located adjacent to a break in the circuit of the current-carrying mould section (Figure 2, *d*), more uniform distribution of flows occurs, while in case of connection of the cable to the middle of the current-carrying section (Figure 2, *e, f*) descending flows are observed in central part of the mould.

Two breaks, located diagonally in the circuit of the current-carrying section electrodes (see Figure 2, *g–j*), make hydrodynamic flows symmetrical. In case of connection of the cables to the wide electrodes (Figure 5, *b*), flows ascend strictly in center of the mould, and two circular horizontal flows, located near narrow electrodes, are also available. In case of connection of the cables to the narrow electrodes, intensity of rotation of these flows reduces, which is, evidently, connected with changes of values of the current, which flows in the circuit of the current-carrying section electrodes. Along the mould walls in direction from places of connection of the cables to the breaks horizontal flows are also formed. It should be noted that increase of the number of breaks in the current-carrying section reduces their speed. If one uses a

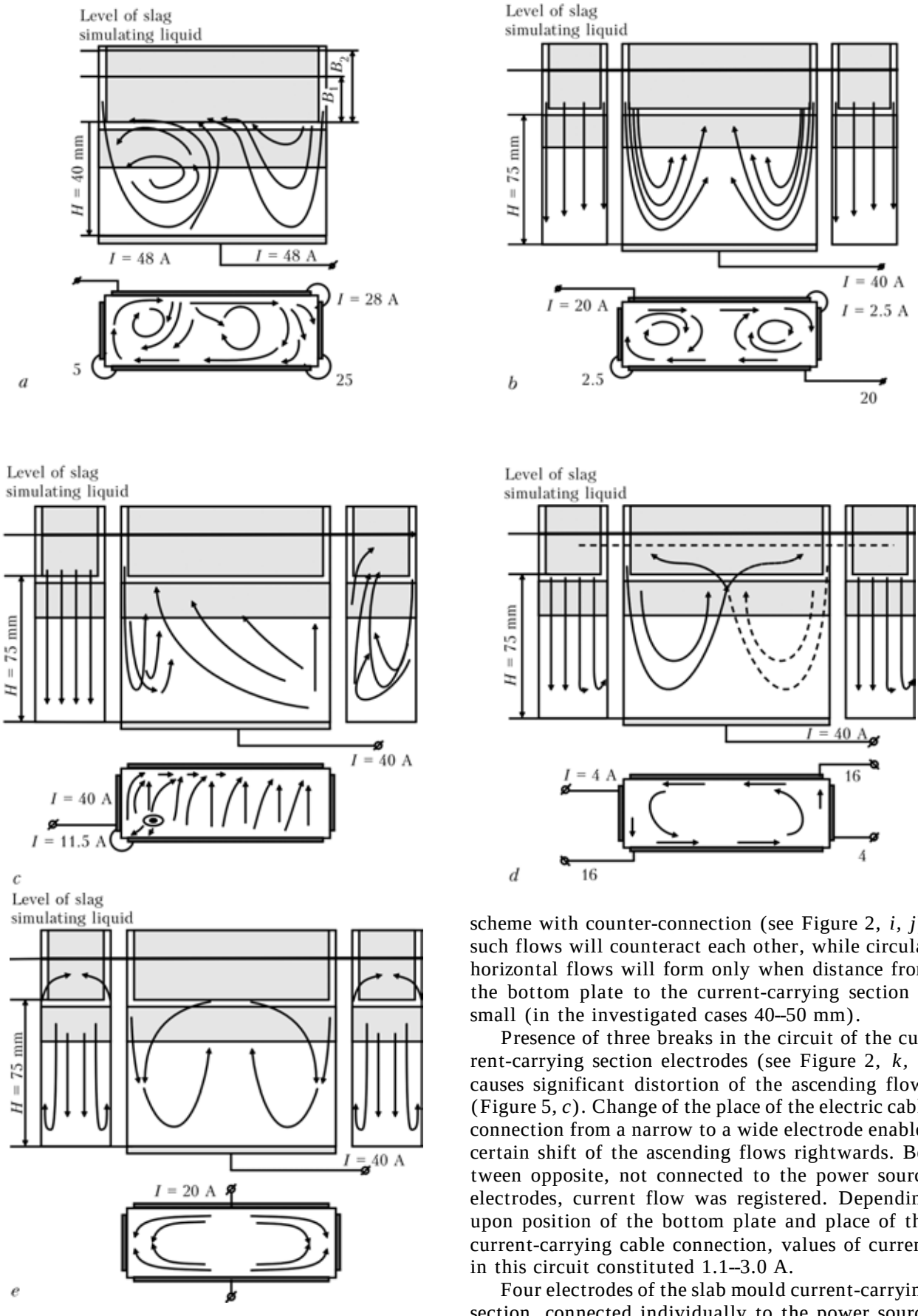

Figure 5. Schemes of flows of liquid, which simulates slag, at different versions of connection of current-carrying section of mould: *a*–*e* — see explanations in the text

scheme with counter-connection (see Figure 2, *i*, *j*), such flows will counteract each other, while circular horizontal flows will form only when distance from the bottom plate to the current-carrying section is small (in the investigated cases 40–50 mm).

Presence of three breaks in the circuit of the current-carrying section electrodes (see Figure 2, *k*, *l*) causes significant distortion of the ascending flows (Figure 5, *c*). Change of the place of the electric cable connection from a narrow to a wide electrode enables certain shift of the ascending flows rightwards. Between opposite, not connected to the power source electrodes, current flow was registered. Depending upon position of the bottom plate and place of the current-carrying cable connection, values of current in this circuit constituted 1.1–3.0 A.

Four electrodes of the slab mould current-carrying section, connected individually to the power source (see Figure 2, *o*, *r*), may, depending upon area of connection, ensure a symmetrical, but rather variable picture of formation of the flows in the slag pool. So,

electrodes, connected in such way that areas of connection of each of them are located immediately adjacent to the breaks of the current-carrying section and do not border with each other, ensure presence of four flows ascending in central part of the mould. They shift in the form of a circular horizontal flow in lower part of the current-carrying section and may reach (depending upon values H and B) surface of the slag pool nearer to narrow sides of the mould, leaving undisturbed central part of its surface (Figure 5, *d*). If areas of connection of electric cables are located in center of the electrodes, shift of vertical flows does not occur. Hear flows, directed from the electrodes downwards along the mould walls to the bottom plate, become practically at once ascending ones and their intensity reduces by means of their approach to the mould center, where even a small descending flow is formed.

Having left a portion of the electrodes unconnected to the power source (see Figure 2, *m, n, p, q, s*) and used not three, like in Figure 2, *k, l*, but four breaks, an attempt was made to compensate distortion of the flows by means of a respective scheme of connection of the current-carrying cables. In case of connection of just two wide electrodes from opposite sides, a pattern of relatively uniform distribution of flows was obtained. Here, like in cases with one and two breaks, horizontal flows of low intensity, directed from the place of connection of the cables along the electrodes over perimeter of the section to the break, were observed. From the connected wide electrodes along the mould wall, vertical flows were formed, which converged in its central part. From narrow non-connected to the power source electrodes, weak descending flows formed. They, evidently, formed due to flow through the narrow electrodes of low current, registered earlier in the circuit of non-connected electrodes. At lower value of current, in comparison with current in the wide electrodes, velocity of such flows is also noticeably lower. In case of the current increase near the current lead areas, formation of intensive eddy flows in horizontal plane occurred. Change of the current lead from the wide electrodes to the narrow ones caused disappearance of the rotating along perimeter of the mould flow and formation of descending flows, directed from central part of the wide electrodes and ascending ones at a certain distance from the narrow electrodes. Into the same area also ascend more intensive flows, formed by the narrow electrodes.

If areas of connection of electric cables are located in center of the wide electrodes, a certain central area of the slag pool remains relatively quite (Figure 5, *e*). Flows of liquid, moving from the wide electrodes to the bottom plate, segregate from their central part and meet near the narrow electrodes. Here these descending flows superimpose on flows from the narrow non-connected electrodes and being repelled from the bottom plate transit into the ascending flows, located at a certain distance from the mould center. One may try to explain such character of distribution of the flows, in contrast to the scheme with individual connection of each electrode in central part, by presence of the horizontal component of current along the wide electrodes and its high value, while connection in center of just narrow electrodes does not create such pattern, which is, evidently, connected with small length of these electrodes. As it was shown earlier, velocity of horizontal flows reduces by means of increase of the number of cuts and reduction of the current-carrying circuit length. That's why horizontal flows in such scheme of connection, evidently, do not reach necessary intensity. Here flows from the narrow current-carrying electrodes to the bottom plate, ascending in central part of the mould, and descending flows of small intensity from the wide electrodes along the mould walls are observed.

It is remarkable that in all schemes with passive non-connected to the power source electrodes, flows are formed, which go from lower edge of the connected electrodes upwards in direction of ends of the non-connected electrodes. In scheme of connection, presented in Figure 2, *m*, such flows move in surface layers of the slag pool, thickness of which is approximately equal to deepening of the current-carrying section, opposite main flows.

Wish to form opposing horizontal flows stipulated testing of the connection schemes, presented in Figure 2, *s–u*. In all these cases distribution of flows was symmetrical. In case of connection of wide electrodes on two opposite sides near each of these walls of the model two vertical ascending flows formed. Ascending flows of lower intensity, which did not reach the bottom plate, also occurred near the narrow not connected to the power source electrodes. In the same place also formed small eddies in horizontal plane. Along the wide electrodes appeared insignificant opposite flows directed from area of connection of the cables. In the connection schemes with E-like pair of electrodes (see Figure 2, *t, u*) horizontal flows were insignificant and distributed according to direction of current from areas of connection of the cables. From areas of connection of the cables two vertical flows formed, descending along the walls and ascending in their center, whereby upper area of the pool, corresponding by its width, approximately, to clearance between the electrodes (in the investigated case 10 mm) and by its depth to deepening of the electrodes, remained relatively quite.

So, carried out preliminary investigations allowed obtaining qualitative pattern of distribution of hydrodynamic flows in a slag pool of the slab current-carrying mould. The most favorable, from the viewpoint of symmetry of hydrodynamic flows in a slag pool, should be considered scheme with two symmetrical breaks in circuit of the current-carrying section electrodes.

The data obtained will be used in designing of the current-carrying moulds and determination of dimen-

sions of the intermediate section and areas of the current lead.

1. Paton, B.E., Medovar, B.I., Emelianenko, Yu.G. et al. (1982) Study of magnetohydrodynamic phenomena in slag pool during ESR. *Problemy Spets. Elektrometallurgii*, Issue 17, 3–8.
2. Emelianenko, Yu.G., Skosnyagin, Yu.A., Andrienko, S.Yu. (1982) Study of the influence of liquid metal and slag movement on conditions of metal pool formation. *Spets. Elektrometallurgiya*, Issue 50, 3–9.
3. Paton, B.E., Medovar, B.I., Emelianenko, Yu.G. et al. (1984) Magnetohydrodynamic phenomena in ESR and crystallization of electroslag ingots. *Problemy Spets. Elektrometallurgii*, Issue 20, 11–15.
4. Medovar, B.I., Samojlovich, Yu.A., Emelianenko, Yu.G. et al. (1985) Investigation of electroslag process by method of physical and mathematical simulation. *Ibid*., **3**, 5–10.
5. Emelianenko, Yu.G., Andrienko, S.Yu. (1986) About balance of hydrodynamic forces in electroslag process. *Ibid*., **1**, 14–18.
6. Medovar, B.I., Troyansky, A.A., Kazimirov, A.N. et al. (1977) Study on the model of nature of consumable electrode melting in production of ESR horizontal ingots. *Spets. Electrometallurgiya*, **33**, 28–32.
7. Medovar, B.I., Bojko, G.A., Serdyukova, V.P. (1978) Physical modeling of the ESR process of consumables electrodes. *Problemy Spets. Elektrometallurgii*, Issue 9, 38–48.
8. Kompan, Ya.Yu., Shcherbinin, E.V. (1989) *Electroslag welding and melting with controlled magnetohydrodynamic processes*. Moscow: Mashinostroenie.
9. Protokovilov, I.V. (2006) *Magnetically-controlled electroslag melting of titanium alloys*: Syn. of Thesis for Cand. of Techn. Sci. Degree. Kiev.
10. Ksyondzyk, G.V. (1975) Current-carrying mould providing the rotation of slag pool. *Spets. Elektrometallurgiya*, Issue 27, 32–40.
11. Tomilenko, S.V., Us, V.I., Kuskov, Yu.M. et al. (1992) Modeling of magnetodynamic processes in current-carrying mould during electroslag melting. *Problemy Spets. Elektrometallurgii*, **4**, 19–21.

INFLUENCE OF SUBSTRATE TEMPERATURE ON FORMATION OF POROUS STRUCTURE OF STAINLESS STEEL IN CASE OF ITS JOINT DEPOSITION WITH NaCl AND KCl VAPORS

A.I. USTINOV[1], **K.V. LYAPINA**[1], **T.V. MELNICHENKO**[1] and **A.A. NEKRASOV**[2]
[1]E.O. Paton Electric Welding Institute, NASU, Kiev, Ukraine
[2]G.V. Kurdyumov Institute for Metal Physics, NASU, Kiev, Ukraine

Porous condensates were produced in joint deposition on a substrate of vapor flows formed by electron beam evaporation in vacuum of the Kh18N10T steel and halogenides of alkaline metals (chloral sodium and chloral potassium). Influence of the substrate temperature on regularities of the porous structure formation of the stainless steel condensate was studied. It was shown that porous structure of open type formed most intensively at such values of the substrate temperature, when boundaries of columnar crystallites loosed their stability.

Keywords: electron beam evaporation and deposition, porous structure, open porosity, shape factor, structural zones

Porous materials or coatings with a high specific surface are widely used as elements of sensor equipment, filters, catalysts, medical implants, etc. In this connection of special interest are technologies of producing high-porous materials with controllable parameters of open and closed porosity. From this point of view new possibilities are opened by the method of formation of porous materials by means of their deposition in vacuum from the vapor phase [1].

By impeding consolidation of crystallites one may ensure their spatially divided origination and growth and thus form a high-porous material. For this purpose so called pore-forming substances ---- inert gases, substances, which transit into gaseous state in heating, and substances, which enter into chemical interaction with a material with formation of gaseous products of reaction, are traditionally used.

So, it is shown in studies [2, 3] that in case of joint deposition of vapor phases of the base material (titanium, aluminium oxide, zirconium oxide, stainless steel) and chloral sodium a material with high volume share of pores is formed. It was assumed on basis of the results obtained that formation of pores in process of the vapor phase condensation is stipulated by both the «shadow» effect during growth of matrix grains exerted by particles of salt, accumulating on the condensation surface, and by interaction of the salt with the metal, which constitutes base of the material, with formation of volatile chlorides.

Using as an example joint condensation of vapor phases of stainless steel and sodium chloride, it was shown that it is possible to affect characteristics of a porous structure by changing technological parameters of the material condensation [3], whereby it was found that maximally open porosity of condensates is formed at the condensation temperature 805–820 °C, and its value depends upon ratio of salt / metal vapor flows.

Increase of the condensation temperature causes reduction of a material porosity, and pores themselves acquire orbicular shape and get closed. Reduction of ratio of the vapor flows insignificantly influences the shape of pores, but enables significant reduction of the porosity volume share. On basis of the results obtained it was assumed that temperature, at which condensates with maximal volume share of open porosity are formed, is determined by two factors: melting point of the salt and temperature, at which condensate being formed has a columnar structure (temperature of the substrate corresponds to the second structural zone [4, 5]).

Taking into account the results obtained, it was assumed that if to use as a porophore halogenides of alkaline metals with different values of the melting point, it will be possible to change temperature conditions, at which condensates with maximal porosity will be formed. From this viewpoint the peculiarities were studied in the work and comparative analysis of the porous structure formation of condensate of stainless steel in case of joint deposition of its vapors with NaCl and KCl salts, melting point temperatures of which are 805 and 750 °C respectively.

Methodology of producing porous materials and investigation thereof. Methodology of deposition of porous condensates in electron beam evaporation and joint deposition of the stainless steel vapor phases and the alkaline metal halogenide on a preliminarily heated up to a certain temperature substrate is described in detail in [3]. Ratio of vapor flows of the salt and the metal varied by change of the salt and the metal rate of evaporation from ingots or position of a substrate relative the ingots. Using these methods, porous condensates of stainless steel were pro-

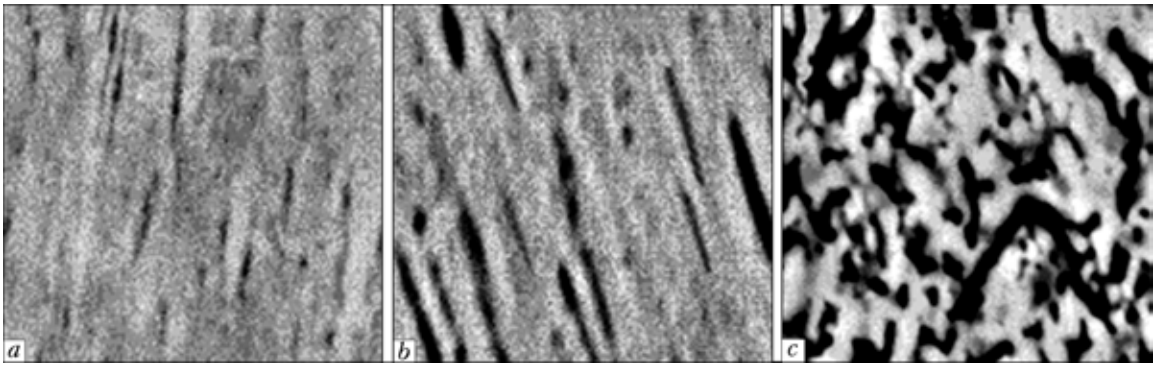

Figure 1. Microstructure of cross section of stainless steel condensates deposited in presence of NaCl vapors at temperature values 700 (*a*), 800 (*b*) and 900 (*c*) °C (×3000)

duced at the substrate temperature values 600–900 °C and fixed ratio of NaCl / metal and KCl / metal vapor flows of 0.3 and 0.6 respectively.

Metallographic analysis of the produced condensates was carried out using the CamScan 4 scanning electron microscope. Quantitative characteristics of the porous structure were estimated by numeric methods of analysis of the microstructure images of cross sections of the condensate. Porosity and ratio of open and closed porosity were determined by the method of mercury porometry [6]. Textural analysis of the condensates was carried out in FeK_α radiation by construction of pole figures with application of the textural attachment to the DRON-4 X-ray diffractometer.

Results of the experiments and their discussion. In Figures 1 and 2 microstructures of porous stainless steel condensates are shown, produced under conditions of joint deposition of the metal and NaCl and KCl salts at different values of the substrate temperature. One can see that at 800 °C condensates of stainless steel with the columnar structure are formed, in which pores of open type are arranged over boundaries of columnar crystallites (Figures 1, *b* and 2, *b*). Reduction of the substrate temperature irrespective of the porophore type (NaCl or KCl) causes reduction of the number of pores and area of their cross section (Figures 1, *a* and 2, *a*), whereby aggregate state of the salt on the condensation surface (NaCl in solid state and KCl in liquid state) does not affect character of the porosity formation. Increase of the condensation temperature in both cases enables change of shape of the pores (they get more equiaxial).

In Figure 3 temperature dependence of general porosity of the condensates is presented, produced at fixed ratio of the salt / metal vapor flows. It was found that porosity changes non-monotonously, achieving the highest values at the condensation temperature 800 °C. Analysis of shapes of the pores, carried out with application of the method of numeric processing of the microstructural cross section images of the condensates, produced at different temperature values, showed that temperature dependence of the pore shape factor (ratio of the pore cross section to its length) is also of non-monotonous character (Figure 4).

The most elongated pores are formed at the condensation temperature about 800 °C. Distribution of pores by their sizes is presented in Figure 5, majority of pores having 18–20 μm size. So, the substrate temperature is a determining factor, which affects main characteristics of porous structure of the condensates formed in joint deposition of salt and stainless steel vapor flows, whereby ratio of the melting point values of the salt and the substrate does not exert significant influence on characteristics of the condensate porous structure. So, one may assume that formation of open pores, located over boundaries of the stainless steel crystallite grains, does not depend upon aggregate state of the salt on the condensate surface.

On basis of carried out analysis one may draw conclusion that the most important factor in formation of porous structure of the condensates is influence of the substrate temperature on morphological peculiarities of growth of the metal condensate grains. For clarifying these peculiarities stainless steel conden-

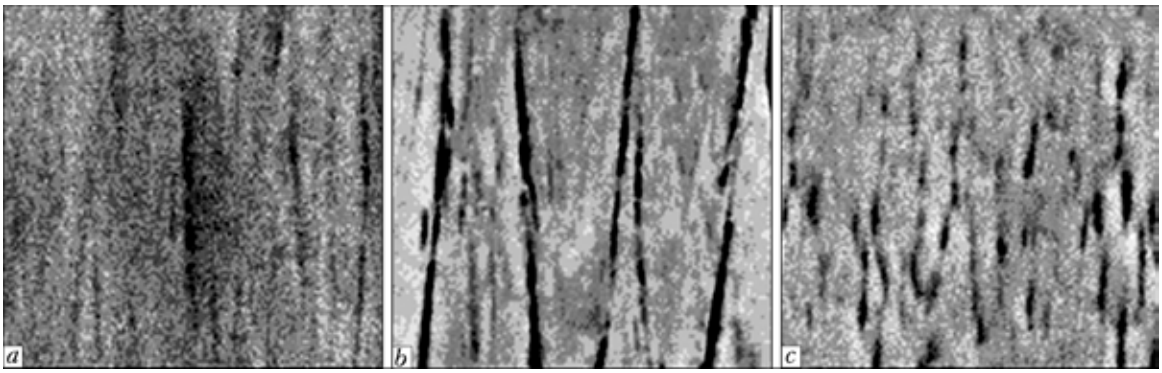

Figure 2. Microstructure of cross section of stainless steel condensates deposited in presence of KCl vapors at temperature values 750 (*a*), 800 (*b*) and 900 (*c*) °C (×3000)

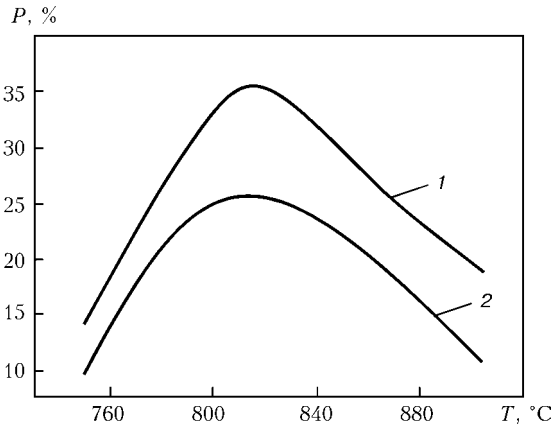

Figure 3. Temperature dependence of general porosity *P* of stainless steel condensates deposited in presence of NaCl (*1*) and KCl (*2*) vapors

sates were produced at the substrate temperature 600–900 °C. It was found that within investigated range of the substrate temperatures the condensates are formed, which have columnar structure with crystallites elongated in the direction perpendicular to the condensation surface, whereby width of columnar crystallites increased by means of the substrate temperature growth.

In Figure 6 temperature dependence of the columnar crystallite width of produced condensates is shown. The most intensive change of the stainless steel crystallite dimensions occurred at the temperature about 800 °C.

Structure formation of the condensates in deposition from the vapor phase follows law of the «zone growth model» [5], according to which columnar crystallites are formed in the area of the condensation temperature equal about $(0.3–0.8)T_m$, whereby at the temperature $(0.5–0.6)T_m$ significant width increase of the columnar crystallites occurs, which is the consequence of the volume diffusion increase at these values of temperature. Significant width increase of the stainless steel columnar crystallites occurs at $0.6T_m$ (Figure 6). Further increase of the condensation temperature causes formation of more equiaxial crystallites, which is connected with dominant role of the volume diffusion in formation of the condensate structure, in comparison with surface diffusion, characteristic of lower values of condensation temperatures, for which shape of the crystallites is mainly determined by the rate of their growth along crystallographic direction that ensures its highest value. In this case the condensates are characterized by both mechanical and crystallographic texture.

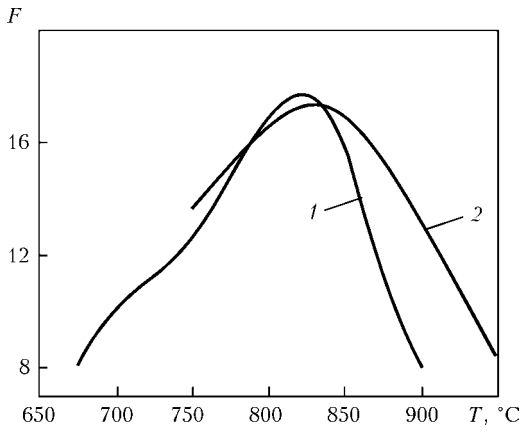

Figure 4. Temperature dependence of shape factor *F* of stainless steel condensate pores deposited in presence of NaCl (*1*) and KCl (*2*) vapors

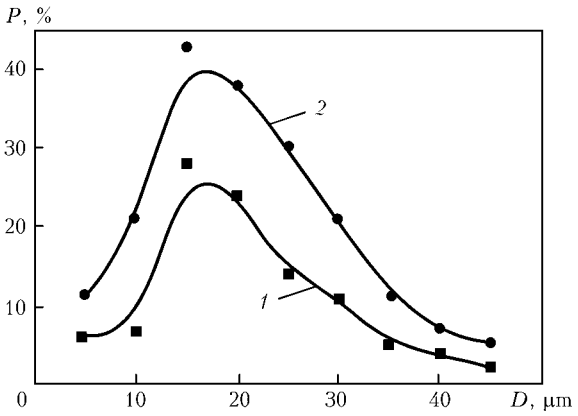

Figure 5. Distribution of pores by sizes *D* in stainless steel condensates deposited in presence of NaCl (*1*) and KCl (*2*) vapors

Analysis of crystallographic texture of the condensates, produced under conditions of the substrate temperature gradient, allows determining temperature, at which change microstructure formation conditions of the condensates.

For this purpose in the work crystallographic texture of the stainless steel condensates, deposited within temperature values 600–900 °C, was analyzed. In Figure 7 characteristic pole figures, obtained in texture analysis of the condensates deposited at 750 (Figure 7, *a*) and 850 °C (Figure 7, *b*), are presented. At the substrate temperature 750 °C the condensate is formed, for which two-component axial <110> + <112> structure is characteristic, that is proved by maximal pole density (110) in center of the pole figure and presence of annular pole density (110) at the distance about 30 circular degrees from the pole figure center. As the substrate temperature increases, maximums of the pole density get blurred, which proves reduction of the texturing degree of the condensates. At temperature value close to 850 °C, texturing of the condensates, as one may see from the pole figures, is practically absent. On basis of the carried out analysis one may draw conclusion that within temperature range close to 800 °C, boundaries of columnar crystallites loose their stability due to domination of vol-

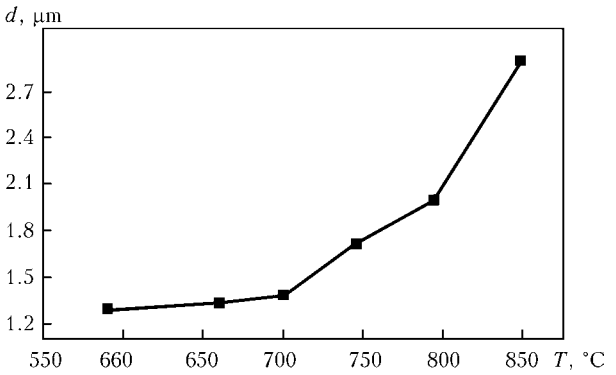

Figure 6. Temperature dependence of width of columnar crystallites *d* of stainless steel condensates

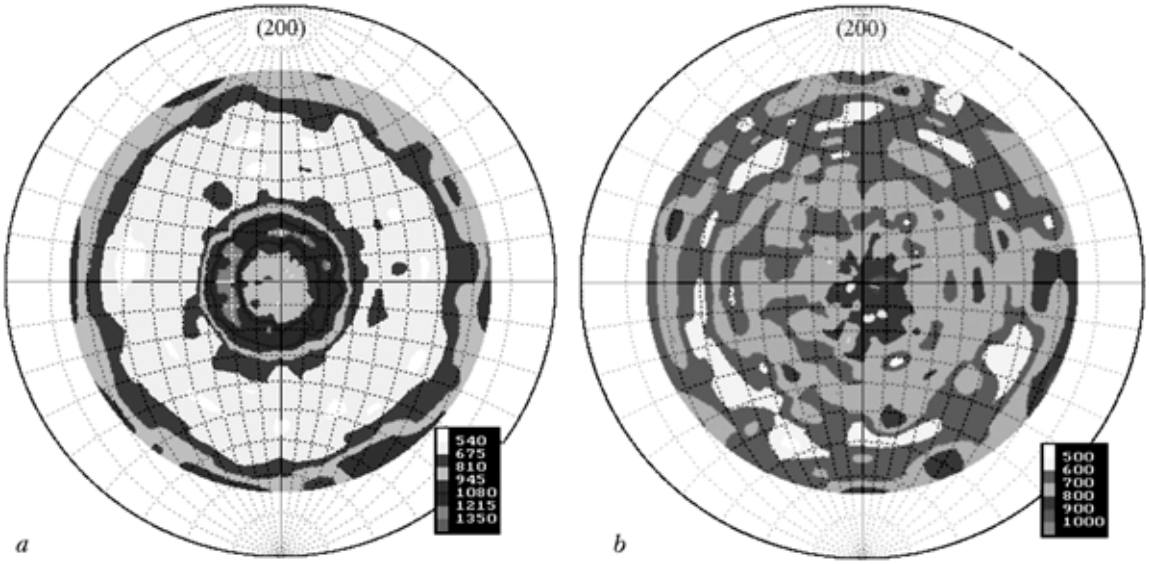

Figure 7. Pole figures of stainless steel condensates deposited at temperature values 750 (*a*) and 850 (*b*) °C

ume diffusion in formation of microstructure of the condensates.

So, peculiarities of growth of crystallites at different values of the condensation temperature are the determining factor of the stainless steel porous structure formation in presence of halogenide vapors. Pores of open type with high values of the shape factor are formed in the area of the deposition temperature of the condensates with columnar structure and characteristic for the metal texture of the crystallite growth, whereby condensation temperature, at which maximal open porosity is formed, coincides with the temperature, at which occurs change of the crystallite growth shape (from the columnar to the equiaxial one), i.e. loss of stability of the columnar crystallite boundaries occurs.

Discovered by us effect may be stipulated by the fact that at the substrate temperature close to 800 °C, role of the volume diffusion in formation of the stainless steel condensates becomes dominant.

Side by side with influence on morphological peculiarities of the crystallite growth under conditions of joint deposition of vapor flows of steel and alkaline metal halogenides, intensification of the volume diffusion will enable formation at boundaries of columnar crystallites of accumulations of defects such as vacancies, impurity atoms, etc. As a result interatomic bonds over boundaries of the grains will get weaker. One may assume that under these conditions role of such pore-formation mechanisms as derangement of the metal crystallite boundaries by liquid salt, removal of the metal particles from the crystallite boundary area due to formation of low-melting halogenides, shadow effects in deposition of salt particles on the condensation surface and their segregation to the places of accumulation of the defects, etc., will increase. Due to this the best conditions for origination and growth of pores will be ensured. Intensification of the volume diffusion at further increase of the condensation temperature will cause curing of pores and change of their shape, which stipulates experimentally registered reduction of porosity of the condensates, transition from open to close form of the pores, and change of their shape.

CONCLUSIONS

1. It is shown that method of electron beam evaporation in vacuum of stainless steel and salts of the alkaline metal halogenides with different melting temperatures (chloral sodium and chloral potassium) allows producing in joint deposition of their vapor flows porous condensates, temperature dependence of porosity of which is of non-monotonous character with maximum in the area of 0.6 T_m temperature with characteristic formation of elongated pores of open type.

2. The results obtained allowed drawing conclusion that dominant factor of porosity formation of the stainless steel condensates are morphologic features of the metal structure formation in the process of the vapor phase condensation, peculiar to this value of the substrate temperature.

3. It was found that maximal share of open porosity is achieved at the condensation temperature, at which change of the crystallite growth shape occurs (from the columnar to the equiaxial one).

4. Important condition that determines formation of porous structure of open type is loss of stability of the boundaries of columnar crystallites due to transition of dominant role of the surface diffusion to the volume one in formation of microstructure of the condensates.

1. Movchan, B.A. (1998) Inorganic materials deposited from vapor phase in vacuum. *Sovremennoe Materialovedenie 21 Veka*, **1**, 327–329.
2. Movchan, B.A., Yakovchuk, K.Yu. (2001) New approach to producing of microporous materials and coatings by electron beam evaporation of inorganic materials. *Problemy Spets. Elektrometallurgii*, **2**, 11–14.
3. Ustinov, A.I., Lyapina, K.V., Melnichenko, T.V. (2005) Regularities of stainless steel porous structure during its deposition from vapor phase in presence of sodium chloride vapors. *Advances in Electrometallurgy*, **4**, 19–24.
4. Movchan, B.A., Demchishin, A.V. (1969) Investigation of structure and properties of thick vacuum condensates of nickel, titanium, tungsten, alumina. *Fizika Metallov i Metallovedenie*, 28(**4**), 653–660.
5. Tornton, J.A. (1977) High rate thick film growth. *Ann. Rev. Mater. Sci.*, **7**, 239.
6. Plachenov, T.G., Kolosentsev, S.D. (1988) *Porometry*. Leningrad: Khimiya.

ELECTRON BEAM COLD HEARTH REMELTING OF HIGH-TEMPERATURE TITANIUM ALLOYS HARDENED BY SILICIDES

A.Yu. SEVERIN, N.P. TRIGUB and **G.V. ZHUK**
E.O. Paton Electric Welding Institute, NASU, Kiev, Ukraine

Technology of electron beam melting of titanium alloys with increased content of silicon is presented. Influence of weight share of elements in the initial charge on their content in ingots is studied, distribution of hardness and microstructure of produced ingots are investigated. A new method for layer-by-layer solidification of ingots, which allows improving their quality, is suggested.

Keywords: electron beam remelting, silicide, high-temperature alloys, layer-by-layer solidification

Development of aircraft and missile construction, nuclear power engineering, chemical machine building and other branches of industry causes the need not just to improve quality of existing structural materials, but to develop new lighter and stronger in operation under normal and increased temperatures materials, whereby they have to be sufficiently ductile, tough, and resistant to action of corrosive environment. These requirements are met by the titanium-base alloys.

Nowadays commercial high-temperature titanium alloys have working temperatures not higher than 600 °C (VT18U and VT-25), and further increase of the level of their properties by means of the solid solution hardening is practically exhausted [1]. That's why lately traditional method of the disperse hardening of the metals by different interstitial phases ---- oxides, nitrides, carbides and borides ---- are used.

The most promising method for improvement of the titanium alloy high-temperature properties is intermetallic hardening. Preferential intermetallic compounds for this purpose are Ti_3Al and TiAl titanium aluminides and Ti_5Si_3 silicide [2, 3].

In recent years great attention is paid to new generation of high-temperature titanium alloys with increased content of silicon [3–6]. These new complex alloyed titanium-base alloys are, in contrast to commercial titanium alloys, characterized by the principally different mechanism of hardening, implemented due to addition of a big volume share of the ceramic component ---- Ti_5Si_3 silicide or, depending upon alloying, ---- Ti, Zr_5Si_3 [5, 6]. Theses materials got the name «cermets» and are «natural» composites, because in the process of their solidification the structure, typical for composite materials ---- plastic matrix, reinforced by stretched and branched crystals of the refractory and high-strength phase (silicides) ---- is formed.

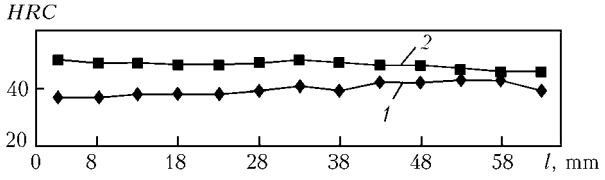

Figure 1. Curves of *HRC* hardness change over section of ingots after one-time electron beam remelting: *1* — No.352; *2* — No.366; *l* — distance from free surface of mould deep into ingot

For increasing high-temperature strength and heat resistance a certain amount of aluminium and zirconium (up to 5 wt.% and more) is introduced into these alloys. Main task of metallurgical technologies in production of multicomponent alloys is ensuring of homogeneity of chemical composition and structure of the ingots, because in the process of electron beam cold hearth remelting (EBCHR) elements with high pressure of vapor, in particular aluminium, evaporate from the melt [2].

In this work the EBCHR peculiarity of the Ti–Al–Si–Zr system alloys is investigated.

According to the calculated conditions experimental melts of ingots in the closed bottom mould, having dimensions 145 × 130 × 490 mm, with content of silicon 2–3 % and aluminium and zirconium 5–6 %, were carried out. Mixing was carried out on basis of previous experience of producing PT-3V and VT-6

Chemical composition of ingots of Ti–Al–Si–Zr alloy system after electron beam remelting

Ingot No.	Weight share of elements, %					
	Al			Si	Zr	Ti
	In charge	Calculation	In ingot			
352	8.4	6.0	6.7	2.22 / 2.2	5.11 / 5.3	84.22 / 85.8
366	7.0	4.7	6.1	3.6 / 3.2	7.0 / 6.4	82.4 / 84.3

Note. In numerator weight share of element in charge, and in denominator in ingot is indicated.

Figure 2. Microstructure of Ti–Al–Si–Zr system alloy with 3.2 % Si (×200)

alloys [2]. Chemical analysis of each ingot was made (Table).

As showed practice, final content of aluminium usually exceeds the calculated one, which requires change of the melt conditions. Mentioned effect is, evidently, connected with peculiarities of phase equilibrium diagram of the Ti–Si system [7]. As far as silicon reduces melting point of titanium almost by 320 °C, evaporation of aluminium occurs to a lower degree, which requires specifying both composition of the charge and conditions of melting. Significant difference in calculated and actual content of silicon and zirconium was not noted.

For the purpose of studying uniformity of distribution of the alloying elements, cutting of the ingots was carried out. On produced after cutting specimens *HRC* hardness was measured along each of them in the direction from surface of solidification deep into the ingot, and microstructure and chemical composition were investigated.

In Figure 1 change of the *HRC* hardness over section of the ingot in the direction from free surface of its solidification deep into its middle is shown. Under free surface of solidification surface of the ingot is meant, which had not contact with the mould and was constantly subjected to the electron beam action. One can see from the presented diagram that hardness changes insignificantly over section of the ingot. This proves sufficient chemical and structural homogeneity of the ingot.

In Figure 2 microstructure of the Ti–Al–Si–Zr system alloy with 3.2 % Si is presented. This alloy relates to hypoeutectic ones and consists of lamellae of α-phase, which occurred inside primary β-grain. Thin interlayers of β-phase are located between lamellae of α-phase and edged by fine silicides of eutectic origin (secondary silicides).

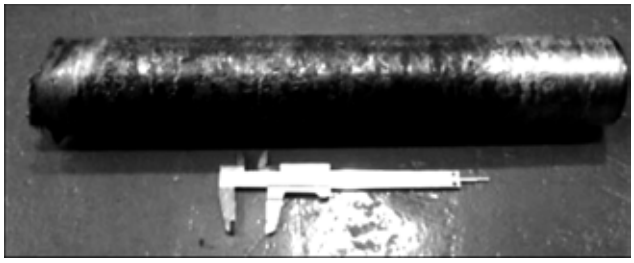

Figure 3. Ingot of 75 mm diameter and 500 mm length of Ti–6.1Al–3.2 Si–6.4 Zr alloy

For increasing chemical homogeneity the ingots were subjected to secondary remelting in open-bottom mould of 75 mm diameter, whereby dimensions of the intermediate unit were increased from $50 \times 110 \times 210$ (used for primary remelting) to $70 \times 225 \times 373$ mm, and additional mixing with necessary components was carried out for ensuring more accurate correspondence of the chemical composition of the ingots to the calculated one. Complex of the investigations was repeatedly carried out, which showed improvement of chemical homogeneity of the ingots. However, certain produced ingots had surface defects in the form of «breaks». In this connection a new technology was developed for melting ingots by the method of layer-by-layer melt solidification in the mould, and optimal conditions of melting were selected.

Method of layer-by-layer solidification consists in the fact that after pouring of next in turn portion of molten metal into the mould, power of electron beams put into the mould is reduced. This allows solidifying of the melt, after which next in turn portion of the molten metal is fed. Produced in this way ingots had good surface without «breaks» (Figure 3); in respect to other properties they did not differ from the ingots described above.

This technology requires for further investigations and approbation on ingots of bigger section.

1. Antashov, V.G., Nochovnaya, N.A., Ivanov, V.I. (2002) Tendency of development of high-strength titanium alloys for aircraft engine industry. *Tekhnologiya Lyog. Splavov*, **4**, 72–76.
2. Paton, B.E., Trigub, N.P., Akhonin, S.V. et al. (2006) *Electron beam melting of titanium*. Kiev: Naukova Dumka.
3. Firstov, S.A., Bankovsky, O.I., Kulak, L.D. (1999) Prospective trends in increase of high-temperature properties of titanium alloys. In: *Electron microscopy and strength of materials*. Kiev: IPS, 73–81.
4. Trefilov, V.I., Firstov, S.A., Mazur, V.I. et al. *Titanium matrix composite*. Pat. 5366570 USA. Publ. 22.11.94.
5. Firstov, S.A., Taran, Yu.N., Mazur, V.I. et al. (1999) New cermet material on titanium base. *Metall i Litio Ukrainy*, **11 / 12**, 42–46.
6. Firstov, S.A., Bulanova, M.V., Bankovskiy, O.I. et al. (2000) Phase composition and mechanical properties of Ti–Si–Al–Zr in situ composites. *Zeitschrift fuer Metallkunde*, **1**, 21–23.
7. Svechnikov, V.N., Kocherzinsky, Yu.A., Yupko, L.M. et al. (1970) Phase diagram of titanium–silicon system. *Doklady AN SSSR*, 193(**2**), 393–396.

ELECTRON BEAM REFINING IN PRODUCTION OF PLATINUM AND PLATINUM-BASE ALLOYS
Information 1. Electron beam refining of platinum

V.A. SAVENKO, N.I. GRECHANYUK and **O.V. CHURAKOV**
SPA GEKONT, Vinnitsa, Ukraine

Commercial technology for production of platinum in ingots with content of the base element not less than 99.99 % was developed.

Keywords: electron beam remelting, platinum metals and alloys, impurity elements, melting conditions

Platinum metals (platinum, palladium, rhodium and iridium) and alloys on their bases are unique structural materials, capable of standing for many hundreds and thousands hours thermal and mechanical stresses in corrosive oxidizing media at extraordinary high homologous temperatures ---- (0.70–0.95)T_m (1200–2300 °C).

Among known high-temperature metal and nonmetal materials platinum metals and alloys have no equivalent substitutes. That's why optimization of composition and increase of high-temperature strength of platinum metals and alloys for the purpose of achieving long service life and efficiency of application of the manufactured from them items is an extremely important task [1]. In majority of cases platinum is base of the materials for production of crucibles, vessels, and feeders for cooking and melting of glasses and manufacturing of different items from them, frequently operating at temperature above 1200 °C in air [2].

As production volumes of quality glasses, glass fibers, and single crystals grow, deficit of platinum metals and first of all platinum continuously increases because of their limited reserves in the earth crust.

According to requirements of GOST 12341–81, 12 impurity elements are regulated in platinum. Practice shows that certain impurities are permissible within certain limits, presence of some of them has to be strictly controlled in special application of the metal, while presence of others causes unsuitability of platinum for application. So, suitable for commodity application is platinum with total content of impurities less than 0.02 %, for work at high temperatures ---- less than 0.01 %, for thermoelectric converters platinum with total content of impurities less than 0.002 % and in production of optical fibers less than 0.001 %, is suitable. The most frequently impurity elements form solid solutions with platinum with melting point lower than that of platinum (copper, iron, nickel, etc.), or low-melting and brittle phases (silver, lead, stannum, silicon, antimony, barium, bismuth, arsenic, aluminium, magnesium, zinc, phosphorus, selenium, tellurium, etc.), which cause failure of platinum under load and high temperature conditions. At majority of enterprises of Ukraine control over content of oxygen and carbon in platinum is absent, which causes wrong estimation of the degree of platinum purity.

Impurity elements in platinum exert great influence on its physical and mechanical properties. That's why purity of platinum is one of important characteristics. Depending upon content of impurity elements platinum is conditionally divided into platinum of technical (99.80 %), chemical (99.90 %), physical (99.99 %), and spectral purity. Company «Johnson Mattie» produces platinum, having purity 99.999 %.

In this connection more and more actual become problems of rational and efficient application of platinum and platinum metals.

Goal of this work is development of the commercial technology for production of platinum in ingots with content of the base element not less than 99.99 %.

Technological scheme envisages hydrometallurgical refining of platinum with production of platinum sponge to be remelted in an induction furnace for production of platinum in ingots. Supplied scrap of platinum materials (platinum, rhodium, palladium) with content of platinum 70.0–99.5 % is subjected to hydrometallurgical refining with separation by elements of platinum metals and their simultaneous cleaning from impurities. The refining process finishes in production for further processing of platinum sponge with platinum content not less than 99.6 %.

Melting of titanium sponge was carried out in the induction high-frequency furnace in the rammed crucible from magnesium oxide that ensured high productivity of the process. However, in induction melting, carried out in air, contamination of platinum by oxygen, nitrogen, hydrogen and other gases, as well as by the crucible material ---- magnesium oxide, occurs.

Production of high-purity platinum (99.99 %) was carried out by its remelting after induction melting in the UE-178 commercial electron beam furnace, de-

Table 1. Chemical composition of platinum ingot before and after EBR, %

Chemical element	Before EBR	After EBR	*K*	Before EBR	After EBR	*K*
Pt	99.94	99.99	–	99.95	99.99	–
Pd	0.004	0.001	4	0.005	0.0013	4
Rh	0.005	0.004	1.25	0.003	0.003	1
Ir	<0.002	<0.002	1	<0.002	<0.002	1
Ru	<0.003	<0.003	1	<0.003	<0.003	1
Au	<0.002	0.0005	4	<0.0005	<0.0005	1
Pb	0.001	<0.0005	>2	0.001	<0.0005	>2
Fe	0.003	0.0025	1.2	0.002	0.001	2
Si	<0.005	<0.005	1	<0.005	<0.005	1
Sn	<0.0005	<0.0005	1	0.0008	<0.0005	>1.6
Al	<0.0005	<0.0005	1	<0.0005	<0.0005	1
Ag	0.001	<0.0005	>2	0.001	0.0001	10
Cu	0.0015	<0.0005	3	<0.0005	<0.0005	1
Ni	0.0008	<0.0005	>1.6	<0.0005	<0.0005	1
Mg	0.04	0.0005	80	0.009	0.001	9
Zn	<0.001	<0.001	1	0.001	0.0001	10
Sb	<0.0005	<0.0005	1	<0.0005	<0.0005	1
$\hat{I}_2$	0.002	0.0001	20	0.001	0.0001	10
Ñ	0.001	0.0001	10	0.002	0.0001	20

signed at the E.O. Paton Electric Welding Institute of the NAS of Ukraine (Figure 1).

In the process of development of melting conditions influence of specific power of electron beam and rate of melting on degree of refining and mass of the evaporated metal was considered.

In Figure 2 dependence of the platinum evaporation rate upon temperature, calculated according to Langmuir equation on basis of the data on pressure of saturated vapors of platinum under conditions of experimental electron beam remelting (EBR), is presented. Langmuir equation [3] describes interconnection between rate of sublimation k_s and pressure P of the substance vapor:

$$k_s = P\sqrt{M/2\pi RT},$$

where M is the atomic or the molecular weight; R is the gas constant; T is the absolute temperature, °C.

One can see from the Figure that the higher is temperature of platinum, the more intensive is process of its evaporation. Critical increase of the platinum evaporation rate was registered at the temperature above 2400 °C.

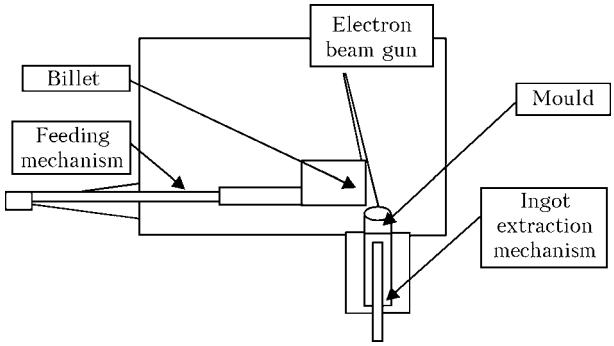

Figure 1. Technological block diagram of UE-178 electron beam installation

As a result of carried out works practical confirmation of the calculated data was obtained. Amount of evaporated and then condensed on screens and internal surfaces of the working chamber metal achieved in some melts 2–4 % of the alloy mass of the remelted metal. Content of platinum in the condensates constituted 92–98 %. That's why subsequent experimental works were directed at determination of optimal EBR conditions, which allow removing impurities at minimal evaporation of platinum.

Experiments in refining of platinum showed that low-melting non-ferrous metals (aluminium, copper, stannum, magnesium, zinc, antimony and lead) are subjected to deep refining (Table 1). Values of coefficient K of removal of mentioned metals vary from 125 to 80. Gas impurities reduce by one order.

Palladium is also volatile in refining remelting of platinum. Mean value of coefficient of its removal from platinum is, approximately, 5. Analysis of experimental melts showed that from the viewpoint of efficiency of cleaning of elements with high volatility it is necessary to overheat the melt to a lower degree. In this case it is rational to carry out EBR at specific power of electron beam 0.50–0.55 kW / cm^2.

Refining of platinum from iron turned out to be rather difficult task. Comparing pressure of platinum and iron vapors [4], one may assume that iron, pressure of vapors of which equals pressure of palladium vapors, may be removed from platinum by means of EBR. However, calculations of degree of separation of the metals, based on pressure of vapors of the ele-

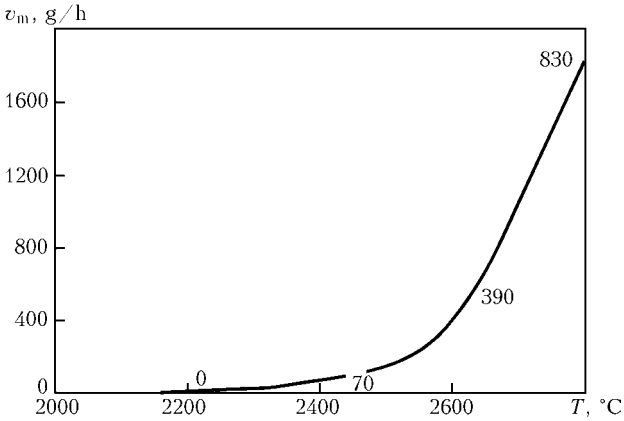

Figure 2. Dependence of platinum evaporation rate upon temperature of melt in EBR

Table 2. Chemical composition of platinum ingot after EBR, %

Chemical element	Platinum sponge	Ingot of induction melting	EBR ingot	GOST 12341–81 (Grade PlA-0)
Pt	99.6	99.95	99.9925	99.98
Pd	0.006	0.006	0.002	Σ 0.015
Rh	0.002	0.002	0.002	
Ir	0.002	0.002	<0.002	
Ru	0.001	0.001	<0.001	
Au	0.002	0.002	<0.001	0.002
Pb	0.003	0.002	<0.001	0.002
Fe	0.003	0.002	0.0015	0.003
Si	0.002	0.002	0.002	0.002
Sn	0.0045	0.004	<0.001	0.001
Al	0.001	0.001	<0.001	0.002
Ag	0.0033	0.003	<0.001	0.005
Cu	0.002	0.002	<0.001	0.002
Ni	0.001	0.002	<0.001	0.001
Mg	0.003	0.008	<0.001	0.002
Zn	0.002	0.002	<0.001	0.002
Ca	–	–	<0.001	Not regulated
Cr	–	–	<0.001	–
K	–	–	<0.001	–
Mn	–	–	<0.001	–
Mo		–	<0.001	–
Zr	–	–	<0.001	–
Sb	0.001	0.001	<0.001	0.001
Î$_2$	0.01	0.006	<0.001	Not regulated
Ñ	0.002	0.002	<0.001	–

ments, show only relative evaporation rate of the components [5]. Experimental data demonstrated that process of iron evaporation in the Pt–Fe system proceeds rather slowly. Triple refining remelting allowed reducing content of iron in platinum from 0.98 to 0.43 %, but evaporation of platinum in this case achieved 9.8 %, which may be explained by high chemical affinity of iron and platinum, unlimited solubility of platinum in γ-Fe, and high level of the interatomic bond strength in the melt.

Degree of platinum refining from impurities may be changed within wide limits by varying rate of remelting, corresponding to sufficient degree of refining at minimal sublimation of platinum. For determining optimal rate of remelting seven experimental melts were carried out at constant specific power 0.5 kW / h and rate from 2.5 to 9.0 kg / h. The investigations resulted in selection of optimal range of the melting rate ––– v_m = 4–5 kg / h [6].

Under optimal conditions of platinum refining more than 20 kg of platinum of not less than 99.99 % purity were produced (Table 2), which is confirmed by the data, obtained by the «Degussa-Huels» company.

1. Rytvin, E.I. (1987) *High-temperature strength of platinum metals*. Moscow: Metallurgiya.
2. Shejko, I.V., Timofeev, N.I., Dmitriev, V.A. et al. (1990) About application of induction remelting in sectional mould for recycling of platinum alloy waste. *Problemy Spets. Elektrometallurgii*, **2**, 9–13.
3. Hirs, D., Paund, G. (1966) *Evaporation and condensation*. Moscow: Metallurgiya.
4. (1985) *Examination of possibility for application of new methods of melting in production of platinum alloy metals*: Report of researches (intermediate). Moscow: Giredmet.
5. Turkdogan, E.N. (1988) *Physical chemistry of high-temperature processes*. Moscow: Metallurgiya.
6. Kadochnikov, V.A., Savenko, V.A., Major, A.V. et al. *Method of refining of platinum and its alloys*. Pat. 75300 Ukraine. Int. Cl. C 22 B 11 / 00. Publ. 15.03.2006.

INVESTIGATION OF PLASMA-SLAG PROCESSES IN SPECIAL AND LADLE ELECTROMETALLURGY OF STEEL

A.A. ZHDANOVSKY, V.A. SHAPOVALOV, G.A. MELNIK, D.M. ZHIROV, M.S. PRIKHODKO and **L.G. ODINTSOVA**
E.O. Paton Electric Welding Institute, NASU, Kiev, Ukraine

Theoretical analysis made it possible to consider advantages of the progressive technology of steelmaking and determine specificity of main processes of the plasma-slag metallurgy, calculate partial pressure of the components and composition of the vapor-gaseous phase above slag of the fluorite–lime and lime–alumina–silicate systems. Experimental investigations allowed specifying some peculiarities of pyrometallurgical reactions in the gas (plasma)–slag–metal system in melting of ball bearing and stainless steels, low carbon iron, high carbon ferrochromium, and alloying of iron by chromium in case of application of the plasma-arc models as heat sources.

Keywords: thermodynamic calculations, fluxes (slag), vapor-gaseous phase, plasma-slag processes, plasma remelting furnaces, plasma ladles-furnaces, out-of-furnace refining of steel from non-metal inclusions and sulfur, top level technology

Ferrous metallurgy of Ukraine within many years developed extensively under conditions of chronic deficit of centralized capital investments, wasteful attitude to mineral-raw material resources, and orientation at unpromising equipment, which was used for decades and exhausted its possibilities. Often many scientific-technical problems were not solved at the proper level within necessary terms, too low rate of mastering of high-tech technologies and as a result sharp disproportion between fundamental-applied investigations and their practical application in production were registered, and in a number of developments serious shortcomings and strategic miscalculations occurred.

Because of these reasons a significant portion of fixed metallurgical assets has high degree of wear, and technological level of certain process stages and production lines is much lower than in the industrially developed countries. Steelmaking production, which determines technical level and results of work of the branch, occupied in 2006 eighth position in the world in regard to gross melting of steel, its structure included huge volume of open-hearth and insufficient development of oxygen-converter and especially electric steel melting conversions, and specific weight of continuous steel casting (CSC) was the lowest among ten countries ---- main producers of steel (Table 1) [1].

These are the reasons of insufficiently high quality of Ukrainian metal products, low level of their certification, limited assortment, high production cost, and low competitiveness both on internal and on external markets. This stipulates urgent need of scientific-technical re-equipment of ferrous metallurgy, modernization and restructuring of its enterprises, and drastic improvement of structure of steelmaking production by gradual liquidation of open-hearth production and its replacement by oxygen-converter and electric steelmaking production in combination with out-of-furnace processing (OFP) and CSC.

In steelmaking production of industrially developed countries concept of the technology of the top level steel production has formed [2]. Its essence consists in application of arc steel furnaces (ASF), oxygen converters or open-hearth furnaces as high-productivity units for melting of semi-manufactured products and maximal ensuring of conditions of operation of the furnaces exclusively for accelerating process of melting of the metal scrap, cast iron and additives. The only element of metallurgical technology, carried out simultaneously with melting of the charge, remains dephosphorization, while all other processes are imposed on OFP (adjustment of the steel chemical composition with regulation of the content of separate

Table 1. Volume of steel production and share of melting methods among first ten countries-main producers in 2006

Country	Total volume of production, mln t	Share of method of melting and casting, %			
		Converter	ASF	Open-hearth	CSC
China	422.7	87.0	13.0	--	94.8
Japan	116.2	74.0	26.0	--	97.7
USA	98.6	43.1	56.9	--	96.7
Russia	70.8	61.6	18.4	20.0	53.8
South Korea	48.5	54.3	45.7	--	98.0
Germany	47.2	68.9	31.1	--	96.3
India	44.0	47.3	50.5	2.3	65.9
Ukraine	40.9	56.4	9.8	33.8	44.7
Italy	31.6	37.4	62.6	--	95.5
Brasilia	30.9	73.9	24.4	1.7*	92.3
All together in the world	1244.2	65.5	32.0	2.4	90.5

*Another method of melting (in energy-optimized furnaces).

elements and the melt temperature; refining of the metal from harmful impurities, gases, and non-metal inclusions; microalloying and modification of steel and control of morphology of non-metal inclusions; improvement of technical-economic parameters of metal production both in steelmaking conversion and within the whole cycle of steel production).

Significant shift in development of plasma technology in 1970–1980s stimulated development of plasma metallurgy as one of promising directions of scientific-technical progress.

That's why in future a special place in steelmaking production plasma metallurgy should occupy, which favorably distinguishes itself not just by high quality of metal, but also by better in comparison with the open arc melting conditions of work and significant environmental advantages. It allows significant increasing of technical level of production; improving quality of the metal (first of all for special-purpose branches of industry ---- aviation, ship building, power-plant engineering, chemical industry, etc.); developing new methods of production of ferroalloys and pure metals with application of lean raw materials with high level of the base component recovery; utilizing slag, slurries and other off-grade wastes of metallurgical production.

Significant contribution into development of powerful plasmatrons was made by the E.O. Paton Electric Welding Institute of the NAS of Ukraine (PWI), Institute of Metallurgy and Materials Science of RAS, TsNIICHERMET (both Russia), companies «Krupp» (Germany), «Plasma energy» (USA), etc. While PWI developed plasmatron mainly for remelting furnaces with water-cooled moulds and tested some of them in furnaces with a ceramic crucible, the «Krupp» company first planned to use such plasmatrons in furnaces with a ceramic crucible, and in future in ladles-furnaces and intermediary ladles of CSC machines. Having at their disposal plasmatrons, operating on alternating current up to 4 kA, this company bought in 1983 from PWI plasmatrons with plasma electrodes, designed for 6 kA current. Early in 1990s this company offered 2–8 MW plasma ladles-furnaces (PLF) of 20–150 t capacity with rate of the metal preheating up to 4 °C / min, equipped with two or three plasmatrons of up to 12 kA current [3].

In 1986 the «Nippon Steel» company (Japan) bought from PWI license for the alternating current plasma heating module (PHM) of up to 5 MW power, which included three plasmatrons of direct action, connected according to the three-phase scheme, sources of their power supply and equipment for controlling electrical and gas conditions. Joint industrial tests of this module on PLF of 100 t capacity confirmed possibility of compensation of heat losses and melt preheating at the rate 0.82 °C / min.

In development and mastering in 1996 of PHM for equipment of the unit for complex out-of-furnace processing of steel of 30 t capacity at «Bummash» Ltd (Russia) the authors used results of theoretical and experimental investigations of PWI, industrial tests of the «Nippon Steel» company and rich experience, received in development of metallurgical alternating current plasmatrons with plasma electrodes and plasma-arc furnaces of different types, and in production of high-quality steels and alloys by methods of remelting, melting and out-of-furnace processing [4].

Plasma metallurgical processes, carried out with supply on surface of a metal pool of slag or with formation of the latter as a result of chemical reactions in the melts and characterized by significant and specific advantages, received name of the plasma-slag ones.

Plasma-arc remelting, in comparison with other methods of producing especially pure metals and allows, allows regulating within wider range atmosphere of the furnace, controlling rates of the billet melting and the ingot solidification, and makes it possible to select different refining agents [5].

Of big scientific and practical interest is investigation of one of the versions of plasma-arc remelting ---- plasma-slag remelting (PSR) [6].

Under PSR conditions, like in electroslag remelting, slag on basis of fluoric calcium, oxides of calcium, aluminium, magnesium, etc. is used. Such slag is continuously or periodically supplied in the form of powders on surface of the metal pool. Consumption of slag per a melt does not exceed 2 % of the produced ingot mass.

Slag for PSR should have a set of necessary properties: high assimilation capacity in relation to oxide and nitride non-metal inclusions; low pressure of vapors; high disulfation capacity; low adhesion relative steels and alloys being remelted; low viscosity within wide temperature range; low oxidation capacity; sufficiently high electric conductivity; stable composition under action of plasma plumes on slag, etc.

Under action of heat of plasma jets and molten metal slag easily melts, spreads over the pool surface, and partially transits into the vapor-gaseous phase. A certain share of the evaporated slag condenses on end of the molten ingot, while its bulk remains on the pool surface and, as a rule, is used for formation of skull between the ingot and the mould wall.

In process of PSR so high temperatures are achieved, at which evaporation of slag is inevitably accompanied by dissociation of its components. Products of slag evaporation, similar to the submerged-arc welding [7], may participate in the metallurgical reactions. For PSR it is necessary to know composition of the vapor-gaseous phase above the used slag. Let us take double CaF_2–CaO and triple CaO–Al_2O_3–SiO_2 systems as an example.

Composition of the vapor-gaseous phase above the melt at different temperatures may be determined by data of dissociation of pure components and their activity in the melt [8].

Thermodynamic calculation of the vapor-gaseous phase composition was carried out at pressure in the

system 0.1 MPa and temperature 1773 K (at overheating of molten CaF_2 by 100 degrees) and at 2773 and 3773 K (boiling temperature of CaF_2 and CaO respectively).

Vapor-gaseous phase above slag of the first system consists mainly of CaF_2. So, at 1773 K partial pressure of CaF_2 exceeds level of pressure of the rest components by 5–15 orders. Increase of temperature causes reduction of this difference: at 2772 K it constitutes 4–10 and at 3773 K — 3–8 orders.

Dilution of CaF_2 by the CaO additive enables certain reduction of partial pressure of evaporation products of CaF_2 and increase of those of CaO.

In the vapor-gaseous phase above CaF_2–CaO melts partial pressure of CaF_2 is significantly higher than of CaF: at 1773 K — by 9, at 2773 K — by 6 orders, and at 3773 K by 4 orders.

Results of calculation of general pressure of vapors in the $CaO–Al_2O_3–SiO_2$ system and composition of the vapor phase indicate at the fact that the slag component, which determines its oxidation potential, is silica. As activity of silica grows, oxidation potential of the slag, which changes slower than the activity, increases. In the considered section activity of silica increases almost 9 times, while oxidation potential of the slag — only 2.25 times.

Growth of the slag oxidation potential is accompanied by increase of the silicon oxide partial pressure. Stipulated by thermal dissociation of the components oxidation potential of the slag is considered its own potential. Partial pressure of the reduction agents — calcium, aluminium, magnesium, etc. — increases by means of consumption of oxygen in vapor.

Considered methodology may be used for thermodynamic analysis of specific slag of multicomponent systems, which lead to the $CaO–Al_2O_3–SiO_2$ quasitriple system. For steel refining in PLF the slag, containing the following components, is used, wt.%: 25–49 CaO; 7–25 MgO; 6–23 Al_2O_3; 14–30 SiO_2; FeO, MnO — not more than 2.0 and 2.5 of each. Because of service conditions of the PLF lining and harmful gas release into environment, CaF_2 content in slag is limited by 2 wt.% [9, 10].

In state-of-the-art remelting processes three stages of metal existence in molten state are singled out: in the form of a film on the billet end being melted, drops, and a metal pool [11]. Thermodynamic analysis of composition of vapor-gaseous phase above the slag allows stating that in contrast to the electroslag remelting, at which the whole molten metal interacts with the homogeneous slag, in PSR metal in the form of a film at the billet end and in the form of drops contacts with CaF_2, while on the pool surface — with the used oxide-fluoric slag.

Refining of steels and alloys from non-metal inclusions may proceed in two ways. If non-metal inclusions are so strong that they do not decompose under conditions of the remelting processes, they may be removed by their carrying out by macrocurrents on interface between the metal pool and the molten slag, which wets and assimilates them. But if at the remelting temperatures non-metal inclusions dissociate into the constituting them elements and the whole oxygen or nitrogen is in the solution, their removal with assistance of the slag proceeds in the form of extraction. Slag as a medium, in which such gases dissolve better than in a metal, tends to equilibrium distribution of gases and absorbs significant share of them from the metal.

Possibility of formation (or decomposition) of non-metal inclusions in steels and alloys depends upon content of constituting them elements in the metal, and temperature and chemical composition of the steel or the alloy, i.e. upon factors, which may exert significant influence on activity of the elements, which form non-metal inclusions.

On basis of thermochemical data [8, 12, 13] temperature dependences of equilibrium constants of the integral reaction of formation of silica in the ShKh15 molten steel, titanium nitride in the Kh18N10T steel, and niobium nitride in the 00Kh16N15M3B steel were calculated:

$$\lg K = \lg (a_{Si} a_{O_2} / a_{SiO_2}) = 24800 / T + 8.70;$$

$$\lg K = \lg [Ti] ([N] / 0.01) = -15390 / T - 0.54 \lg T - 0.046 \cdot 10^{-3} T + 0.323 \cdot 10^{5} T^{-2} + 8.06;$$

$$\lg K = \lg [Nb] ([N] / 0.01) = -11838 / T - 0.03 \lg T - 0.036 \cdot 10^{-3} T - 0.42 \cdot 10^{5} T^{-2} + 6.12.$$

In Figure 1 results of calculation of temperature dependence of oxygen content in the ShKh15 steel, equilibrium with slag A (97.25 % CaF_2 and 2.75 % SiO_2) and slag B (70 % CaF_2 + 27.25 % CaO + 2.75 % SiO_2). It was assumed in the calculation that in case of equilibrium between the metal and the slag the whole oxygen reacts only with silicon, and activity coefficients of silicon and oxygen in steel and activity of silicon in slags A and B were taken into account. Curve *1* (Figure 1) corresponds to equilibrium with slag A, curve *2* — with slag B, and lines *3* and *4*

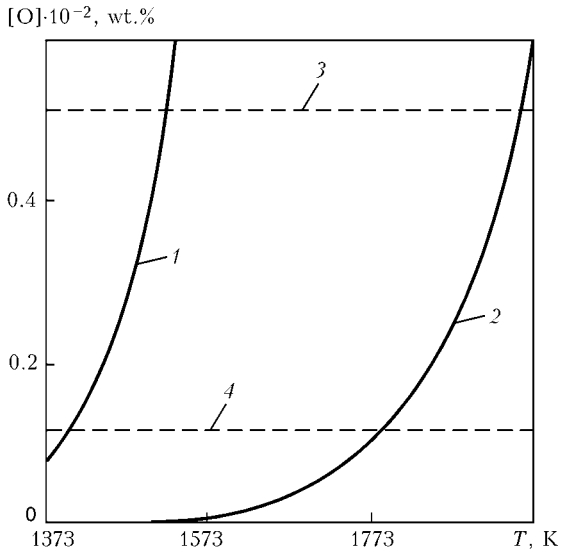

Figure 1. Dependence of oxygen content in ShKh15 steel upon temperature, and its actual content in metal

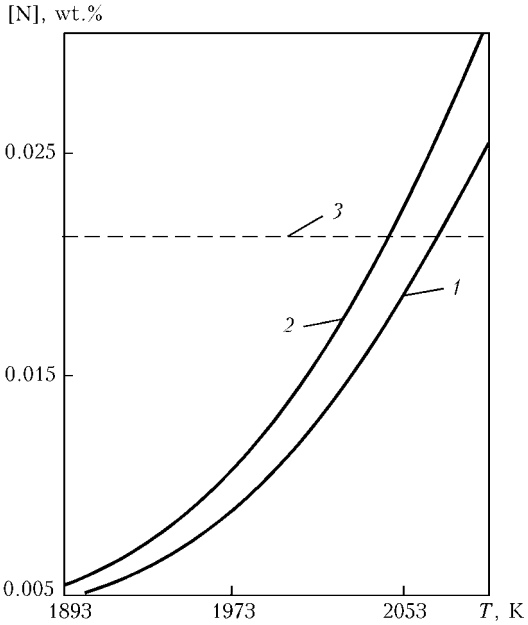

Figure 2. Dependence of equilibrium content of nitrogen in Kh18N10T steel upon temperature and titanium content

show actual content of oxygen in the billet and in the ingot respectively. Having analyzed Figure 1, one may draw conclusion that silicon is stable in steel in equilibrium with slag A at the temperature below 1453–1530 K, and in presence of slag B silicon dissociates into constituting it elements (up to the temperature 1453–1530 K). So, one may assume that refining of the ShKh15 steel from silicate inclusions occurs mainly on melted end of the billet, and removal of oxygen from the metal pool under slag — by the extraction method.

In Figure 2 curves of equilibrium content of nitrogen are presented, which correspond, according to our experiments, to maximal (curve *1* — 0.50 %) and minimal (curve *2* — 0.14 %) content of titanium in the Kh18N10T steel, and curve *3*, which corresponds to actual content of nitrogen. One can see that at 0.5 % content of titanium in steel, the titanium nitride dissociates at the temperature not lower than 2073 K.

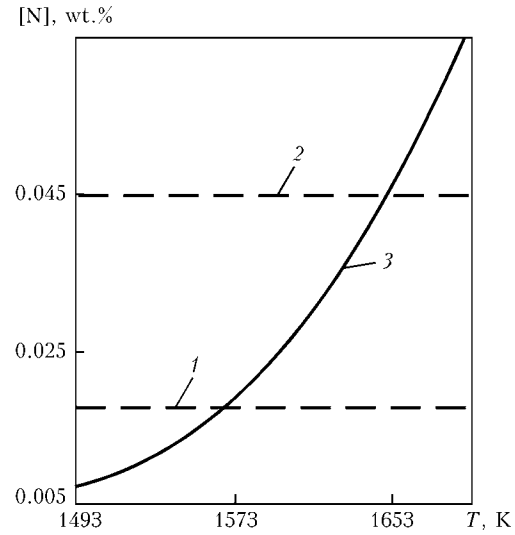

Figure 3. Temperature dependence of equilibrium content of nitrogen in 00Kh16N15M36 steel at 0.045 wt.% Nb

Reduction of the titanium content down to 0.14 wt.% causes reduction of its dissociation temperature down to 2053 K. As far as at PSR in a water-cooled mould, main bulk of the metal does not reach so high temperature, titanium nitride in the Kh18N10T steel will not dissociate.

Dash lines *1* of minimal (0.019 wt.%) and *2* of maximal (0.045 wt %) concentrations of nitrogen in the 00Kh16N15M3B steel intersect with solid line *3* of its equilibrium content at the temperatures 1573 and 1653 K respectively (Figure 3). So, at PSR niobium nitride dissociates in this steel.

It is established in [14, 15] that nitrides of the transition metals, aluminium and silicon are well wetted by the lime-silica slags of the AN-29 type and somewhat worse by silica-fluoric slags of the ANF-6 type, etc. In addition, lime-silica slags have maximum solubility of nitrogen. That's why there is ground to assume that dominant part in removal of nitrides and nitrogen from stainless steels in PSR is played by the metal pool.

The most perfect OFP units are installations of the arc ladles furnaces (ALF) type, in which possibility of the molten steel heating and a set of devices for its stirring, addition of lumpy and injection of powder materials are envisaged. At present any OFP and CSC technologies and equipment, introduced at national metallurgical enterprises, are mainly of foreign production, which lags behind by 10–15 years from state-of-the-art technical and technological decisions. The only exclusion are put into operation at Enakievo Metallurgical Plant two new lines with CSC machines complete with two ladle-furnace installations, produced at Novokramotorsk Machine-Building Works [16].

Further way of improvement of ladles-furnaces is application of single-sleeve or current-conducting electrode holders, transition of the latter on direct current supply, conversion of conventional arcs into plasma ones by means of feeding argon into the hollow graphitized electrodes, replacement of the latter with plasmatrons, development of PLF, etc.

Application of the alternating current plasmatrons creates the following advantages [17–20]:

- application of the inert atmosphere prevents saturation of the metal with gases (nitrogen, hydrogen, oxygen) or will make it possible to alloy the metal by nitrogen, and make easier regulation of content of the elements with high affinity to oxygen and increase their assimilation;
- absence of the need to use graphitized electrodes will allow refusing from the steel decarburization process, that will simplify and make easier process of movement of the plasmatrons;
- possibility of operation of three plasma arcs at zero point will enable efficient heating of the slag and deep desulfuration and refining of the metal;
- stability of burning of the plasma arcs makes it possible to direct them neater to the ladle center, reduce wear and increase durability of the lining.

Table 2. Chemical composition of initial slags and slags produced after PSR of pellets, ferrochromium and chromium steel

Slags	Weight share of components, %									
	MnO	TiO_2	CaO	MgO	FeO	Al_2O_3	Cr_2O_3	SiO_2	CaF_2	S
Initial										
VO-1	–	–	50.0	–	–	30.0	–	20.0	–	–
VO-2	5.0	10.5	45.0	5.0	9.5	10.0	–	15.0	–	–
ANF-1	–	–	1.8	–	–	0.5	–	–	96.7	–
EZF*	–	–	0.3	44.7	–	17.6	4.1	30.4	–	–
Produced										
PO-1	–	–	–	–	80.0	–	–	19.5	–	–
PO-2	–	–	13.0	–	67.0	–	–	17.9	5.8	–
PO-3	–	–	13.4	–	65.7	–	–	18.2	3.2	–
PO-4	–	–	6.8	–	74.8	2.3	–	15.6	–	–
PF-1	–	–	13.2	6.3	3.9	5.3	42.7	29.3	–	–
PF-2	–	–	17.1	6.8	3.6	5.6	34.4	33.4	–	–
PL-1	–	–	48.5	1.3	–	26.4	0.4	22.6	–	0.6

*Is given for comparison.

Specificity of the PSR processes allows considering them as physical-chemical models of plasma OFP. Thermodynamics of the PSR processes can not have differences. Mass transfer may be equalized by variation of the process rate, soaking of the metal in the crucible, and intensity of the melt mixing in OFP, when the same interaction surface areas of gaseous, slag and metal phases are achieved.

The OFP and the CSC processes as technological components of the combined systems are characterized by a rather wide range of potential possibilities for their development and improvement, which are quite within the power of Ukrainian metallurgists and machine builders, provided their efforts are consolidated [21].

Experimental investigations, simulating plasma OFP, were carried out on the OB-1501 test bed, re-equipped into the plasma-arc installation for melting, soaking and casting of the metal by adding a specially developed melting-casting fitting-out. This allowed carrying out melts in a copper water-cooled or ceramic crucible. In the first case interaction of the metal and the slag melts with refractory lining was excluded, which ensured purity of the experiments, and in the second case favorable conditions were created for thermal and energy investigations and for investigation of operation of the ladle-furnace slag-line area.

In PWI a complex of laboratory installations was developed and successfully used [22, 23], on which physical-chemical properties of the slag melts, used in special electrometallurgy, were investigated [24, 25]. We investigated temperature dependences of viscosity and electric conductivity of the VO-1 and VO-2 slags for OFP of steels (Table 2). Partial replacement of calcium oxide for magnesium oxode, silicon dioxide for manganese oxide, and dialuminium trioxide for ilmenite enable significant reduction of viscosity (Figure 4) and increase of electric conductivity (Figure 5) of the slag.

Metallized pellets, produced at Oskol Electrometallurgical Plant (Russia), wastes of carbonaceous ferrochromium casting, supplied by Aksu Plant of Ferroalloys (Republic Kazakhstan), and the VO-1 and the ANF-1P slags, produced in melts carried out in Ukraine, were used as the charge material.

Plasma-arc melts were carried out in inert atmosphere after loading into the crucible about 20 kg of the charge. In first series of melts iron from the pellets was produced, in second series ---- ferrochromium from the wastes of its casting, and in third series ---- chromium steel by means of alloying of iron by ferrochromium. At the beginning of each melt of first and second series intensive removal of volatile substances and moisture from the charge were detected. This was proved by the character of voltage change of the plasmatrons ---- increasing, achieving the maximum, and then reducing down to the nominal value. After achievement of the latter the melt was subjected to soaking while the plasmatrons continued to work, for a period of, approxi-

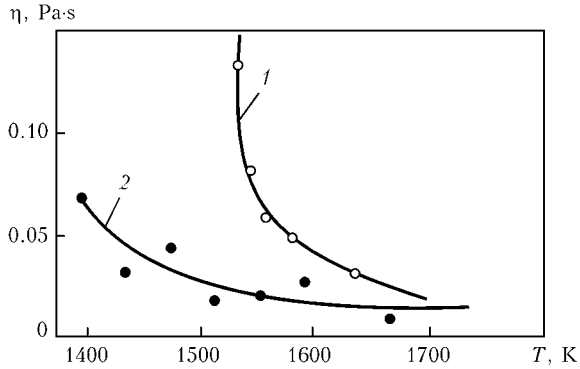

Figure 4. Dependence of viscosity of VO-1 (*1*) and VO-2 (*2*) out-of-furnace processing slags upon temperature

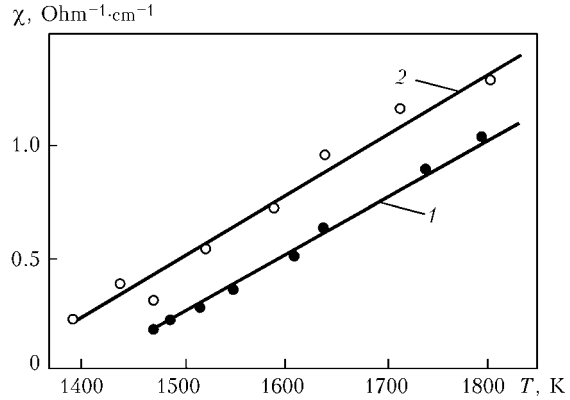

Figure 5. Temperature dependence of electrical conductivity χ of VO-1 (*1*) and VO-2 (*2*) slags

mately, 10 min for finishing of the chemical reactions and homogenization of the metal.

Metallized pellets were melted according to three technological options: without addition of synthetic slags (PO-1) and with addition to 20 kg of the pellets of 1.3 kg of the ANF-1P (PO-2 and PO-3) and the VO-1 (PO-4) slag. In majority of these melts current of each plasmatron was 2 kA, while in case of melting with PO-3 it was increased up to 2.4 kA. Chromatographic analysis of the furnace atmosphere composition showed formation in the gaseous medium of hydrogen and carbon oxides, growth of their content at initial period of the melting, achievement of the maximum, and their smooth reduction down to full disappearance (Figure 6). Synchronism of the content change of these gases and voltage of the plasmatrons in the course of a melt should be noted.

In melting of the ferrochromium wastes the charge was used in the state, in which it was supplied (PF-1), or was subjected to calcination at the temperature 800 °C that caused reduction of its mass by 5 %.

It became possible to produce low-carbon iron (0.013–0.027 wt.% C) and ferrochromium, chemical composition of which meets requirements of GOST 4757-89, according to the described technology (Table 3).

Data of this Table have to be considered in greater detail. So, in plasma melting of pure pellets, 80 % of the slag constitutes iron oxide, the rest is silica. Addition of the ANF-1P slag reduces content of iron oxide down to 67 wt.%, while increase of current

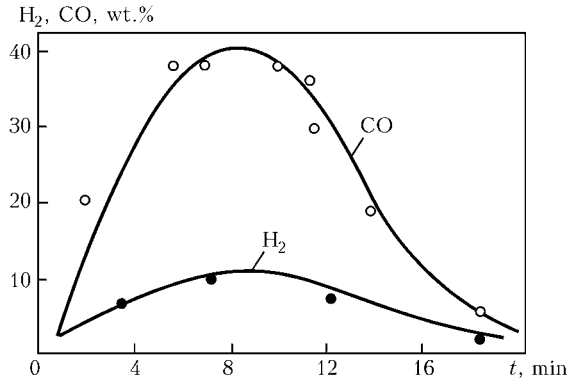

Figure 6. Dynamics of content change of hydrogen and carbon oxide in gaseous medium in plasma melting of pellets

Table 3. Chemical composition of metal produced by PSR

Slags	Weight share of elements, %				
	Fe	Cr	C	S	P
PO-1	Base	–	0.027	0.019	0.014
PO-2	Same	–	0.013	0.018	0.012
PO-3	»	–	0.013	0.018	0.012
PO-4	»	–	0.014	0.015	0.013
PF-1	23.5	71.6	5.400	0.080	0.031
PF-2	20.7	73.6	5.700	0.120	0.031
PL-1	Base	8.9	0.860	0.005	0.018

enables deeper change of the slag composition evidently due to a fuller progress of the reaction between calcium fluoride and iron oxide with formation of the volatile iron fluoride. Absence of calcium fluoride when the VO-1 slag is added causes reduction of the iron oxide content in the final slag only up to 75 wt.%. Slag, formed in melting of ferrochromium wastes in the water-cooled crucible, differs from conventional slag of the carbothermal production by a very high content of dichrome trioxide and calcium oxide and low content of magnesium oxide and dialuminium trioxide, weight share of silicon dioxide being constant.

Products of the melts of first and second series were used as the charge for melting of chromium steels. For investigation of the desulfuration processes, about 4 kg of ferrochromium and iron of general mass 20 kg were loaded into the skull crucible, and the VO-1 slag, aluminium, and sulfurous iron were added to them, and then melting was carried out. Due to such melting significant degree of desulfuration was achieved owing to high efficiency of plasma heating and increased activity of the slag caused by high temperature. So, slag of OFP, similar to the PShP [26] and EShP [27] slags, allows ensuring achievement of high coefficients of sulfur distribution between the slag and the metal in plasma melting both in the described experiments and according to data of the work [10].

Alloying of steel by chromium, accompanied by reduction of the melt temperature because of endothermicity of the process, became the reason of reduction of the degree of overheating of water, which cools melting crucible [28].

Ladle refining of metal is an important link in production technology of steel of both special-purpose and general designation. Progress achieved within the last years in improvement of production technology of refractory materials, design of the installations, application of plasma heating, and other technological measures created premises for deepened investigation of the processes, which proceed in ladles-furnaces. This allowed significant improving quality of steel and controlling not just amount, but also chemical composition of the non-metal inclusions [29].

CONCLUSIONS

1. Thermodynamic analysis of composition of the vapor-gaseous medium above some slags of plasma remelting and out-of-furnace processing was carried out.

2. Carried out plasma-slag melts allowed specifying peculiarities of behavior of gases in stainless and bearing steels.

3. Plasma melts of the metallized pellets and ferrochromium wastes for production of chromium steels were carried out.

1. (2007) Main steelmaking countries and their technological processes. *Metallurg. Kompas Ukraina-Mir*, **6**, 54.
2. Lopukhov, G.A., Katsov, E.Z. (1989) State-of-the-art of steelmaking. Production of cast iron and steel. In: *Results of science and technique*, Vol. 19. Moscow: VINITI AN SSSR, 9–88.
3. Bebber, H., Espenoliller, B. (1991) Plasma torch clean up the ladle furnace. *Steel Times*, 219(**12**), 665–666.
4. Zhadkevich, M.L., Melnik, G.A., Zabarilo, O.S. et al. (1998) Design and implementation of plasma ladle-furnace. *Problemy Spets. Elektrometallurgii*, **1**, 42–48.
5. Paton, B.E., Lakomsky, V.I., Dudko, D.A. et al. (1966) Plasma-arc remelting of metals and alloys. *Avtomatich. Svarka*, **8**, 1–5.
6. Paton, B.E., Medovar, B.I., Movchan B.A. et al. (1967) Some ways of increase in quality of steels and alloys for welded structures. *Svarochn. Proizvodstvo*, **11**, 7–10.
7. Dyatlov, V.I. (1951) Specifics of metallurgical processes in submerged-arc welding. In: *Coll. dedicated to 80th anniversary and 55th years of scientific activity of E.O. Paton*. Kiev: AN Ukr. SSR.
8. Kulikov, I.S. (1969) *Thermal dissociation of compounds*. Moscow: Metallurgiya.
9. Elansky, G.N. (1988) Out-of-furnace treatment of steel. Iron- and steelmaking. In: *Results of science and technique*, Vol. 18. Moscow: VINITI AN SSSR, 120–188.
10. Neuschutz, D., Schubert, K.-H., Bebber, H. (1991) Metallurgical results from a 30-t AC plasma ladle furnace. *Steel Research*, **9**, 390–394.
11. Lakomsky, V.I. (1967) Macrokinetics of metal refining in current processes of remelting. *Fizika i Khimiya Obrab. Materialov*, **4**, 57–62.
12. (1966) *Thermodynamic properties of inorganic materials*. Ed. by A.P. Zefirov. Moscow: Atomizdat.
13. Elliot, D.F., Glejser, M., Ramakrishna, V. (1969) *Thermochemistry of steelmaking processes*. Moscow: Metallurgiya.
14. Sryvalin, I.T., Burylev, V.P., Korpachev, V.G. et al. (1970) To thermodynamics of delaminated oxide and fluoride systems. System $CaO–SiO_2–CaF_2$. *Izvestiya Vuzov. Chyorn. Metallurgiya*, **10**, 5–9.
15. Ershov, G.S., Kovalenko, A.M. (1968) Adhesion of nitrides to liquid alloy steels and slag melts. *Izvestiya AN SSSR. Metally*, **1**, 84–90.
16. (2005) How the Ukrainian steel is melted. *Metall*, July, 6–7.
17. Zhdanovsky, A.A., Zabarylo, O.S., Melnik, G.A. et al. (1993) Comparative analysis of main parameters of arc ladles-furnaces and steel-smelting furnaces. *Problemy Spets. Elektrometallurgii*, **3**, 50–58.
18. Zhdanovsky, A.A., Zabarylo, O.S., Melnik, G.A. et al. (1994) Analysis of main parameters of energy mode of industrial plasma ladles-furnaces. *Ibid*., **1/2**, 53–60.
19. Melnik, G.A., Zabarylo, O.S., Zhdanovsky, A.A. et al. (1991) Prospects of application of plasma heat sources in units for out-of-furnace treatment of steel. Report 1: *Ibid*., **2**, 60–66; Report 2: *Ibid*., **3**, 86–92.
20. Paton, B.E., Latash, Yu.V., Zabarilo, O.S. et al. (1985) Three-phase plasma heating devices and prospects of their application. Report 1: *Ibid*., Issue 1, 50–55; Report 2: *Ibid*., Issue 2, 53–57.
21. Dubodelov, V.I., Smirnov, A.N. (2006) Second meeting of interdepartmental scientific-technical council (MNTO) of Ukraine on problems of out-of-furnace treatment and continuous casting of steel. *Elektrometallurgiya*, **5**, 46, 47.
22. Zhdanovsky, A.A., Lakomsky, V.I., Grigorenko, G.M. et al. (1976) Machine for examination of slag melt viscosity. *Problemy Spets. Elektrometallurgii*, Issue 4, 102–106.
23. Zhdanovsky, A.A., Latash, Yu.V., Gorchinsky, O.A. et al. (1978) Machine for measurement of electroconductivity of melted fluxes. *Ibid*., Issue 8, 113–115.
24. Latash, Yu.V., Fetisova, T.Ya., Voronin, A.E. (1986) Examination of viscosity of slags (fluxes) of $CaF_2–CaO–Al_2O_3–SiO_2$ system. *Ibid*., **2**, 3–8.
25. Latash, Yu.V., Fetisova, T.Ya., Voronin, A.E. (1986) Electroconductivity of slags (fluxes) of $CaF_2–CaO–Al_2O_3–SiO_2$ system. *Ibid*., **3**, 25–30.
26. Zhdanovsky, A.A., Latash, Yu.V., Bakumenko, S.P. et al. (1978) On problem of sulfur-absorbing capability of plasma-slag remelting fluxes. *Ibid*., Issue 8, 115–120.
27. Biktagirov, F.K., Latash, Yu.V., Levkov, L.Ya. et al. (1989) Procedure of experimental determination of sulfide capacity of oxide-fluoride fluxes. *Ibid*., **3**, 6–11.
28. Kazachkov, I.P. (1982) *Alloying of steel*. Kiev: Tekhnika.
29. Nicholson, A., Gladman, T. (1986) Non-metallic inclusions in secondary steelmaking. *Ironmaking and Steelmaking*, 13(**2**), 53–69.

STRUCTURE AND STRENGTH PROPERTIES OF BRAZED JOINTS OF JS26NK CAST NICKEL ALLOY Part 2*

V.V. KURENKOVA[2], **E.V. ONOPRIENKO**[2], **I.S. MALASHENKO**[1], **A.F. BELYAVIN**[1] and **L.V. CHERVYAKOVA**[2]
[1]Research Center «Pratt and Whitney Paton», Kiev, Ukraine
[2]E.O. Paton Electric Welding Institute, NASU, Kiev, Ukraine

Materials science problems of formation of brazed joints in the JS26NK cast nickel alloy are considered. Physical-chemical properties of brazed joints, produced with application of standard boron-containing brazing alloy and brazing alloy containing silicon as second depressant, and different binders are presented. It is shown that application of a binder in the form of solution of acrylic acid in acetone is efficient in case of application of complex brazing alloys containing 20 % of the Ni–12 % Si (NS12) commercial brazing alloy powder. Achieved at room temperature strength and fracture toughness of a brazed joint from the JS26NK alloy exceed similar characteristics of the JS26VI alloy. Connection of mechanical properties of brazed joints with direction of dendrite growth in the metal being brazed is shown.

Keywords: brazing in vacuum, JS26NK cast alloy, complex boron- and silicon-containing brazing alloy, NS12 brazing alloy, brazed joint, hardness, elongation, failure, structure, fusion line

Deformation process is often brought under laboratory conditions to uniaxial extension. The most interesting results, registered at such action on the investigated joints, are abnormal tensile properties and character of strain hardening of a specimen, whereby main attention has to be paid to elongation of the specimen [8].

Multiphase character of the brazed joint metal structure and shrinkage microporosity are main reasons of premature failure of brazed joints (BJ) in loading. Type of the fracture and microstructure of the specimen in locus of failure are main sources of information of the BJ being investigated [9, 10].

In making analysis of the brazed structure failure, when it was necessary to find locus of failure in the seam, heat-affected zone or base metal, both parts of the failed specimen were investigated, because work with just one half of the fracture is ineffective.

Fractography of tensile BJ specimens. Strain hardening curves (see Figures 4 and 5 in No.4, 2007) of BJ are supplemented with results of the fractography investigation of fractures of respective specimens [11]. Character of deformation of the specimens is stipulated by different crystallographic orientation of dendrites in structure of the brazed metal. This is confirmed by pictures of failure, presented in Figures 10–12, obtained on longitudinal microsections of BJ specimens of the JS26NK alloy of directed solidification (DS). Fracture character of the specimens was connected with chemical composition of brazing alloys, used at first stage of the investigations (Table 4).

Different character of two types of the strain hardening curves of the BJ specimens, formed with application of brazing alloy #1 + 20 % NS12 + 60 % Rene-142 (see Figure 4) [11], is confirmed by the fractographic analysis data of typical Z1 and Z5 specimens (Figure 10, *a–d*). Failure in these specimens with sufficiently high value of ultimate tensile strength (1065–1067 MPa) and relatively low yield strength (i.e. maximal strain hardening) occurred in the base metal.

In fracture of the Z5 specimen tough structure of the base metal was detected with clear direction of growth of branches of main dendrites (Figure 10, *b*). On surface of the fracture axes of dendrites had clear single directedness and loss of orientation in relation to main direction of applied load.

One may judge by structure of the base alloy on picture of failure and microstructure of the brazed seam in plane of applied load about possible crystallographic orientation of dendrites in the Z5 specimen, corresponding to <111>. Steepness of strain curves of Z5 and Z1 specimens confirms existence of this orientation.

Trajectory of main crack propagation in the Z5 specimen passes over boundaries of dendrites of 2nd and 3rd order (i.e. over interdendrite carbide phases). BJ failure originated in surface of end part of the flat specimen and propagated over interdendrite spaces of adjacent dendrites of 2nd order.

In this case width of the formed seam did not exceed 250 μm. High quality of the BJ with minimal amount of secondary carbide phases in matrix solution was noted. In specimens with <111> orientation insignificant development of the diffusion zone was reg-

*Part 1 see in No.4, 2007.

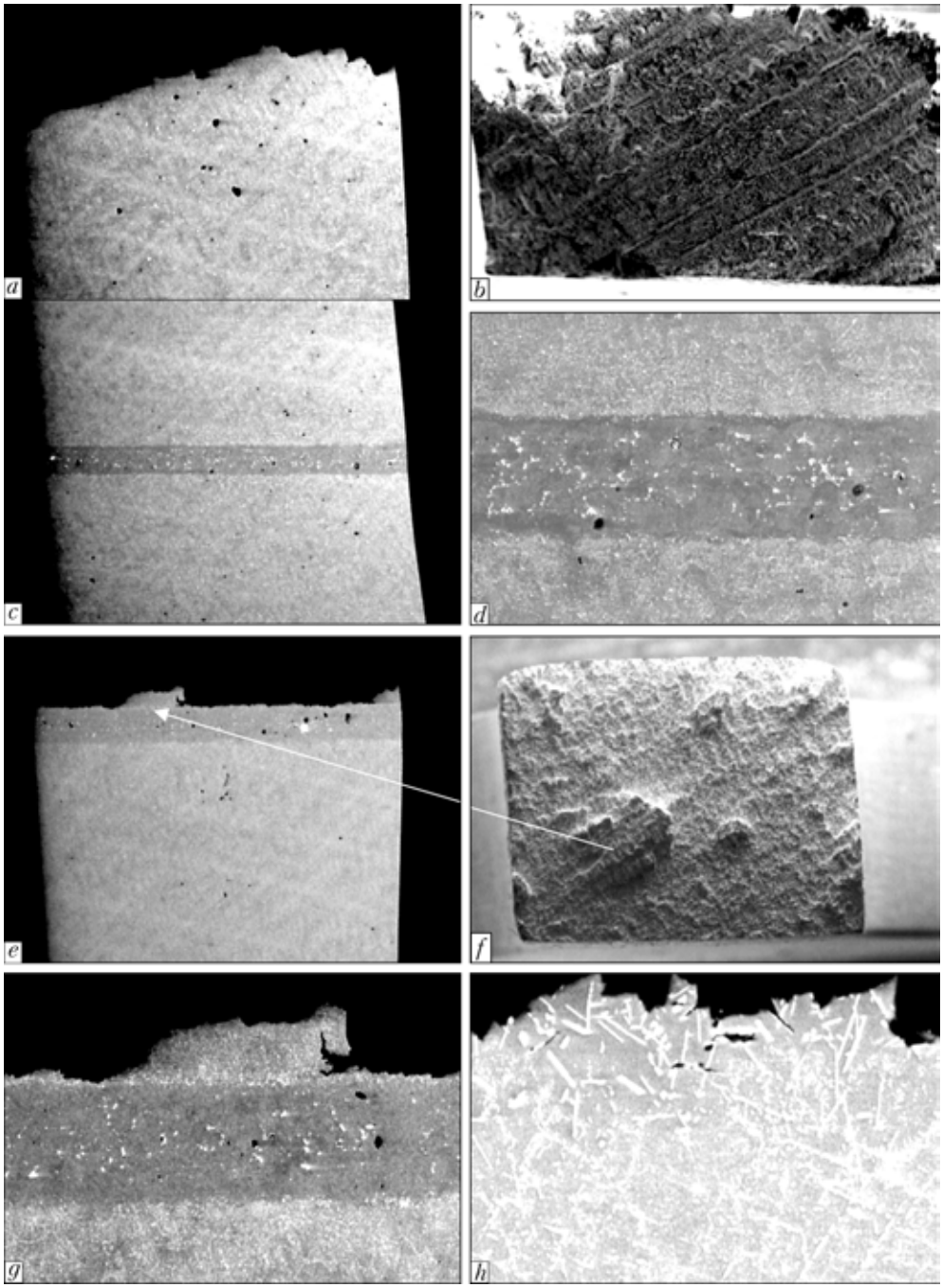

Figure 10. Picture of fracture of BJ specimens, formed with application of 20 % NS12 + 20 % #1 + 60 % Rene-142 complex brazing alloy, of JS26NK alloy of different crystallographic orientation: *a–d* — specimen Z5 with <111> orientation (σ_t = 1065 MPa, ε = = 23 %); *e–h* — Z3 with <111> orientation (σ_t = 823 MPa, ε = 17.3 %); *a*, *b*, *e*, *f* — fractography of failure of specimens (×50); *d*, *g* — BJ microstructure (×100)

istered. Course incising carbide phases were completely absent in the seam at boundary of fusion with the base metal. Quality of BJ in the considered experiment was guaranteed by fulfillment of full heat treatment cycle, including high-temperature ageing at 1050 °C for 4 h. The heat treatment ensured full diffusion interaction of solidified brazing alloy with the base metal and refining of secondary phases in the seam body and at the interphase boundary. This allowed uniform redistributing of applied load within the brazed seam volume.

Another type of failure had Z3 and Z9 specimens. These BJ are peculiar for minimal disperse hardening, and strain curves had sufficiently flat character, whereby yield strength achieved 657–674 MPa and ultimate strength — 760–823 MPa. Failure of the Z3 specimen, produced by the complex brazing alloy (with silicon), occurred over fusion line and went deeper into the base metal (see Figure 10, *e–h*). On pictures of failure direction of growth of dendrites in the brazed metal is registered.

Trajectory of the crack propagation demonstrates good connection between metal to be brazed and seam metal. The diffusion zone in case of other orientations of growth of dendrites in the BJ specimens is more developed (has significant width and contains big

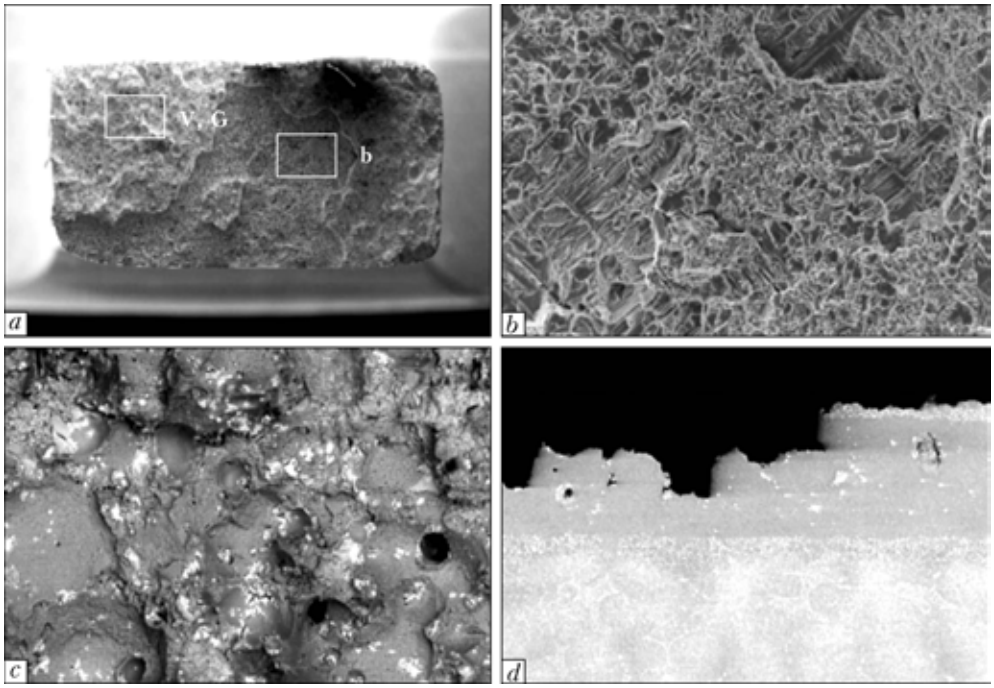

Figure 11. Fractography of brittle fracture of specimen Z11 formed with application of 20 % NS12 + 20 % #1 + 60 % Rene-142 complex brazing alloy: *a* — general picture of failure (×50); *b*, *c* — passage of main crack over base metal and diffusion zone respectively (×200); *d* — trajectory of specimen failure over fusion line (×100)

amount of secondary hardening phase, in particular acicular Me_6C carbides characterized by incising properties under loading).

So, in the BJ specimens in case of <111> orientation failure occurred mainly in the base metal over the diffusion zone. Formed seam in the Z3 specimen had quality structure with minimal amount of carbide phases. Available discrete microporosity did not enable formation of microcracks in the seam under loading. General relative elongation of BJ, equal to 17.3 %, proved high density of the seam metal, determined by parameters of brazing and conditions of the finish heat treatment. Big elongation of BJ is connected, in our opinion, with the fact that in test of the joint coincidence of direction of preferential growth of dendrites with the applied load vector was registered. Failure of the specimen is caused by cracking of the acicula-like carbide phase near the fusion line (see Figure 10, *h*).

General pattern of brittle fracture of the Z11 BJ specimen of the JS26NK alloy actually at the yield strength ($\sigma_{0.2}$ = 613 MPa, σ_t = 615.8 MPa, ε = 0.85 %) is reflected on longitudinal microsection (see Figure 11 *a*, *b*). This specimen is an exception from general pattern of fracture of the BJ specimens, formed with application of brazing alloy #1 + 20 % NS12 + 60 % Rene-142. At small width of the natural gap (up to 200 μm) and relative homogeneity of the brazed seam results of mechanical tests turned out to be rather low. In the failure transcrystalline fracture over seam metal and diffusion zone was combined with tough fracture of the base metal (see Figure 11, *a*, *d*). The crack propagated over carbide phase in the seam body and fusion line on side of the seam metal (see Figure 11, *d*).

Seam metal and base alloy had good cohesion bond due to development of the diffusion processes at the interphase boundary in finish heat treatment (ageing at 1050 °C). Microporosity, detected in the fracture, turned out to be one of the reasons of reduced BJ strength due to weakening of free cross-section area of the seam in case of extension of the specimen. Mainly intergranular character of failure is stipulated by precipitation of excessive carbide phases over boundaries of the seam grains. Trajectory of failure covers the brazed metal, which is proved by tough fracture, containing elements of brittle fracture that include skeleton-like interdendrite carbide phases over boundaries of axes of 2nd and 3rd order (Figure 10, *c*).

In case of application of the base boron-containing brazing alloy #1 + 60 % Rene-142, results of mechanical tests were satisfactory.

Strength, as well as ductility of BJ, depends upon filling of the gap (density of the seam metal). If the gap is wide, greater volume of metal solidifies with formation of shrinkage microporosity and even looseness. Such dependence is especially clearly seen when classic system of brazing alloy #1 + 60 % Rene-142 with a higher toughness in comparison with silicon-containing brazing alloys is used. In this case seam metal is a weak place in the BJ specimen, and fracture in case of uniaxial extension occurs in it. This is illustrated by the fact that at the minimal 125 μm gap in the Z8 specimen maximal 23 % elongation was achieved. Load curve of this specimen proves its monotonous strain hardening and correspondence of growth of the dendrites of <111> orientation (see Figure 5). Picture of the Z8 specimen failure demonstrates dendrite structure of the specimen material,

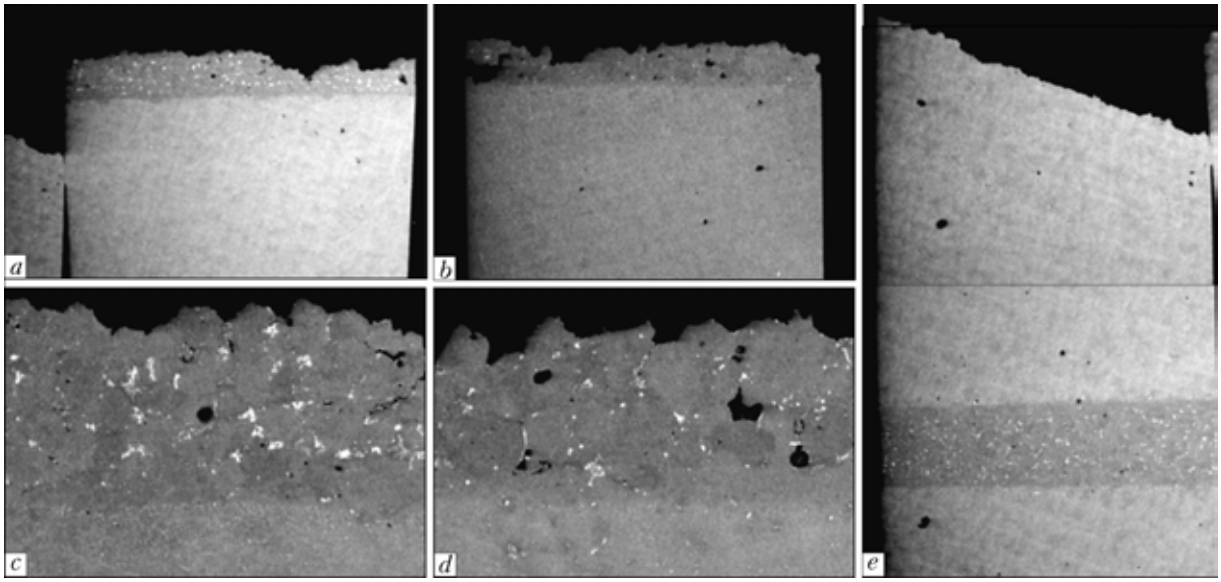

Figure 12. Typical microstructures of fracture surface of BJ specimens, formed with application of 20 % NS12 + 20 % #1 + 60 % Rene-142 complex brazing alloy, at different directions of cutting out of NK billet: *a*, *c* — longitudinal over fusion line (×50; ×100); *b*, *d* — cross over seam metal (×50; ×100); *e* — cross (over base metal) (×23)

direction of which coincided with long of the specimen axis (see Figures 7, *g* and 13, *c*).

Peculiarity of the considered specimen is the fact that its natural gap was minimal in comparison with the rest ones (see Table 1). Due to this structure of the seam metal had high degree of homogeneity — secondary carbide phases were practically absent in it (see Figures 11, *d* and 13, *c*). At high toughness of classic brazing alloy #1 + 60 % Rene-142 application of its minimal volume share in the gap and finish annealing at 1050 °C within 4 h allowed obtaining structure of the brazed seam with satisfactory characteristics of strength and ductility of the joint close to the ideal one.

In absence of secondary phases in the seam main crack in case of failure propagated mainly over diffusion zone in the fusion area (see Figure 11, *a*, *c*). Wavy relief of the fracture surface is connected with oriented growth of dendrites, when a grain body elongates in direction of the acting load, and interphase base–brazing alloy boundary is strengthened by precipitates of secondary carbide or carboboride phases, which make easier transfer of plastic flow of the matrix through boundary from grain to grain.

Typical for the BJ specimens, formed with application of the base brazing alloy #1 + 60 % Rene-142, was transcrystalline or intergranular failure over the solidified seam metal. By means of growth of volume share of a rather tough complex brazing alloy and the gap width from 225 to 400 μm, heterogeneous structure of the seam with different kinds of secondary hardening phases was formed.

These brittle phases acted as stress concentrators in the tests. This is confirmed by fractography of the Z6 specimen fracture with 1.2 % elongation and ultimate strength 822.3 MPa (see Figure 7, *b*, *f*, *h*). Fracture occurred over interdendrite areas of the seam metal, where precipitation of phases was registered, consisting of enlarged carbide particles (see Figure 7, *d*). Picture of similar brittle fracture of the Z0 specimen with zero ductility is illustrated by the diagram of its extension (see Figure 5) [11].

So, in case of application of base brazing alloy #1 + 60 % Rene-142 in brazing of the JS26NK alloy fracture of the BJ specimens in tensile tests occurred mainly over solidified seam metal because of their more pronounced multiphase character (see Figure 13, *d*).

In case of application of brazing alloy #1 + 20 % NS12 + 60 % Rene-142, BJ failure occurred most frequently over the base metal or line of fusion with it. At relative homogeneity of the seam metal and minimal content of secondary phases in the seam, front of failure in the tests shifted into the diffusion zone area, where after high-temperature ageing disperse carbide phases and carbides of acicular type in a limited amount precipitated from the solution during cooling.

At second stage of the investigations when width of the natural gap was increased the BJ specimens, formed with application of complex brazing alloy #1 + 20 % NS12 + 60 % Rene-142, had rather stable mechanical properties irrespective of direction of growth of dendrites in the brazed billets (see Table 1) [11].

Longitudinal specimens had insignificant strain hardening and relative elongation within 3.9–5.5 % (see Table 1). For these specimens developed diffusion interaction between the base being brazed and the seam metal is characteristic as a result of annealing at 1050 °C within 5 h (see Figure 12, *a*, *b*). The specimens mainly failed over the BJ fusion line. Diffusion processes at the boundary are connected with direction of growth in the specimen billets and crossing by the forming brazed joints of boundaries of the growing dendrites, which are favorable places for progress of metathetical processes in the cast alloy.

In case of cross specimens, when the formed brazed joints are parallel to axes of dendrites in the billets,

Table 4. Chemical composition of different phases in metal of BJ seams produced with application of two kinds of brazing alloys in process of isothermal brazing after tests at 950 °C

System of brazing alloy	Analysis spectrum	Weight share of components, %													
		Si	C	Al	Ti	V	Cr	Co	Ni	Nb	Mo	Hf	Ta	W	Re
#1 + 60 % Rene-142	1	–	2.74	5.10	0.87	0.98	5.01	8.66	60.59	0.73	0.64	–	–	13.11	1.57
	2	–	2.21	5.54	–	–	8.36	10.44	63.47	–	0.88	–	2.58	4.80	1.73
	3	–	1.82	5.23	–	–	8.04	12.02	65.37	0.14	0.75	–	3.01	3.24	0.37
	4	–	6.86	3.83	0.34	–	2.29	4.44	41.88	0.62	0.06	14.33	23.10	1.54	0.71
	5	–	3.47	4.64	–	–	8.83	11.57	63.58	0.25	0.67	0.21	2.45	2.79	1.52
	6	–	5.68	2.65	–	–	7.79	9.38	47.02	0.54	0.67	10.34	13.54	1.84	0.54
	7	–	3.66	–	–	–	48.69	4.75	4.99	0.13	5.46	–	0.14	12.99	19.20
	8	–	3.80	1.47	–	–	22.33	5.18	17.45	–	8.05	–	5.36	28.55	7.79
	9	–	3.58	0.22	–	–	47.18	4.41	5.16	–	5.44	–	–	14.42	19.60
	10	–	4.09	4.64	0.47	0.78	5.34	8.63	55.31	0.70	1.33	–	–	17.90	0.81
	11	–	4.01	–	–	0.43	28.80	4.31	7.74	–	10.88	–	4.21	30.51	9.10
#1 + 20 % NS12 + + 60 % Rene-142	1	–	1.55	5.16	0.93	0.96	4.77	8.82	61.80	1.44	0.94	0.45	–	12.00	1.23
	2	–	3.19	6.91	1.86	0.77	2.11	7.24	67.50	3.16	0.71	–	–	6.59	–
	3	1.25	2.42	4.67	–	–	7.29	10.80	65.80	–	0.38	–	2.33	3.58	1.43
	4	1.92	3.08	4.73	–	–	7.20	10.30	65.70	–	0.68	–	2.29	2.82	1.29
	5	–	4.83	–	–	0.41	23.10	3.00	6.27	0.75	12.60	–	4.03	33.20	11.80
	6	–	5.63	–	–	–	24.00	2.73	5.98	–	10.10	4.05	13.00	21.30	13.10
	7	–	3.94	3.72	0.38	0.50	5.05	8.29	51.40	0.67	1.43	–	2.87	20.60	1.19
	8	–	3.96	3.92	0.29	–	5.83	9.54	55.60	0.40	1.50	–	4.12	13.00	1.82
	9	1.36	3.02	4.54	–	–	6.92	9.57	65.10	–	0.65	–	3.31	3.73	1.80

a limited diffusion interaction was detected between the metal being brazed and the brazing alloy. This may be explained by the fact that the solidified seam metal contacts mainly with axes of dendrites of 1st order, because the brazed joint is parallel to the growing dendrites, whereby direct contact of the seam metal with boundaries of main hydrides is weakened. That's why in case of tensile testing of the cross specimens the occurring crack passes either over defects of the seam metal (microporosity) (see Figure 12, *c, d*) or over the base metal (see Figure 12, *e*). In the latter case influence of a wide natural gap is compensated by reduced toughness of the silicon-containing brazing alloy, good filling of the gap, and flawless quality of the seam being formed.

In tests of the cross specimens small reduction of yield strength was noted (down to 681–752 MPa), ultimate strength being 766–927 MPa. Insignificant growth of strain hardening of the base metal in comparison with longitudinal samples was also registered (see Figure 7).

Increase of the natural gap width in the BJ specimens did not exert significant negative influence on quality of the formed brazed seams and mechanical characteristics thereof (see Table 1). In case of the gap width increase up to 630–780 μm, in BJ σ_t = = 890.0–926.8 MPa (specimens Nos. 14 and 17) at relative elongation 9.5–10.5 % (see Table 1).

Comparison of fracture pictures of the JS26NK alloy BJ specimens, produced with application of different brazing alloys, tested at 950 °C (Figure 14), showed that their general feature is high cohesion strength of the seam metal and the metal being brazed in comparison with strength of central (axial) part of the seam. BJ failure occurred over the seam metal, but in case of a standard bi-component brazing mixture, when a seam contained course carbide phase, the metal disintegrated into separate grains, demonstrating noticeable weakening of the boundaries at high temperature. At the same time the seam, formed from the complex brazing mixture, which included silicon, showed an increased density and higher strength of BJ, combining transcrystalline fracture with intergranular one. This was ensured by a higher dispersiveness of the carbide phase and reduction of weight share of boron in the seam metal in comparison with the first case. Smaller size of the hardening phase over the boundaries creates prerequisites for formation of small microvoids around the particles.

So, character of failure of BJ, produced by the high-temperature brazing method, is in direct dependence upon phase composition of the seam metal, determined by its heat treatment.

In the solidified seam metal, formed with application of the #1 + 60 % Rene-142 composite boron-containing brazing alloy, after multistage heat treat-

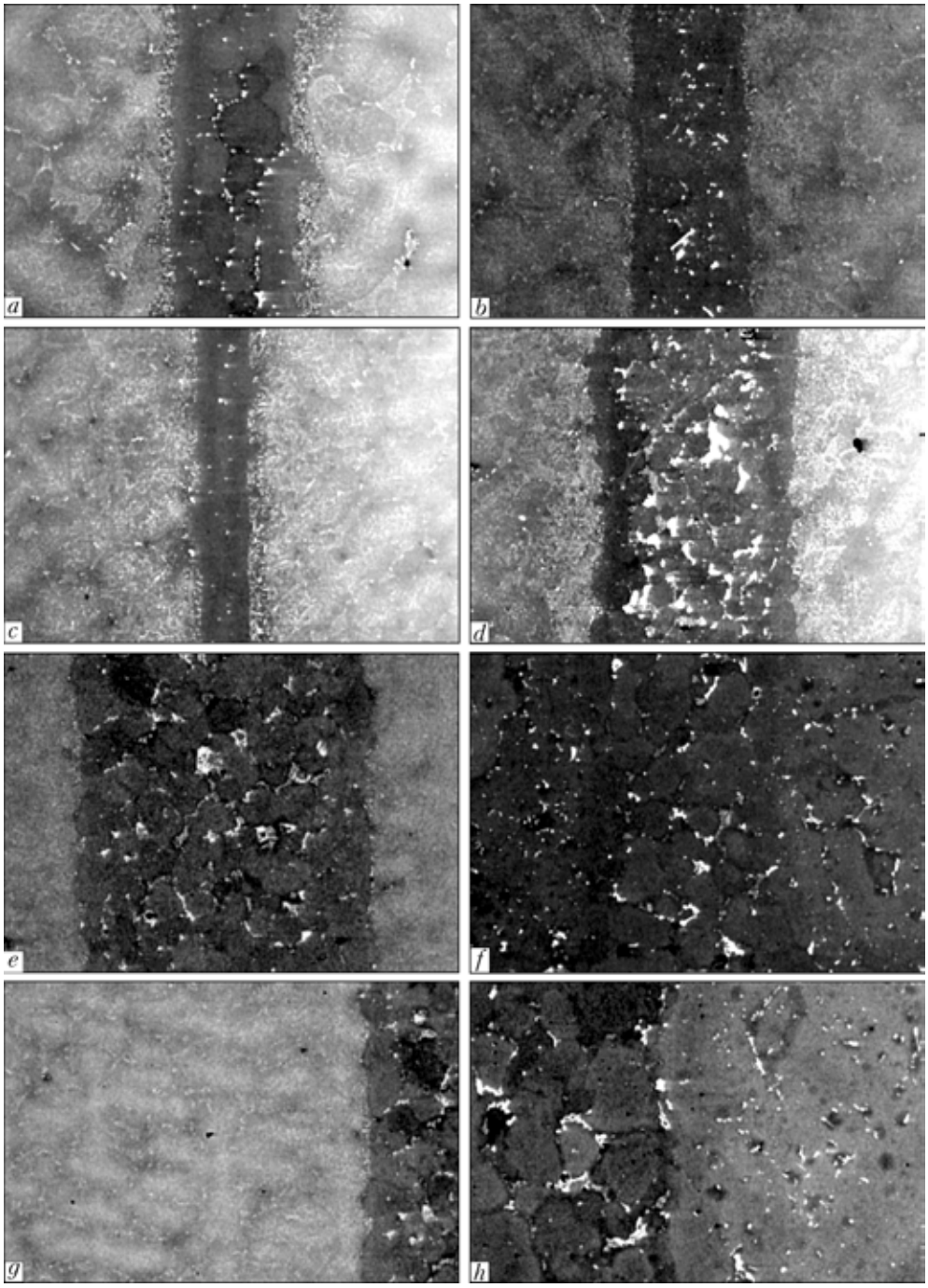

Figure 13. Typical microstructures (×100) of BJ specimens formed with application of complex 20 % NS12 + 20 % #1 + 60 % Rene-142 (*a*, *b*, *e*–*h*) and standard 40 % #1 + 60 % Rene-142 (*c*, *d*) brazing alloys: *a*, *b* — specimens Z9 with <111> orientation and Z5 with <111> orientation (*c*, *d*); *e* — specimen Z18 cut out in cross direction; *f* — specimen Z20 cut out in longitudinal direction; *g*, *h* — diffusion zone in BJ in case of cross and longitudinal cutting out of specimens, respectively

ment boundary course carbide phases of the $Me_{23}C_6$ type on basis of chromium, tungsten, molybdenum, rhenium and phases of eutectic type, corresponding to the Me_6C formula with maximum content of tungsten (up to 30 %), are available (see Table 4 and Figure 15).

In case of application of silicon-containing brazing alloy with 20 wt.% NS12, content and structural diversity of secondary phases in the solidified seam metal sharply reduce. They are represented manly by rare Me_6C carbides on basis of tungsten, molybdenum, rhenium and disperse MeC carbides on basis of hafnium, tantalum and tungsten (see Table 4 and Figure 15).

Discussion of the results obtained. Quality of BJ, determined by continuity of the seam, depends upon intensity of the molten metal feeding to the interdendrite areas in those parts of the joint, where process of solidification has already started. Continuity is achieved when conditions of full flowing through the gap of the brazing alloy melt, under which solidification terminates, are ensured. Density (quality) of the metal is determined by optimal values of temperature of the isothermal brazing process and rate

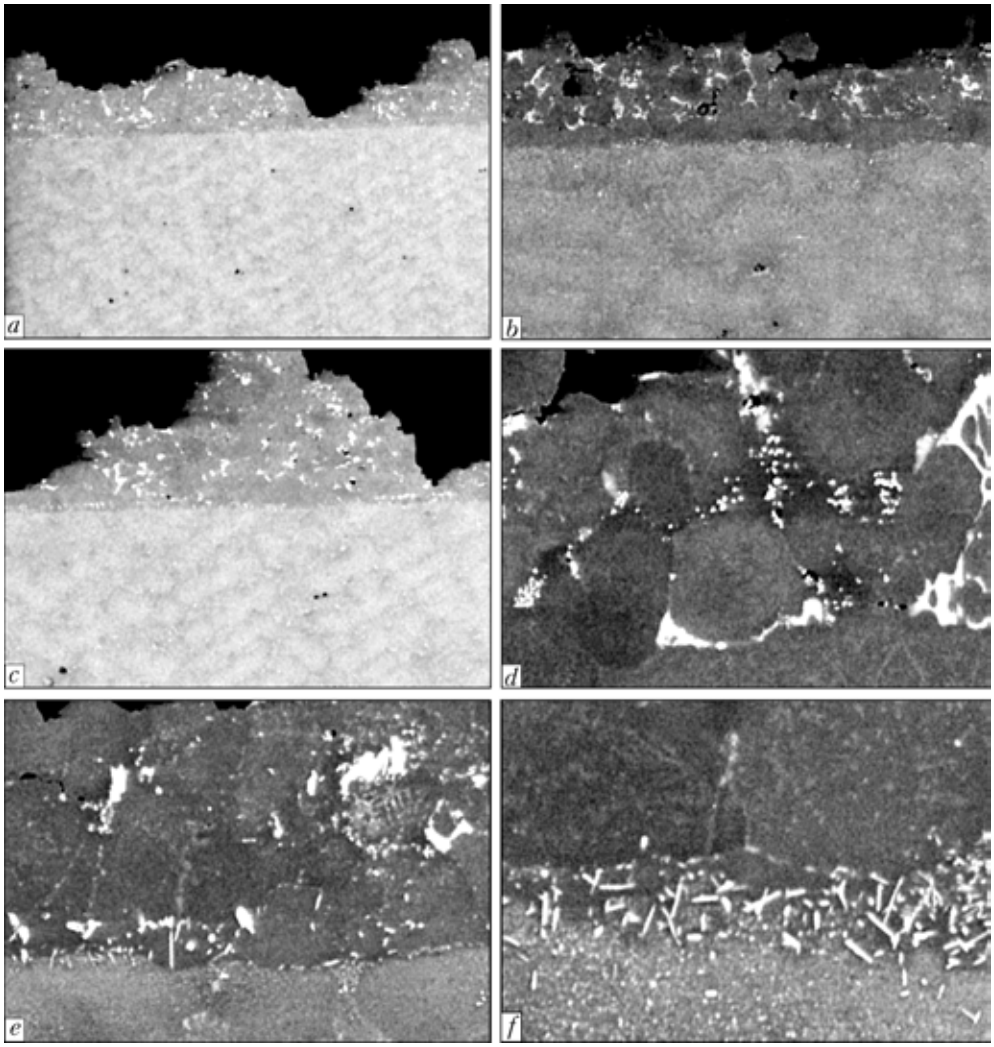

Figure 14. Character of fracture of seam metal of JS26NK alloy BJ produced with application of standard #1 + 60 % Rene-142 (*a*, *c*, *e*) and complex #1 + 20 % NS12 + 60 % Rene-142 (*b*, *d*, *f*) brazing alloys at 950 °C: *a* — ×50; *b*, *c* — ×100; *d*, *e* — ×500; *f* — ×1000

of hardening (solidification) of the formed seam, which ensure completeness of phase transformations, occurring in the seam metal.

Process of brazing of the directed solidification alloy does not provide single-crystal or oriented structure in the seam metal. However, crystallographic orientation of grains in the seam metal may be repeated, when direction of growth in the base metal is clearly pronounced in relation to the BJ seam being formed.

Chosen conditions of isothermal brazing of specimens from the JS26NK alloy allowed forming BJ of good quality with minimal number of microdefects in seams at different natural gaps (see Figure 13).

It was found at the first stage that the joints, produced with application of complex (silicon- and boron-containing) brazing alloy #1 + 20 % NS12 + 60 % Rene-142, had denser homogeneous structure of the seam metal (see Figure 13, *a*, *b*) than in case of application of the #1 + 60 % Rene-142 brazing alloy (see Figure 13, *d*). In first case amount of secondary carboboride phase in the seam reduced, grain has refined, and intergranular complex alloyed eutectics were absent. The #1 + 60 % Rene-142 brazing alloy enabled formation of cellular solidification with structurally developed interdendrite areas.

Two-stage conditions of heat treatment after brazing, which included homogenization at 1160 °C and high-temperature ageing at 1050 °C for 4 h, reduced structural inhomogeneity of the seam metal, enabled development of the diffusion metathetical processes at the brazed metal–brazing alloy boundary and thus ensured higher level of strength and plastic properties of the joints. Development of mutual diffusion of components on fusion line of BJ is pledge of their high strength. In tensile tests failure of the specimens mainly occurred over the diffusion zone, containing, in addition to fine disperse carbide phases, Me_6C phases of acicular type, which affect with their «incisivezz» morphology process of origination and propagation of a crack in BJ.

It is determined that optimal chemical composition of a brazed seam metal after homogenization annealing and high-temperature ageing, which ensures high functional parameters of BJ, is the following, wt.%: Ni (base)–(11.2–12.4) Co–(6.3–6.7) Cr–(4.2–4.6)

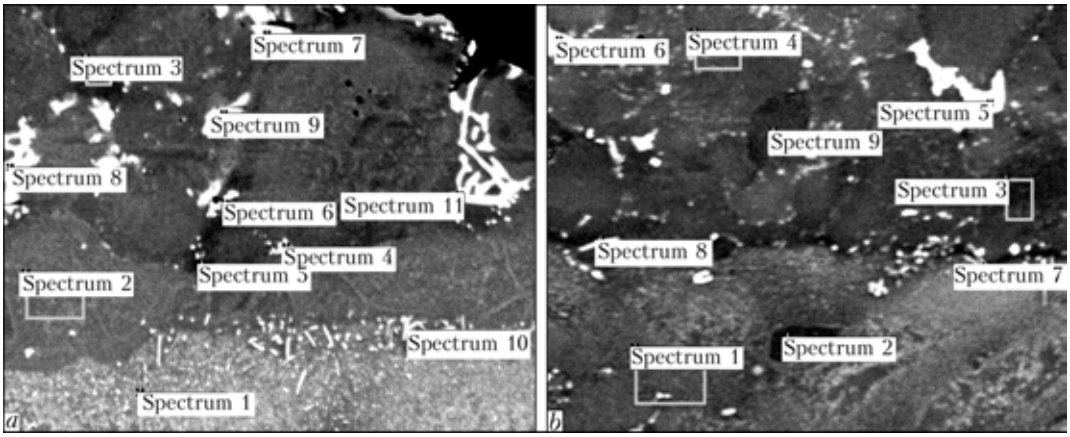

Figure 15. Areas of X-ray spectral microanalysis of separate phases, which constituted seam metal after BJ tests at 950 °C (see Table 4), ×500: *a* — #1 + 60 % Rene-142; *b* — #1 + 20 % NS12 + 60 % Rene-142 brazing alloy

W–(1.0–1.3) Mo–(2.9–3.5) Ta–(0.5–0.7) Nb–(3.5–4.3) Al–(1.2–1.5) Re–(0.7–0.8) Si–(0.6–1.0) Hf–1.0 B–0.12 C.

For avoiding formation of developed multiphase diffusion zone, at second stage of the tests time of annealing at 1050 °C was increased up to 5 h, which allowed avoiding formation of the diffusion zone with acicular carbide phases. On the microstructures smooth transition from matrix solution of the seam metal to matrix of the base alloy was detected (see Figure 13, *e, f*).

Width of the natural gap of the formed brazed joint did not effect development of the diffusion zone at the interphase boundary. Difference was registered only in the BJ specimens in second series of the experiments with different (longitudinal or cross) direction of cutting of the billets.

In longitudinal specimens direction of growth of dendrites was perpendicular to the brazed seam axis. Crossing of the array of the directing dendrites and subsequent contact of the incision surface with the brazing alloy melt ensured penetration of liquid phase over boundaries of butted dendrites of 1st order. Thermal diffusion interaction of the molten brazing alloy with the metal being brazed ensured satisfactory level of BJ strength and development of mutual diffusion in longitudinal specimens (see Figure 13, *f, h*). Diffusion proceeded without formation of course carbide phases or carboboride barriers. Distribution of components in separate zones of BJ was determined by X-ray spectral microanalysis. Width of the mutual diffusion zone was, approximately, 180–250 μm.

In cross specimens, where direct contact of the brazing alloy molten metal with boundaries of dendrites of 1st order was absent (the seam is parallel to direction of growth of dendrites), mutual diffusion processes proceeded feebly at the depth up to 30 μm (see Figure 13, *g*).

Fine (γ–γ')-microstructure of main BJ zones, produced with application of #1 + 20 % NS12 + 60 % Rene-142 brazing alloy, is presented after finish heat treatment in Figure 16. Uniform precipitation of hardening γ'-phase in the seam metal, diffusion zone, and metal being brazed was detected (Figure 16, *a*, *c*, *e*, *h*). In the course of homogenization partial dissolution of primary γ'-phase occurred in the base, and during cooling (together with the furnace) — its precipitation from solid solution of hardening γ'-phase. In the course of subsequent ageing at 1050 °C for 4 h the precipitated hardening phase enlarged, and in the process of cooling additionally precipitated disperse γ'-phase from the matrix γ-solution (Figure 16, *c*).

In long-term ageing share of the supersaturated matrix solution exceeded share of γ'-phase both in the base metal, diffusion zone, and over axes of dendrites of the alloy being brazed.

In high alloy diffusion zone at the seam–JS26 alloy interphase boundary at temperature of ageing in solid solution, carbides of Me_6C type have formed in the form of plates (aciculae) in the places enriched with tungsten. Such morphology of carbides and their edging by the pellicle γ'-phase prove beginning of carbide transformations in high alloy matrix at the interphase boundary (Figure 16, *g*).

Variation of the finish heat treatment conditions (at second stage of the experiment) caused change of the BJ (γ–γ')-microstructure. So, in the base metal growth of the volume share of hardening phase of clear cubic shape and smaller size (up to 0.2–0.7 μm) was detected (Figure 16, *d*). Content of γ'-phase increased both in the seam metal and in the diffusion zone (Figure 16, *f, h*), whereby size of the latter reduced.

In second series of the experiments after homogenization at 1160 °C and cooling with furnace the BJ specimens were not removed from the furnace, but were soaked at 650–700 °C within 10 min, which might affect stability of precipitated from the matrix solution stoichiometric γ'-phase, which in the course of further ageing was less subjected to dissolution and preserved primary shape of the particles. Increase of the ageing duration up to 5 h increased diffusion of components at the boundary, but did not create premises for transition of the alloying elements from joints into the matrix solution and progress of subsequent processes of carbide formation at the fusion line.

Me_6C carbides, formed at the saturated with alloying elements high-alloy interphase boundary, ex-

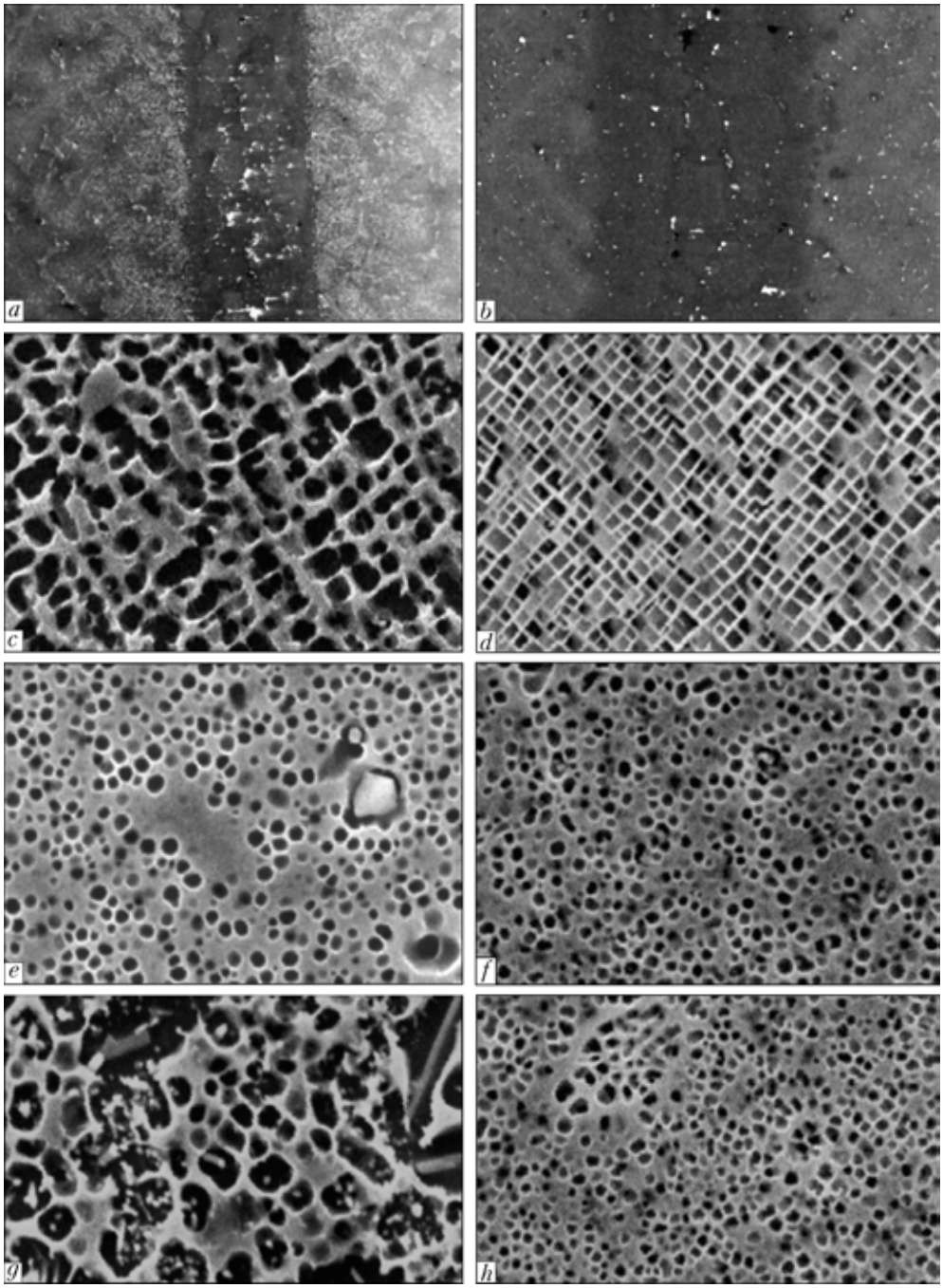

Figure 16. Peculiarities of BJ (γ–γ')-microstructure under different conditions of finish heat treatment: *a*, *c*, *e*, *g* — ageing at 1050 °C for 4 h; *b*, *d*, *f*, *h* — ageing at 1050 °C for 5 h with preliminary soaking in vacuum at 700 °C (10 min); *a*, *b* — general appearance of seams after different finish heat treatments; *c*, *d* — precipitates of γ'-phase in base metal; *e*, *f* — in seam metal; *g*, *h* — in diffusion zone

erted harmful influence on fatigue properties of the alloy being brazed. Increase of the high-temperature ageing duration and stabilization of stoichiometric γ'-phase enabled intensification of the mutual diffusion processes and reduction of content of strongly segregating elements (tungsten, titanium, niobium, hafnium and rhenium) at the base–brazing alloy boundary, and this, in its turn, prevented formation of plastic (acicular) carbide phases of the Me_6C type.

Refining of hardening γ'-phase and increase of its volume share in γ-solution enabled increase of yield strength of the alloy being brazed and small reduction of its ductility.

High dispersity of γ'-phase in the alloy being brazed ensured higher yield strength of BJ of the specimens at second stage of the investigations. For example, yield strength of the Z23 BJ specimen was 803 MPa, while that of the Z1 specimen was 652 MPa (Figure 16).

CONCLUSIONS

1. Materials science fundamentals of high-temperature brazing of the JS26NK high-temperature nickel alloy with application of standard boron-containing Ni–Co–Cr–Al–2.5 % B brazing alloy, silicon-containing NS12 brazing alloy (20 wt.% Si) and 60 wt.% of

filler in the form of powder of the Rene-142 alloy were developed.

2. It was shown that stable strength of BJ of the JS26NK alloy, produced with application of the NS12 complex brazing alloy, exceeded strength of the JS26VI joints after similar heat treatment. Difference consisted only in the fact that in case of the NK alloy duration of high-temperature ageing was 4–5 h, while in case of the JS26VI alloy — 2 h. Maximal BJ strength value was 1067 MPa, relative elongation — 15–23 %.

3. Application of the complex brazing alloy, in which simultaneously boron and silicon were used as the depressant, allowed producing BJ, characterized by stably high values of ultimate strength and relative elongation in comparison with BJ, produced with application of the #1 + 60 % Rene-142 base brazing alloy.

4. It was found that in case of coincidence of the dendrite growth direction with vector of the applied load, strength of the specimens and their ductility depended upon crystallographic orientation of growth of dendrites in the NK alloy.

5. It was shown that BJ mechanical characteristics of the JS26NK alloy, determined on the specimens cut out both along and across of the dendrite growth direction, are close at room temperature. Yield strength of longitudinal specimens is somewhat higher than that of the cross specimens.

6. Application of the #1 + 20 % NS12 + 60 % Rene-142 complex brazing alloy allowed producing high-strength flawless BJ of the JS26NK alloy with natural gap 400–780 MPa at the brazing temperature 1225 °C (15 min).

7. The weakest place in case of extension of the BJ specimens of the JS26NK alloy is fusion line, in which segregations of carboboride phases and Me_6C carbides of acicular shape was detected. Heat treatment (ageing at 1050 °C, 4–5 h) allows forming BJ structure with uniformly distributed hardening γ'-phase. In case of increase of its volume content growth of yield strength of the BJ metal was registered.

8. Balter, M.A., Lyubchenko, A.P., Aksyonova, S.I. et al. (1987) *Fractography as a mean of diagnostics of fractured parts*. Moscow: Mashinostroenie.
9. (1982) *Fractography and atlas of fractograms*: Refer. Book. Ed. by J. Fellous. Moscow: Metallurgiya.
10. Engel, L., Klingele, G. (1986) *Scanning electron microscopy. Fracture*: Refer. Book. Ed. by M.L. Bernshtejn. Moscow: Metallurgiya.
11. Malashenko, I.S., Kurenkova, V.V., Belyavin, A.F. et al. (2007) Structure and strength properties of brazed joints of cast nickel alloy JS26NK. Part 1. *Advances in Electrometallurgy*, **4**, 31–38.

IMPROVEMENT OF STRUCTURE AND PROPERTIES OF CAST FERRITE-PEARLITE STEELS FOR TRANSPORT MACHINE BUILDING

A.V. RABINOVICH[1], **Yu.A. BUBLIKOV**[2], **G.N. TREGUBENKO**[2], **G.A. POLYAKOV**[2], **A.V. PUCHIKOV**[2] and **Zh.A. DEMENTIEVA**[2*]

[1]National Metallurgical Academy of Ukraine, Dnepropetrovsk, Ukraine
[2]Z.I. Nekrasov Institute of Ferrous Metallurgy, NASU, Dnepropetrovsk, Ukraine

Technology for complex modification of casting from low-alloy ferrite-pearlite steels by titanium, aluminium and nitrogen was developed, which ensures increase of the lower level of yield strength in normalized (≥ 380 MPa) and temper hardened (≥ 450 MPa) state, the rest requirements to mechanical properties of the 20GL steel being preserved.

Keywords: steel, casting, carbonitride hardening, titanium, aluminium, nitrogen, grain index, yield strength, impact toughness

Main task of freight railway car building is increase of the car run before the first planned repair from 100–120 to 500 thou km, whereby guaranteed service life of cast elements of the carriage and the car as a whole should be not less than 16 years before the planned repair, its full service life being up to 32 years [1].

An efficient measure for ensuring these requirements, in addition to new design solutions, is improvement 1.2–1.3 times of strength characteristics of metal of the railway car cast elements, first of all yield strength up to ≥ 380 MPa, the rest mechanical properties being not lower than the normative ones (according to the valid standards).

The simplest solution of this task is increase of degree of steel alloying by the elements, which form substitution solution with iron (silicon, manganese, chromium and nickel). Application of the latter is

*Student of the group TsM-03 of National Metallurgical Academy of Ukraine A.A. Katrich also participated in this work.

connected with significant rise in price of steel and need to make import purchases. Increase of content of just silicon and manganese, alloys of which are comparatively cheap and accessible in Ukraine, without taking additional measures is limited because of reduction of plasticity level, especially impact toughness of steel, and worsening of weldability. As a rule, content of silicon in these steels should not exceed 0.4–0.6 wt.%, its ratio with manganese being not more than 1:2 [2].

For refining of the grain and suppression of its growth during heating, including welding, modification of steel by its microalloying with nitrogen and elements characterized by increased affinity to it ---- mainly vanadium [3], less often niobium [4], is used. Disadvantage of such solution, in addition to very high cost of the microalloying elements, is relatively low thermodynamic strength of nitrides of these elements, dissociation of which occurs during heating in the process of heat treatment and in the near-weld zone in welding, which reduces effect of the grain refining.

In works of National Metallurgical Academy of Ukraine and the Z.I. Nekrasov Institute of Ferrous Metallurgy of the NAS of Ukraine, which concern production of rolled stock of broad size assortment, efficiency of replacement in steels modified by carbonitrides, of expensive vanadium and niobium by relatively low-cost and less deficient nitride-forming elements ---- titanium and aluminium [5], is shown, whereby possibility is established of achieving required properties of hot-rolled stock by alloying the carbonitride hardened (CNH) steel just by silicon and manganese without using chromium and nickel.

Adaptation of these principles of microalloying to casting in railway car building allows evaluating possibilities of ensuring requirements, established for cast elements of freight railway cars of new generation.

At present according to OST 32.183–2001, the 20GL steel and its modifications 20GFL, 20GTL and 20KhGNFTL are used for cast components of carriages of 1520 mm gauge double-axle freight railway cars (side frame and the above-spring beam). For achieving maximal strength of cast components of the freight car carriages, the 20GL steel is alloyed by chromium and nickel, which increase solid solution hardening of ferrite, and by vanadium and titanium, carbides of which enable dispersion hardening, whereby regulated level of the 20KhGNFTL cast steel yield strength ($\sigma_y \geq 373$ MPa) anyway remains somewhat lower than that established in new recommendations [1]. In addition, application of this steel is limited by very strict requirements in regard to content of phosphorus and sulfur (≤ 0.02 % for each element), which causes the need of prolonging both oxidation and reduction periods of melting, practically complete removal of phosphorus slag prior to the refining, increase of consumption of deoxidizers, lime and fluxes, and taking other technological measures.

In a number of works [6, 7] possibility of improving properties of the cast metal by its alloying with nitrogen in combination with titanium or aluminium is considered. However, selected level of content of these elements (up to 0.025; 0.150; ≥ 0.100 wt.%) causes significant reduction of the metal plasticity and increases inclination of steel to crack formation in the processes of manufacturing and operation of the castings. That's why we carried out investigations, directed at optimization of composition of the 20GL cast steel, complexly modified by titanium and aluminium nitrides.

Experimental melts were carried out in the IST-0.06 induction furnace with acid lining. The materials, used in melting of the 20GL steel in arc furnaces (wastes of the arc melted 20GL steel, the FS65 ferrosilicon, the MnC17 ferromanganese silicon; the FTi35 ferrotitanium; alumocalcium wire), were used as the charge in order to be closer to conditions of commercial production.

For introducing into the steel required content of nitrogen, the nitrogen-containing ALK master alloy, produced on the basis of the FMn78 standard ferromanganese, was used [8]. Content of the additive nitrogen-containing master alloy varied within 0.83–7.50 kg / t (0.05–0.45 kg per melting). Weight share of titanium, which is jointly with nitrogen one of the main hardening additives, in all experimental melts was increased in comparison with standard 20GL steel, and in majority of cases varied within 0.008–0.025 %. In a number of melts upper limit was increased for investigation purpose up to 0.07–0.11 wt.% [6, 7]. It should be noted that according to valid normative-technical documentation addition of deoxidizers and modifiers without limitation of their kinds and residual contents is allowed in melting of the 20GL steel for transport machine building. Content of the rest alloying elements, carbon and impurities was maintained within requirements of standards on the 20GL steel. Only in two melts content of silicon was somewhat increased (up to 0.72 wt.%) for getting static dependences of silicon content.

For getting comparable results, standard melting of the 20GL steel without addition of nitrogen-containing master alloy and ferrotitanium was carried out in addition to the experimental one.

Charging, which consisted completely of the 20GL steel wastes, was carried out in several stages by means of foundering and settling down of the loaded charge.

After full melting of the charge and soaking for the purpose of the melt preheating a sample was taken for analysis of the metal, and the required amount of ferromanganese silicon and ferrosilicon was consecutively added into the furnace. After a short soaking for full assimilation of the alloying elements, temperature was measured by means of an immersion thermocouple. Tapping temperature (approximately 1650 °C) was adjusted by means of soaking of the metal in the switched on furnace, assuming rate of

Chemical composition and results of tests of commercial 20GL steel modified by nitrides of titanium and aluminium

Series	Number of melts	Consumption of ALK, kg / t	Weight share of elements, %				
			C	Si	Mn	$Ti \cdot 10^4$	$Al \cdot 10^4$
I	1	0.83	0.19	0.53	1.33	46	72
II	11	1.25	0.17–0.22	0.33–0.78	1.18–1.50	8–24	19–52
III	1	2.50	0.20	0.42	1.35	60	60
IV	5	5.00	0.21–0.24	0.35–0.45	1.30–1.44	22–31	21–60
V	1	7.50	0.20	0.47	1.36	110	60
VI	1	–	0.22	0.38	1.29	2	23
Commercial melts	2314	–	0.17–0.24	0.20–0.60	1.05–1.50	≥4	10–82
OST 32.183–2001			0.17–0.25	0.30–0.50	1.10–1.40	–	20–60***

Table (cont.)

Series	Mechanical properties						
	After normalization*				After temper quenching**		
	σ_y, MPa	σ_t, MPa	KCU^{-60}, J / cm^2	Grain index	σ_y, MPa	σ_t, MPa	KCU^{-60}, J / cm^2
I	410 / 380	610 / 580	55–63 / 31–37	9, 10 / 8, 9	560 / 460	740 / 650	44–53 / 53–55
II	405–460 / 360–440	580–660 / 560–640	27–67 / 25–63	8, 9, 10 / 8, 9 (7)	520–580 / 440–530	680–690 / 620–700	40–65 / 31–56
III	410 / 370	610 / 610	37–50 / 36–41	9, 10 / 8	650 / 520	750 / 730	37 / 22–28
IV	415–470 / 390–440	610–660 / 590–630	19–51 / 25–50	10, 9 / 9, 8 (7)	495–540 / 480–510	660–690 / 600–660	45–59 / 27–55
V	440 / 380	640 / 610	19–31 / 19–35	9, 10, 8 / 8, 9	630 / 540	760 / 710	25–37 / 19–22
VI	390 / 370	600 / 580	35–36 / 12–14	8, 9 / 7, 8	520 / 460	660 / 640	26 / 32
Commercial melts	– / 305–400	– / 490–660	– / 10–105	– / 7, 8, 9 (6)	– / 400–530	– / 550–700	– / 25–100
OST 32.183–2001	≥ 343	≥ 490	≥ 24.5	≥ 8***	–	–	–

*In numerator data after heat treatment under laboratory conditions, in denominator ---- under workshop conditions are presented.
**In brackets grain index, registered in some specimens, is shown. ***Requirements, introduced by RZhD since 01.01.2007.

its heating was about 10 °C / min. The melt was tapped into the preliminarily heated ladle with acid lining.

For the purpose of improving assimilation of titanium and nitrogen, deoxidizing of the metal was performed in two stages. Immediately before tapping, half of the required amount of alumocalcium wire was fed on bottom of the ladle. After approximately 1 / 3 of the ladle was filled, the rest aluminium, ferrotitanium and nitrogen-containing master alloy were added under the jet. The metal was cast in three standard test bars (GOST 977–88), which were subjected to heat treatment (normalization at 920–950 °C) or high-temperature temper quenching. Results of the carried out investigations are given in the Table.

As far as it's not chemical and phase composition of steel, which exerts significant influence on structure and properties of the metal in heat treatment in continuous industrial furnaces, but conditions of heating and cooling of the items of big mass, for getting more substantiated conclusions about role of the carbonitride hardening, normalization of the specimens of all experimental melts and hardening of a portion of them were performed in parallel under workshop and laboratory conditions.

One can see from Figure 1 and the Table that irrespective of consumption of the nitrogen-containing master alloy and chemical composition of steel concerning base elements and modifiers, in all melts rather rapid cooling of the billets ensured presence of a finer grain and, respectively, increase of the yield strength level. Size of the grain being the same, the 20GL steel modified by titanium and aluminium nitrides significantly exceeds conventional steel and is characterized by the required level of $\sigma_y \geq 380$ MPa even after heat treatment under industrial conditions. This conclusion is confirmed by processing of the results of commercial and experimental melts concern-

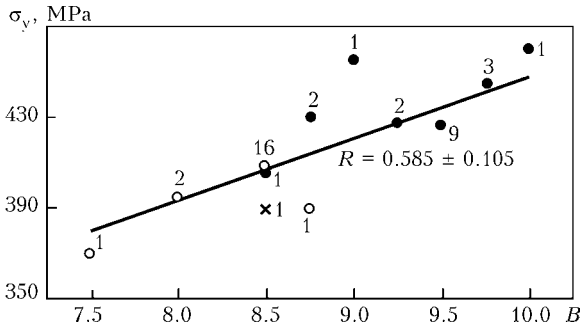

Figure 1. Influence of ferrite grain index *B* in 20GL steel on its yield strength after normalization under workshop (○) and laboratory (●) conditions: × — melting without CNH; figures near points indicate number of melts; *R* — correlation factor

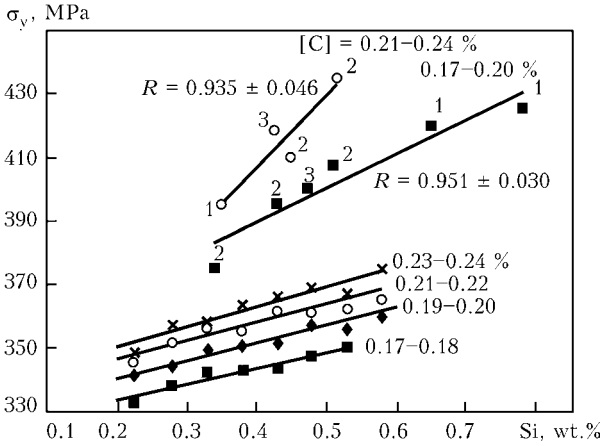

Figure 2. Influence of silicon and carbon on yield strength of commercial (lower curves, 2314 melts) and modified (upper curves) 20GL steel after normalization under industrial conditions (designation of points and figures near points hear and in Figures 3–6 are the same as in Figure 1)

ing function of content of base elements ---- silicon and carbon (Figure 2). In connection with relatively small number of experimental melts, their processing was carried out only proceeding from two ranges of carbon content.

Similar dependences exist in relation to manganese. That's why for ensuring necessary level of the

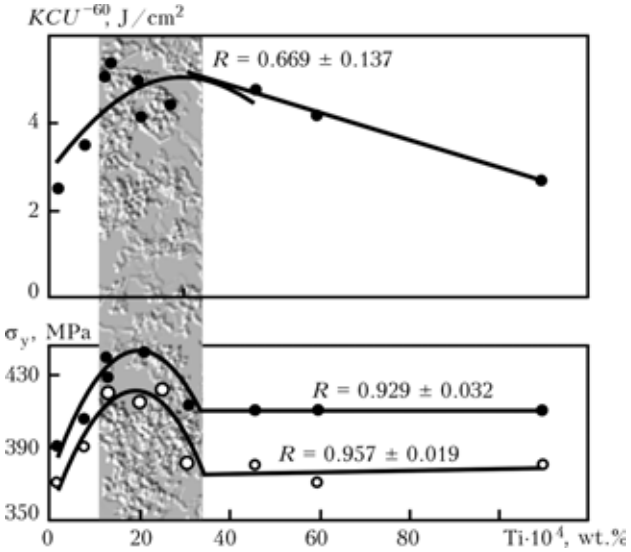

Figure 3. Influence of titanium content on yield strength and impact toughness of 20GL steel with CNH

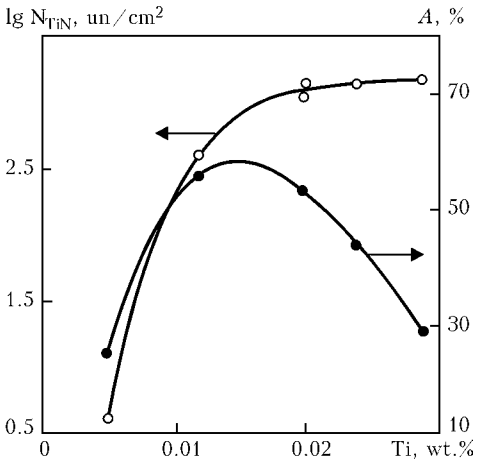

Figure 4. Influence of titanium content on share *A* of fine carbonitrides in 20GL steel

commercial casting hardness it is recommended in addition to complex modifying of steel by titanium, aluminium and nitrogen to narrow allowable ranges of content of base elements, having increased lower limit for carbon up to 0.2, for silicon up to 0.4 and for manganese up to 1.2 wt.%.

In contrast to the base elements influence of titanium on mechanical properties of the 20GL steel is of extreme character (Figure 3), which fits well change of content and size of formed titanium carbonitrides (Figure 4). As their content increases up to 0.015 wt.%, share *A* of fine carbonitrides, which regulate size of the primary grain, grows, and then it starts to fall, thus reducing both dispersion and grain boundary hardening.

Respectively, for sufficiently reliable ensuring required level of mechanical properties of the commercial casting recommended content of titanium in steel with CNH is 0.013–0.035 wt.% (outlined area in Figures 3, 5 and 6).

Extreme character is also registered in consumption of ALK with optimum in the area of 2.0–3.7 kg / t

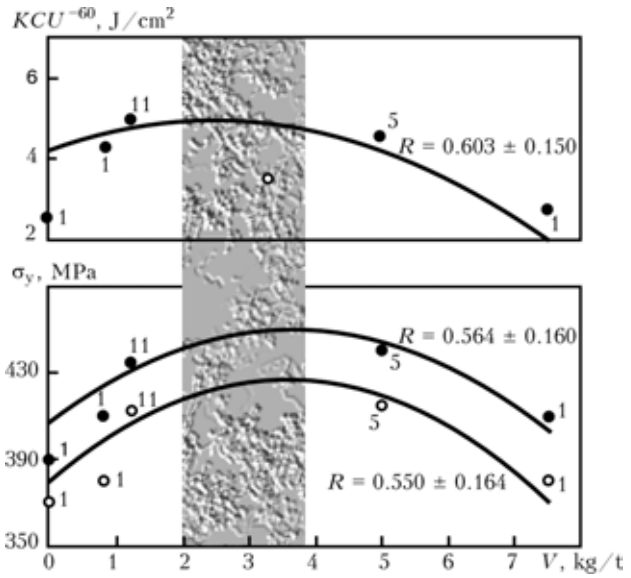

Figure 5. Influence of consumption *V* of ALK on yield strength and impact toughness of normalized 20GL steel

both for normalized steel (Figure 5) and for high-temperature temper quenched steel (Figure 6).

As it follows from presented in the Figures correlation factors, value of ratio R / σ_y for all experimental dependences exceeds 3, which corresponds to the level of fiduciary probability of the data obtained ($\alpha \geq \geq 0.95$) and is rather high value for multifactor investigations. This allows speaking about high statistic reliability of the data obtained and predicting their reproducibility in melting of the 20GL steel with CNH in industrial furnaces.

CONCLUSIONS

1. Modification of the 20GL ferrite-pearlite steel by titanium, aluminium and nitrogen in combination with rather narrow ranges of content of base elements (silicon, manganese and carbon) corresponds to the level of requirements, established for cast elements of freight railway cars of new generation.

2. The results obtained have high statistic reliability and are accepted for industrial application.

1. (2004) *Development of transport machine-building in Russia «Zheldormashinostroenie-2004», experimental circular railway VNIIZhT*: Recommend. of Participants of Int. Conf. (Shcherbinka, June 29–30, 2004). Moscow: Center of Assistance to Development of Transport Science.
2. Pirogov, V.A., Chernenko, V.T., Martsiniv, B.F. et al. (1994) *New low-alloy silicon steels for metal structures.* Moscow: Central Research Institute of Information and Technical-Economical Studies in Ferrous Metallurgy.
3. Shipitsyn, S.Ya., Babaskin, Yu.Z., Kirchu, I.F. (2004) Application of steels with carbon-nitride hardening is the essential increase in reliability and life of rail tracks and trains. *Metall i Litio Ukrainy*, **1 / 2**, 39–42.

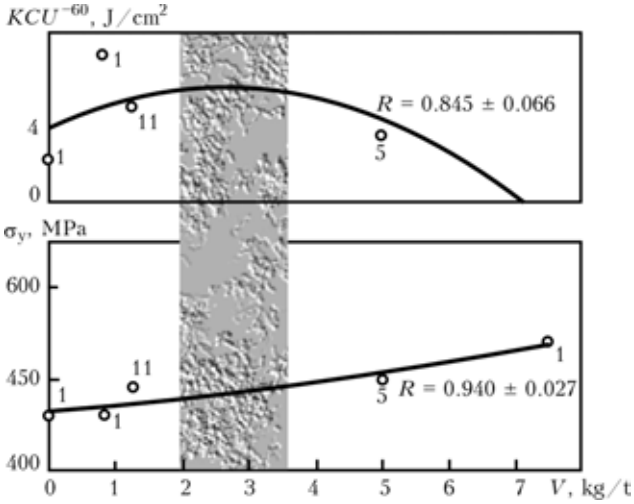

Figure 6. Influence of ALK consumption V on yield strength and impact toughness of high-temperature temper quenched 20GL steel

4. Goldshtejn, M.I., Grin, A.V., Blum, E.E. et al. (1970) Hardening of structural steels by nitrides. Moscow: Metallurgiya.
5. Rabinovich, A.V., Tregubenko, G.N., Tarasiev, M.I. et al. (2001) Development of composition and technology for production of efficient structural steels with carbon-nitride hardening. In: *Transact. of NMetAU on Current Problems of Metallurgy*. Vol. 3. Dnipropetrovsk: Sistemni Teknologii.
6. Kalliopin, I.K., Gavrilin, I.V., Ershov, G.S. (1976) Modification of nitrogen- and sulfur-containing steel by titanium. *Izvestiya Vuzov. Chiorn. Metallurgiya*, **2**, 64–67.
7. Lunev, V.V., Pirozhkova, V.P., Burova, N.M. (2003) Examination of structure and nonmetallic inclusions in steels 20G2L and 40G2L modified by nitrogen with different sulfur additions. *Teoriya i Praktika Metallurgii*, **1**, 21–26.
8. Nizhegorodov, B.O., Ignatov, M.V., Rabinovich, O.V. et al. *Method of production of nitrogen-containing master alloys*. Pat. 20492, Ukraine. Int. Cl. C 22 C 35 / 00. Publ. 15.10.2001.

ANALYSIS OF TECHNOLOGICAL DEVELOPMENT OF FINISH METAL PRODUCT TREATMENT

V.K. POSTIZHENKO

National Technical University of Ukraine «KPI», Kiev, Ukraine

Review of existing in the world methods of the rolled metal heat treatment and technological directions of coating application on metal products is made. Results of technological development analysis of finish metal product treatment are presented. The most rational technological schemes of finish metal product treatment are suggested.

K e y w o r d s : heat treatment, quality metal product, anticorrosion coatings, controlled rolling

Intensive development of construction and automotive industry within postwar period up to nowadays required high amount of quality metal products.

Improvement of the rolled stock quality is to a significant degree ensured in the process of the fourth metallurgical process stage (heat treatment, heat hardening, and application of protective anticorrosion coatings).

Quality metal product is rather wide idea. One of its components is rolled stock from alloyed, low-alloy, carbon and low-carbon steels, produced by the method of controllable rolling, heat treated in separate units after rolling, subjected to heat treatment in rolling heating, with metal or non-metal coatings. Growth of volume of production of quality steels is presented in Figure 1.

Special attention has to be paid to wish of the metal product consumers to get it in the form, suitable for manufacturing of their products.

That's why metallurgical plants try to produce rolled stock with preset properties –– a combination

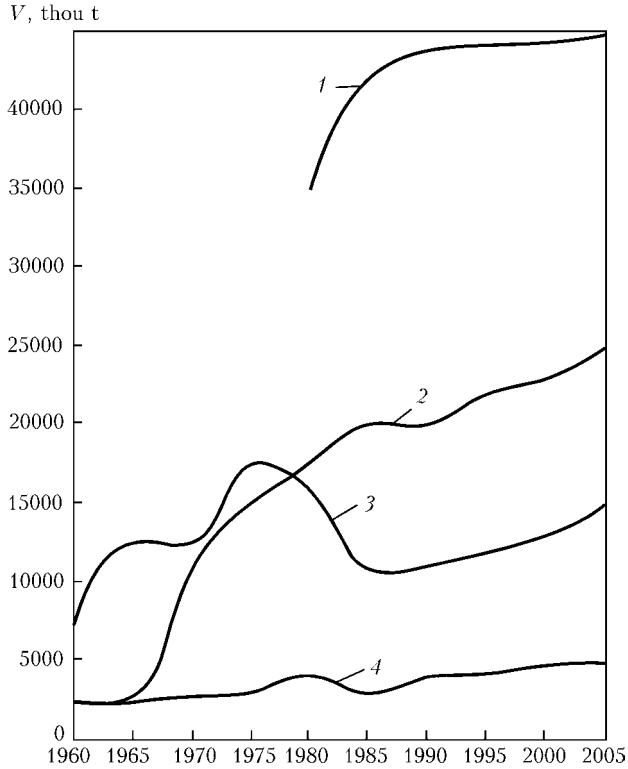

Figure 1. Volume *V* of quality steel melting in economically developed countries; here and in Figures 2 and 3: *1* — USA; *2* — Japan; *3* — France; *4* — Brazil

of the required values of strength, ductility, and service characteristics.

Mentioned changes in conditions of the metal product supply are based on radical perfection of the metal production at the ferrous metallurgy plants. From this viewpoint of great significance is registered in a number of countries transition from production of relatively high-alloy structural steels, subjected to heat treatment at a metallurgical plant or at the enterprise-consumer of this metal, to production of high-strength rolled stock without application of separate heat treatment and with minimal content of alloying additives.

Mentioned statement should not be interpreted as refusal of metallurgists from application of the metal heat treatment as a measure for improving mechanical and technological properties. Development of processes in ferrous metallurgy follows at present the way of achievement of the required results using simpler, cheaper and, as a result, more rational methods, while heat treatment may be used in order to meet more strict requirements, for example in production of heavy-duty steels [1].

Technologies of metal product finish treatment based on processes of heat treatment. Improvement of the steel rolled stock mechanical properties is frequently achieved due to application of controllable rolling, at which hot deformation (and for rolled stock in reels or rolls also reeling) is performed under strictly regulated temperature conditions. Significant share of general reduction is performed at the temperatures below the level of austenite transformations. So, the controlled rolling is actually thermomechanical treatment of the metal.

It should be noted that effect of the controlled rolling is connected with special change of steel microstructure and is manifested provided certain conditions are observed, main of which is that the steel has to be clean in regard to sulfur and non-metal inclusions. The highest effect is achieved on oxygen-converter steels that passed out-of-furnace treatment.

In production of coiled steel on broad-strip continuous mills a regulated rolling is used. In this case intensity of cooling and temperature of the strip reeling into rolls are strictly controlled [2].

They started to use controlled rolling in industry in 1960s on plate mills. Later they started to use it on broad-strip and section mills. At big metallurgical enterprises about 20 % of produced plate rolled stock are subjected to the controlled rolling.

At present mentioned processes are used at such state-of-the-art metallurgical enterprises as inter-branch regional centers of thermal metal products [3].

Methods of application of protection coatings on final metal products. More and more frequently ferrous metallurgy assumes function of finishing of the rolled stock surface. This is explained by high efficiency of continuous application of coatings on a steel strip. Application of coatings serves first of all for long-term protection of metal products against corrosion. In addition, steels with coatings are imparted decorative and special properties. Surfaces of sheets and strips from corrosion-resistant steels and aluminium are also subjected to finishing. Among methods of production of steel corrosion-resistant products at enterprises of ferrous metallurgy production of rolled sheet with coatings occupies first position.

Sheet metal with coating. Tinplate occupies first position as to the volume of its production. In Figure 2 data on production and consumption of tinplate in capitalist and developing countries within 1980--2005 are presented [4, 5]. As one can see from the Figure, production of tinplate in developing countries increases every year.

The biggest producer of tinplate and sheet metal as a whole continues to be the USA despite reduction of volumes of production in comparison with the maximal achieved level (6.2 mln t in 1968) [6]. In 2003 general dispatches of sheet metal constituted 3684.7 thou t. In Japan (second position in the world in regard to production of tinplate and coated sheet metal as a whole) volume of tinplate production in 1997 constituted 1977 thou t, and in 1980s it somewhat reduced [7]. The biggest in the world exporters of tinplate are Japan (48.2 % in 2002), in Western Europe ---- France, FRG and Netherlands. Great Britain achieved maximal volume of tinplate production in 2001 ---- 1283 thou t.

Volumes of production of hot-dipped tinplate, used in canning industry, are significant only in countries of former socialist camp, but nowadays process

of their reduction is registered. Production of hot-dipped tinplate in industrially developed capitalist countries in some cases revives, although it is not used anymore in canning industry.

Production of chrome-plated sheet metal is stable or increases in the producer-countries. Although in the USA it is lower than maximal achieved level (1.2 mln t in 1973), from 1995 on it was rather constant, in particular, 850 thou t / year. In 2000 its dispatched volume constituted 857.1 thou t, in 2003 ---- 1041.8 thou t. Leader in production of chromium-plated sheet metal at present is Japan, where production increases at high rate and constitute at present approximately 1.2 mln t, whereby 25 % of chromium-plated sheet metal are exported.

Rolled sheet with galvanized coatings from zinc alloys. To the galvanized rolled sheet relates rolled metal with coatings from zinc and its alloys, which are applied by method of dipping into the melt (hot-galvanized, with thermal diffusion coating by iron-zinc alloy, with coatings from alloys of zinc with aluminium (4.5–5.0, 15, 30 and 55 wt.%) and small additives of other elements), coatings produced by electrolytic method (zinc ones, from alloys of zinc with iron, nickel, manganese, and other types including multilayer ones, in which zinc is present in one or two layers). Zinc may be also applied on a steel strip by deposition from vapor phase in vacuum, but this technology is still rarely used.

Growth of the galvanized rolled sheet production in main capitalist countries in 1980–2003 is shown in Figure 3. In Japan its volume in 1986 constituted 9088 thou t, in 2002 ---- 18197 thou t, i.e. it continues to increase.

According to estimation, made in 1981, annual volume of subjected to galvanization ferrous metals constituted all over the world about 35 mln t (about 3 bln m^2 of surface) [8].

In FRG about 150 enterprises applied in 1979 for protection against corrosion coatings on 3 mln t of ferrous metals (approximately 270 mln m^2 of surface). Consumption of zinc for hot galvanization constituted about 165 thou t, about 70 thou t of which were used for piece galvanization, approximately 10 thou t ---- for galvanization of wire and pipes, and about 75 thou t ---- for galvanization of strips [9]. Volume of production of hot-galvanized sheets and strips in this country in 1979 constituted about 1.49 mln t, in 1990 and 1995 ---- 1.5 mln t. Volume of production of hot-aluminized strips, and sheets and strips, produced by the method of dipping into a melt, constituted in 1985 1.7 mln t, and their share in general volume of production of thin sheet in the country equaled more than 20 %. Beginning from 1959, from eight installed broad-strip units for application of coatings by the method of dipping into a melt at present only six operate and produce about 8 % of the products, produced at almost 200 known in the world broad-strip units for application of coatings by the method of dipping into a melt [10].

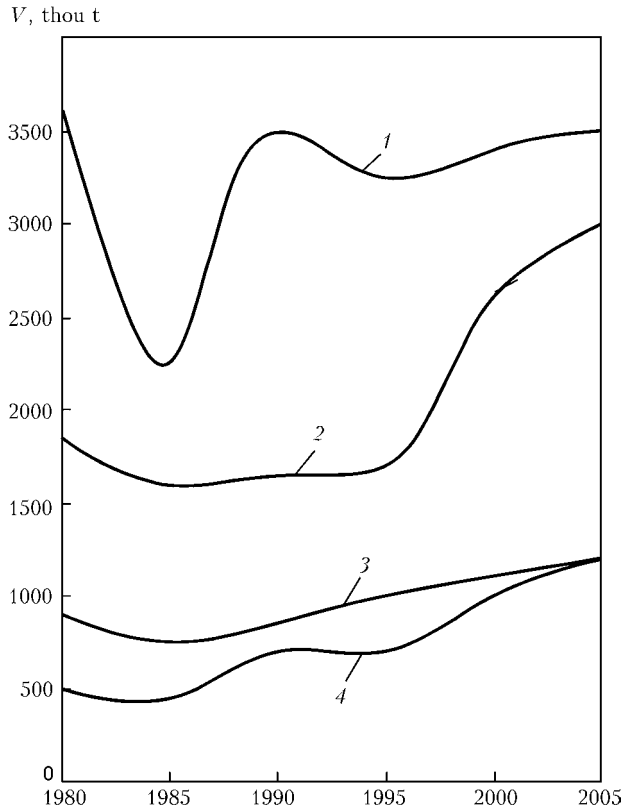

Figure 2. Volume of tinplate production in developed and developing countries

As it follows from [11], general volume of produced in the world beginning from 1972 galvalum achieved more than 7 mln t; annual production of galvalum equals at present 1.5 mln t / year and had

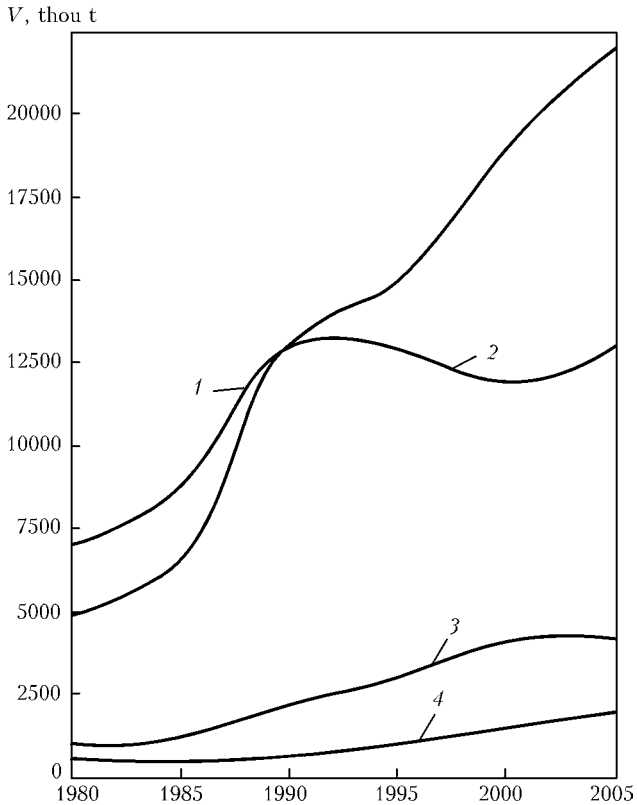

Figure 3. Growth of rolled galvanized sheet production in developed and developing countries

to double by 1989. About 300 thou t of galvalum was produced in Western Europe in 1986. It was assumed that in 2005 it would constitute 950 thou t. For production of the galvalum strip 22 licenses were sold, developer of which is the «Bethlehem International Engineering Corp.», USA [11].

Pilot production of strip with galfan coating on hot-galvanization unit was carried out in France in 1981. Information about this was not discovered. In 1985 volume of its production constituted more than 60 thou t. It was assumed that in Japan by 2005 production of steel with galfan coating could achieve 20 % of hot-galvanized steel production. By 1987, 32 licenses were sold for production of strip, wire and pipes with galfan coating [12]. Cost of the license for production of strip with galfan coating in 1981 was 50 thou USD for first unit, 40 thou USD for second and 30 thou USD for each subsequent unit. Developer of the coating was International Lead and Zinc Research Organization (ILZRO) [13].

Production of strip with lavegal coating (30 % Al) started in 1985 in Italy at a new combined unit for hot-aluminizing and application of the lavegal coatings of 140 thou t / year productivity of the «Nuova Italsider» company [14]. The product was developed by a group of metallurgical companies with participation of the Metallurgical scientific-research center. In 2005 demand for this product in Italy constituted 170 thou t.

There is no sufficient statistical data about production of rolled electrolytically coated by zinc and its alloys metal. In the USA production of the electrolytically galvanized rolled sheet constituted in 1982 490 thou t, in 1983 ---- 610 thou t, and in 1984 ---- more than 700 thou t [15]. In connection with simultaneous commissioning of big number of new highly productive electrolytic galvanization units in 2003, production of this kind of rolled sheet with the coating had to sharply increase. In FRG volume of production of the electrolytically galvanized rolled sheet constituted in 1981 190 thou t, in 1982 ---- 230 thou t, and in 1983 ---- 300 thou t [16]. According to statement of specialists of Japanese company «Nisshin Steel», production of the electrolytically galvanized rolled sheet constituted in January–November 1987 3 mln t (hot-galvanized sheet ---- 4.59 mln t), and rates of growth, in comparison with previous period in 1986, were the highest (19.5 % in comparison with 11.2 % for the hot-galvanized one). Judging from commissioning of big amount of new capacities for electrolytic galvanizing of steel strip, rates of growth in 2000s of electrolytically galvanized steel were high not just in Japan, but also in other industrially developed capitalist countries.

Hot-aluminized sheet steel. As it follows from mentioned above, production of the hot-aluminized sheet steel in the world constitutes more than 1 mln t. In CIS countries 137 thou t of aluminized sheet steel were produced in 1970, in 1984 ---- 308 thou t, and in 1987 ---- 405 thou t. Import of Japan in 1987 constituted 15 thou t. Production of hot-aluminized steel in Japan achieves, approximately, 500 thou t / year [4].

In 1960–1970s more than ten continuous specialized or combined units for production of hot-aluminized sheet steel were installed in the USA, Japan, Great Britain, FRG, France, CSSR, BPR and Argentine [4]. In 1980s new continuous units (all of them combined ones) were installed in Luxemburg and Italy (one in each) and were planned for putting into operation in the USA (1988) and the USSR (1989). In the USA among companies-producers of hot-aluminized sheet steel «Armco Steel» and «Inland Steel» are mentioned.

A unit was put into operation in 1972 in Middletown, which was designed for aluminizing strip of 0.4–2.5 mm thickness and up to 1525 mm width with two changeable baths for production of hot-aluminized steel of type I (Al–Si) and type II (Al) [10]. At present primary productivity of the unit has been increased from 200 to 300 thou t / year. American company «United States Steel» (present USX) switched over since 1983 to production of galvalum.

A new unit for hot galvanization (aluminizing) of 270 thou t / year productivity was installed in Follansbee by joint American-Japanese company «Willing-Nisshin». In Japan two companies produced hot-aluminized steel (of type I) ---- «Nippon Steel Co.» and «Nisshin Steel» (the latter one supplies 79 % of this product).

The «Nisshin Steel» company used two units (they are installed at the «Hanshin» plant in Sakai) ---- combined ones for hot galvanization and aluminizing of 164 thou t / year productivity [4]. The company informed about development of technology for one-side hot aluminizing with application of masking coating on other side of the strip, which is roasted in the annealing furnace and then cleaned off by a brush [17].

Unit of the «Nippon Steel Co.» (Japan) of 60 thou t / year capacity, installed at the plant in Yawata, is also a combined one for hot galvanization / aluminizing. In Germany the only producer of hot-aluminized sheet steel was the «Tissen Stahl» company, which produced it on the combined galvanization / aluminizing unit.

In France at plant of the «Ziegler» company in Muson a continuous double designation unit of 120 thou t / year productivity was installed for processing of a strip of 0.5–2.0 mm thickness and up to 1500 mm width.

In Italy a combined unit for hot aluminizing / production of a strip with lavegal coating of 140 thou t / year productivity was put into operation. Need in hot-aluminized steel in Italy in 1990 was estimated at the level of 50 thou t.

In1982 at the «Galvalenge» plant in Dudelenge, Belgium, unit for hot aluminizing / production of galvalum (the company name is aluzink) was put into operation for processing of a strip of 0.3–1.75 mm

thickness and 700–1500 mm width with speed of movement up to 140 m / min. Its maximal productivity was 35 t / h.

In Great Britain the only producer of hot-aluminized sheet steel became the only non-metallurgical company «Coated Metals». It produced 45 thou t of the product.

As a whole, production of the hot-aluminized steel is less adaptable to streamlined production than production of the hot-galvanized steel. It requires for higher temperatures of the melt heating (660–680 °C), which can stand only ceramic bathes. Characteristic feature for state-of-the-art units, designated for both hot aluminizing and hot galvanization, is application of non-oxidizing heating in annealing furnaces with utilization of the waste gas heat, application of air knives for regulation of the coating thickness, straightening-stretching machines, and temper mills. For additional chemical treatment of a strip with coating the chromate treatment may be used. The issue of prevention of thick layer of iron-aluminium alloy formation is successfully solved by increase of the strip movement speed.

Hot-aluminized steel of type I (Al–8–12 % Si) is characterized by improved deformability, high heat resistance, and heat-reflecting capacity. Silicon in the melt suppresses growth of iron-aluminium alloy. Investigations, carried out in Japan and other countries, showed high resistance of this steel against atmospheric action in comparison with galvanized steel.

Lead-plated sheet steel. According to the assessment made in 1982, more than 600 thou t / year of lead-plated steel were produced in the world on continuous or sheet lead-plating units or using electrolytic method [6]. Continuous hot lead plating units were installed in the USA (three), Great Britain and France (two in each), Japan, FRG, Australia, Belgium and the USSR (one in each). The most state-of-the-art and productive in 1982 was the unit for continuous lead plating, installed in Japan at plant of the «Nippon Steel Co.» in Yawata instead of the old continuous unit, productivity of which was 81 thou t / year. Productivity of the new unit is 210 thou t / year. Strips of 0.4–2.3 mm thickness and 610–1230 mm width in coils of up to 22 t mass were processes on it at strip movement speed up to 70 m / min (the highest speed for hot lead plating units). Nominal mass of the two-side coating is 75–150 g / m^2. Technology of the nickel sublayer application in amount of 1 g per 1 m^2 by electrolytic method was used for the first time on this unit. As a result a difficult for the hot lead plating units task of ensuring quality adhesion of a coating from the Pb–Sn melt to steel base was solved, it became possible to reduce content of stannum in the alloy from 15 to 8 %, more uniform fine crystalline structure of the alloy with minimal amount of pinholes was achieved, and duration of etching was reduced from 45 to 3–5 s.

Corrosion resistance of the lead plated according to the new technology sheet steel is by 25 % higher than of the steel plated according to conventional technology. Other peculiarities of the unit consist in application of air knives and, in some cases, of chemical treatment. Technology of nickel sublayer application was introduced by two American companies, which produced lead-plated sheet steel ---- «Armco Steel» at the plant in Middletown and «United States Steel» at the plant in Pittsburg. Maximal width of the lead-plated sheet steel, produced at the continuous unit in Middletown, was 1245 mm [18].

A continuous unit for electrolytic galvanization / lead plating (installed in 1972, retrofitted into the double-purpose one in 1978) operates at plant of the «Estel Ziegerlandwerke» company in Dortmund, FRG. It is designed for production of one- and two-side lead plating of sheet steel with Pb–7 % Sn coating of 2.5 and 5.0 μm thickness (5.0 μm correspond to the coating of 38 g per 1 m^2). The product may be supplied in sheets of up to 5000 mm length and strips with minimal width 20 mm; its quality does not differ from that of the hot lead plated product [6]. Old unit for electrolytic galvanization was reequipped into the unit for electrolytic lead plating at the plant in Fukuyama by the «Nippon Kokan» company, Japan. Volume of production of the lead-plated sheet steel was 24–36 thou t / year.

Lead-plated steel rolled stock is produced from mild non-alloyed cold-rolled steel, characterized by good stamping capacity. Coating in stamping is characterized by the lubrication effect. Lead-plated sheet steel has high corrosion resistance against action of petrol, diesel fuel, and salt spread over the roads. The sheets are subjected to soldering and brazing, spot and seam welding, and then they are painted. Main designation of the lead-plated sheet rolled stock is its application in fuel tanks of automobiles and in manufacturing of the radiator frames and filter parts, housings of gas meters, oil bathes, housings of condensers and other purposes.

New in technology of hot lead plating is application as a basis of a strip from the corrosion-resistant steel. For the first time production of the new product of construction designation was mastered by the «Strip Tinning» company, Great Britain. Strip of 0.25–3.00 mm thickness and 700 mm width from steels 304 and 306 was produced (application of other corrosion-resistant steels is possible) with two-side coating by lead-stannum alloy (20 % Sn–80 % Pb).

Rolled sheet with organic coatings. World production of steel rolled sheet with organic coatings in 1984 equaled 6 mln t or 1.2 bln m^2, share of North America in which constituted 47, Western Europe ---- 26, Japan ---- 22, and the rest countries ---- 5 %. Comparison with other data [19] showed that share of countries of Western Europe is by several percent less, while that of the North America countries is respectively higher. Consumption of the sheet rolled stock per capita in 1984 constituted: in Western Europe ---- 4, FRG ---- 5, North America and Japan ---- almost 10, Austria with New Zealand ---- approxi-

mately 13 kg [20]. Assumed world production of rolled aluminium sheet with organic coatings had to constitute 1.85 bln t in 2003.

In the North America countries (the USA, Canada and Mexico) the biggest dispatches of rolled sheet (steel and aluminium one) with organic coatings were in 1984 ---- 3.63 mln t. In 1985 they constituted 3.56, and in 1986 ---- 3.46 mln t (reduction of the dispatches was mainly caused by reduction of zincrometal consumption) [21]. Share of Canada and Mexico constituted 8–10 % of the dispatches. In 1996 among general amount of dispatched rolled sheet 2.82 mln t constituted steel rolled sheet and 0.64 mln t ---- aluminium one [22].

In the Western Europe countries 1.8 mln t of rolled sheet with organic coatings were produced in 2000. In FRG volume of its production constituted 837 thou t in 2000; at average 0.7 mm thickness of the strip it corresponds to application of coating on the area of 180 mln m^2 (area of one side of a strip is taken into account). For this purpose about 9000 t of coatings, applied in molten state, were used, including coatings for sheet steel of zincrometal type and coatings of back side of the strip.

In Japan, proceeding from the generalized data, volume of production of steel rolled sheet with organic coatings constituted 2.34 mln t in 2002. Volume of dispatches of preliminarily painted galvanized sheet achieved 1965 thou t in 1999. Aluminium was not widely used as a base in Japan because of high cost of electric energy [23].

As of 2002, the highest rates of increment of production of the rolled sheet with organic coatings were in Japan. This country became almost as big producer in this field as the USA.

Tasks of the metal product finish treatment development in ferrous metallurgy of Ukraine. The most important task of metallurgy of Ukraine is increase of high-tech character of the produced product and its competitiveness on the metal product market, and main directions are increased quality of the metal products, expansion of the technological process in the course of further processing of this product, and preparation of the latter for its use by the consumers.

For this purpose it is necessary to fulfill the following measures:

- develop and use scheme of development of new kinds of the products jointly with metallurgists and consumers;
- expand assortment of the metallurgical products;
- widely use technology of heat and heat deformation treatment of the metal from the rolling heating;
- establish a number of interbranch centers for heat treatment of metal products (such centers were established within last 15–20 years and successfully function in industrially developed countries);
- significantly increase production of rolled sheet from carbon steels with protection coatings;
- organize in big research centers laboratories for carrying out standard and special tests of rolled stock with coatings.

High quality of the products, produced on the units for hot galvanization and application of electrolytic, organic and other coatings, enables expansion of the field of their use. Rolled sheet with coating is corrosion-resistant. In many cases it may be used as a decorative facing and roofing material, it has special properties and is subject to cold forming to shape and has a number of other designations. Absence of corrosion of the steel is guaranteed for the period of 5–40 years.

1. Myrtsymov, F.M. (1978) *Ferrous metallurgy of industrialized and developing countries*. Kiev: Naukova Dumka.
2. Medovar, B.I. (1990) *Metallurgy yesterday, today and tomorrow*. Kiev: Naukova Dumka.
3. Dejneko, L.N. (2004) Heat treatment as one of the effective methods in increase of competitiveness of metal products. In: *Metallurgical science for enterprises of the Trans-Dniester Region*. Dnepropetrovsk: Sistemni Tekhnologii.
4. (1988) Annual world tinplate survey. *Tin International*, 61(**2**), 6–11.
5. (1986) *Ibid.*, 59(**4**), 156.
6. (1982) *JJSS Commentary*, May, XI-5, 72.
7. (1985) French tinplate sales expand as world market dips. *Metal Bulletin Monthly*, **170**, 18, 19.
8. (1987) *Tin International*, 60(**10**), 324.
9. (1984) Mehr verzinkte Bleche. *Baender Bleche Rohre*, **6**, 145.
10. Albrecht, J., Gerhard, E., Furken, L. et al. (1987) Stand der Technik bei der Herstellung von Schmelztauchueberzugen. *Stahl und Eisen*, 107(**21**), 973–979.
11. (1987) Europe may follow USSR into galvalume. *Metal Bulletin*, **7224**, 21.
12. (1986) Galfan — the zinc–aluminum coating. *Iron Age*, 229(**15**), 46, 49.
13. Radtke, S.F. (1981) Ganvan — zink bietet Galvalume paroli. *Metall*, **15**, 909, 910.
14. Memmi, M., Jardetti, J., Bonaretti, A. (1987) Lavegals — a new coating on the base of Zn–Al–Mg for sheet steel. In: *Paper for Symp. of Ital. Firms «Italsider» and «Italimpianti»* (Moscow, October 15–16, 1987). Moscow.
15. (1984) Mehrere Elektrolytische Verzinkungsanlagen geplant. *Stahl und Eisen*, 104(**14**), 11.
16. Meuthen, B., Meyer zu Bexten Jobst, H. (1985) Electrolytic zinc-coated steel sheet for the automotive industry: state of the art in West Germany. *Iron and Steel Eng.*, 62(**6**), 26–28.
17. (1985) *Jahrbuch Stahl*. Duesseldorf: Stahleisen, 153–158.
18. Wrigley, Al. (1985) 2 auto firms employ terne-coated steel tanks. *American Metal Market*, 93(**47**), 20.
19. (1985) World coil coating capacity. *Sheet Metal Industries*, **22**, 90.
20. (1985) *Tetsu-to-Hagane*, **12**, 1252.
21. Meuthen, B., von Laer, P., Nolter, A. et al. (1985) Jahre Stahlbreitbandbesichtigung — eine Leistungsbilanz der deutschen Stahlindustrie. *Stahl und Eisen*, 105(**22**), 119–126.
22. (1987) Westeuropa: Bandbesichter wachsen weiter. *Ibid.*, 107(**20**), 77.
23. Guseva, N.E. (1987) *Zincrometal and its modification*. Moscow: Chermetinformatsiya.

HEAT EXCHANGE IN MOLTEN POOL IN LIQUID-PHASE MELTING OF ORE-COAL PELLETS

V.N. KOSTYAKOV[2], **E.B. POLETAEV**[2], **G.M. GRIGORENKO**[1], **S.N. MEDVED**[2], **E.A. SHEVCHUK**[2], **A.A. YASINSKY**[2] and **O.A. YAKOVISHIN**[2]

[1]E.O. Paton Electric Welding Institute, NASU, Kiev, Ukraine

[2]Physical-and-Technological Institute of Metals and Alloy, NASU, Kiev, Ukraine

Results of the heat exchange investigation in a pool in liquid-phase melting of the ore-coal pellets are presented. Dependence of heat-transfer coefficient from the slag to a pellet upon intensity of the slag mixing in the furnace pool is established.

K e y w o r d s : pellet, slag, reducer, heat-transfer coefficient, speed, mixing, melting, metal

Melting of the ore-coal pellets in the arc furnace is characterized by diversity of heat and mass transfer processes, stipulated by action of both heat engineering and combination of physical-chemical factors, which accompany decarburization of the pool, slag formation, oxidation of the metal by oxygen of the furnace atmosphere, etc.

Combination of all processes, occurring in the furnace, represents for the time being irresolvable task and can not be described mathematically.

For real conditions and mathematical description construction of the model is simplified, if one takes into account a number of issues, characteristic of melting of metallized pellets in the arc furnace at different types of charging.

One may assume that for melting with application of the metallized pellets process of their dissolution in the molten pool is of a subordinate character in comparison with melting, because temperature of the molten metal is higher than melting point of the pellets. Among all questions of interest is determination of peculiarities of the process, stipulated by thermal physics characteristics of the material, because they are different in the pellets and the scrap.

The assigned task may be solved first of all by the model of heat exchange between a pellet being heated and the molten metal (the slag). Kinetics of heating and melting of a pellet may be considered on basis of the model of heat transfer by heat conductivity in the body of spherical shape under boundary conditions of third kind, i.e. at constant temperature of the metal (the slag).

Duration of the pellet melting, heated in the course of the convection heat transfer, depends upon thermal physics properties of the material and coefficient of heat exchange at the interface between the body and the medium. Heat exchange between the body and the medium, characterized by heat exchange coefficient α, may vary under real conditions within much wider range than physical properties. In the arc furnace heating and melting of the metallized pellets occurs both in the slag and at the slag–metal interface.

The investigations showed that values of coefficient of heat exchange between the metal and the melting in it scrap or a metallized pellet change within a narrow range. So, in melting of slag in a converter values of the heat exchange coefficient achieve α = 58–62 J / (m^2·s·°C) [1].

Investigation of melting of cylindrical steel specimens and metallized pellets in the induction furnace showed that heat exchange coefficient at a relatively low intensity of mixing equaled 13 J / (m^2·s·°C); at maximum power (intensive mixing) its values were within 139–220 J / (m^2·s·°C).

Taking into account somewhat overstated latter values, one may assume that the heat exchange coefficient in melting of a pellet in the molten metal may constitute 11–146 J / (m^2·s·°C) [2]. Because of a lower heat conductivity, density and increased viscosity of the slag in comparison with the molten metal, its heat exchange coefficient may be by several orders lower than in the molten metal–pellet system.

As a rule, heating and melting of the metallized pellets is accompanied by release of gases, stipulated by reaction between carbon and iron oxides. It is found [2] that noticeable release of gases (mainly CO) starts at 800 °C. As rate of a pellet heating increases, maximum of gas release shifts in direction of high temperatures. Recalculation of intensity of the CO release into rate of decarburization at heating rate 250 °C / min will give intensity 0.2 % C per minute, and share of carbon, which entered into reaction, — more than 1 %. High level of the gas release intensity from surface of a pellet in heating in slag or at the slag–metal boundary stipulates significant intensity of mixing of the melt layers, which directly contact with the pellet and, as a result, increased heat exchange.

Under real production conditions at continuous loading of pellets into the pool conditions of heat exchange between the medium and a pellet in the process of heating and melting change in direction of the heat exchange increase. This is explained by

change of mean density of the pellets (due to which they move from the slag lower to the slag–metal interface) and development of the decarburization reaction in the pellet, which intensifies heat exchange owing to increased degree of turbulence of the slag or the molten metal flows, which wash the pellet.

At correctly organized pellet melting technology heat exchange in the slag and at the slag–metal boundary is characterized by values α_{sl} = 3.6 J / (m^2·s·°C) and α_{sl-m} = 36–73 J / (m^2·s·°C) [2].

At the heat exchange coefficient value less than 3.6 J / (m^2·s·°C) and typical for the pellets size of the sphere, values of the Biot criterion constitute 0.5–2.0. At this ratio of internal and external heat flows heating of a pellet occurs in such way that by the time of the melting point achievement, temperature gradient on its surface gets insignificant over its radius.

In Physical-and-Technological Institute of Metals and Alloys (FTIMS) of the NAS of Ukraine heat exchange in melting of the ore-coal pellets in motionless and boiling slag were investigated.

Goal of this work was investigation of heat exchange in the pool in liquid-phase melting of the ore-coal pellets. The investigations were carried on experimental installation (Figure 1), the design of which included Tamman furnace, a frequency converter (FR-5520-0.4K), an electric motor, and a graphite crucible. By rotation of the crucible with slag intensity of the slag boiling in melting of the ore-coal pellets was simulated.

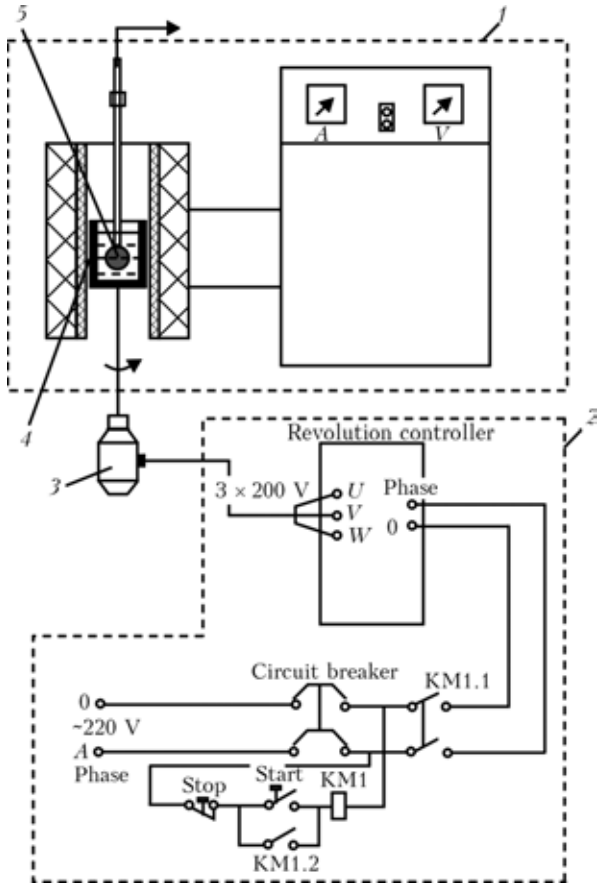

Figure 1. Scheme of experimental installation: *1* — Tamman furnace; *2* — controller of revolutions with power supply scheme; *3* — electric motor; *4* — crucible; *5* — ore-coal pellet with thermocouple

In the experiments lime-silica slag (55.5 % CaO, 44.5 % SiO_2) was used with melting point 1475 °C. Mass of the slag in all experiments was constant — 0.3 kg.

For manufacturing of the ore-coal pellets an iron-ore concentrate, a carbon-containing reducer and the grade 400 cement, which functioned as a binder in formation of the pellets, were used. Content of the cement constituted 15 % of total mass of the ore concentrate and the reducer.

Electrode scrap, containing 86 % C, was used as the reducer. Consumption of the reducer exceeded by 30 % its quantity, theoretically necessary for full reduction of iron in a pellet. Weight share of components in the mixture was as follows, %: ore concentrate — 66.7; reducer — 19.0; cement — 14.3.

The pellets were produced by ramming the mixture in a specially made mould. In center of the pellet the VR-20 / 5 tungstenrhenium thermocouple was placed. For protection of the thermocouple junction against direct contact with iron and its oxides protective electrocorundum coating was applied on the surface. The pellets were subjected to hardening drying at room temperature within 7 days and then to low-temperature (300 °C) drying in the drying chamber.

Mass of a pellet was 0.009 kg, density — 2150 kg / m^3. Chemical composition of the ore-coal pellets was as follows, wt.%: 1.33 FeO; 58.6 Fe_2O_3; 7.34 SiO_2; 0.82 Al_2O_3; 10.92 CaO; 0.6 MgO; 0.02 TiO_2; 16.34 C; 0.34 K_2O; 0.06 P_2O_5; 0.63 S.

At the beginning of the experiment the crucible with slag was installed in isothermal zone of the furnace, the furnace was turned on, and the slag was melted. The slag temperature was measured by the tungstenrhenium thermocouple, junction of which was protected by a quartz tip. Readings of the thermocouple were registered by the M1108 portable millivolt-ammeter.

After melting of the slag and its overheating up to (1550 ± 5) °C the crucible with the slag was imparted rotational movement at a preset speed, and the pellet was immersed into the slag. In process of the experiments speed of the crucible rotation equaled 0; 0.01; 0.02 and 0.04 m / s.

Temperature of the pellet center from the instant of its immersion into the slag was registered by the UPIT portable universal instrument, developed by FTIMS of the NAS of Ukraine and designed for periodic measurements of temperatures by means of the converters. Error of the temperature measurement equaled ± 1 °C. Time interval between previous and subsequent measurements of the pellet center temperature was constant and equaled 5 s. Time of the pellet heating was registered by a stop-watch.

Duration of a pellet heating was determined by its stability. Failure of the specimen being heated was detected at high temperatures; it was stipulated by intensive gas release of the iron reduction reaction products in internal layers of a pellet and swelling

and loss of strength of a pellet because of phase and structural transformations during heating [3].

Change of the pelt surface temperature and coefficient of convective heat exchange between the pellet surface and the slag depending upon intensity of the slag boiling and time of heating were determined using data presented in Figures 2 and 3. These graphs are built according to calculated values of the Fourier criterion and analytical solution results of differential equation of heat conductivity in case of heating of bodies of spherical shape under non-stationary conditions in the constant temperature environment [4]. They are applicable for this case because mass of the slag is 30 times higher than that of the pellet.

The graphs are drawn in the form of the following equation:

$$\theta = f\left(\mathrm{Bi},\ \mathrm{Fo},\ \frac{r}{R}\right)$$

or

$$\theta = f\left(\frac{\alpha R}{\lambda},\ \frac{a\tau}{R^2},\ \frac{r}{R}\right),$$

where θ is the dimensionless variable temperature; Bi is the Biot criterion, which determines character of temperature distribution within volume of the pellet being heated; Fo is the dimensionless time; r / R is the dimensionless coordinate; r is the current value of the pellet radius, m; R is the pellet radius; λ is the pellet heat conductivity, J / (m^2·s·°C); a is the pellet heat diffusivity coefficient, characterized by its heat inertia properties, m^2 / s.

Heat diffusivity coefficient is determined from the expression

$$\alpha = \frac{\lambda}{c\rho},$$

where c is the pellet heat capacity, J / (kg·°C); ρ is the pellet density, kg / m^3.

Presented in Figures 2 and 3 dependences are drawn for two values of the dimensionless coordinate: $r / R = 0$ and $r / R = 1$, which correspond to the pellet center and its surface.

Heat exchange coefficient α and the pellet surface temperature were determined according to the calculated Fourier criterion and dimensionless temperature of the pellet center for each instant of the time, at which temperature of the pellet center was measured. In calculation of the heat diffusivity coefficient heat capacity and heat conductivity of the pellet material were assumed to be constant and represent mean values of mentioned thermal physics properties within temperature range of 0–1200 °C.

Necessary for calculation of the heat capacity and heat conductivity values were taken from [5].

Dimensionless temperature of the pellet center θ_c was determined from the expression

$$\theta_c = \frac{T_c - T_0}{T_{sl} - T_0},$$

where T_c is the measured temperature of the pellet center, °C; T_0 is the pellet temperature prior to its immersion into the slag, °C; T_{sl} is the slag temperature, °C.

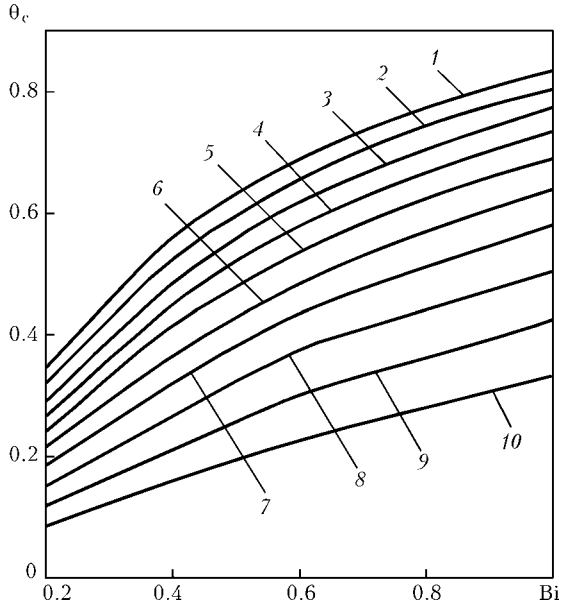

Figure 2. Curves for determination of Biot criterion by known values of Fourier criterion and dimensionless temperature of sphere center at Fo: *1* — 0.840; *2* — 0.770; *3* — 0.700; *4* — 0.640; *5* — 0.580; *6* — 0.515; *7* — 0.450; *8* — 0.386; *9* — 0.320; *10* — 0.257

Using found values of dimensionless temperature of the pellet center and the Fourier criterion value, the Biot criterion was found with application of the data, presented in Figure 2.

Heat exchange coefficient α was determined from the expression

$$\alpha = \frac{\mathrm{Bi}\lambda}{R}\ [\mathrm{J} / (\mathrm{m{\cdot}s{\cdot}^{\circ}\tilde{N}})].$$

Dimensionless temperature of the pellet surface was determined using data of Figure 3.

Temperature of the pellet surface T_s was determined from the expression

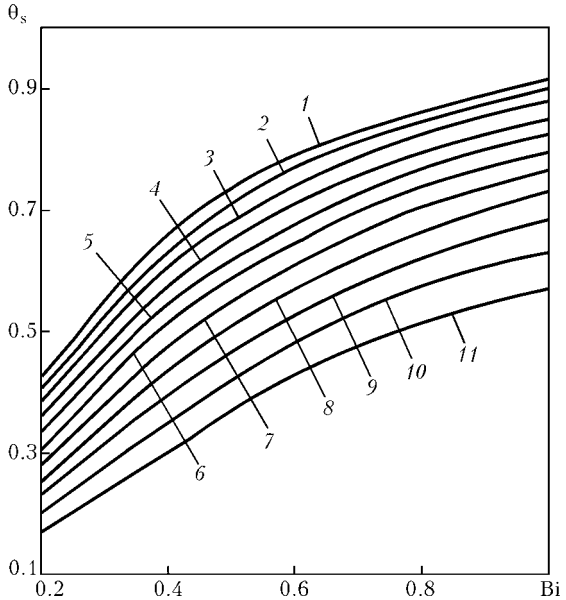

Figure 3. Curves for determination of dimensionless temperature of sphere surface by known values of Fourier and Biot criteria at Fo: *1* — 0.900; *2* — 0.840; *3* — 0.770; *4* — 0.700; *5* — 0.640; *6* — 0.580; *7* — 0.515; *8* — 0.450; *9* — 0.386; *10* — 0.320; *11* — 0.257

Table 1. Values of absolute and dimensionless temperatures of pellet center and surface, and Fourier and Biot criteria in case of pellet heating in immovable slag

τ, s	T_c, °Ñ	θ_c	Fo	Bi	θ_s	T_s, °Ñ
5	81	0.040	0.064	--	--	--
10	116	0.063	0.129	0.550	0.217	353
15	173	0.100	0.193	0.405	0.246	396
20	248	0.149	0.257	0.385	0.277	444
25	322	0.197	0.320	0.370	0.325	517
30	395	0.245	0.386	0.360	0.368	583
35	465	0.290	0.450	0.355	0.405	640
40	530	0.333	0.515	0.355	0.445	701
45	597	0.377	0.580	0.355	0.483	759
50	664	0.421	0.640	0.365	0.515	808
55	726	0.460	0.700	0.370	0.544	852
60	784	0.500	0.770	0.373	0.575	900
65	843	0.538	0.840	0.375	0.595	930
70	894	0.571	0.900	0.380	0.627	979
75	941	0.602	0.965	0.387	--	--

Note. Here in all cases Bi_{av} = 0.366, α_{av} = 73.26 J / (m^2·s·°Ñ).

$$T_s = \theta_s(T_{sl} - T_0) + T_0 \ [°Ñ],$$

where θ_s is the dimensionless temperature of the pellet surface.

Experimental and calculated values of parameters of the pellet heating process in molten slag are presented in Tables 1–4.

It follows from the presented data that initial period of heating of the pellets is characterized by increased values of the Biot criterion. At this period change of temperature field significantly differs from initial thermal state of the body. That's why character of mentioned process is not determined unambiguously by conditions of heating and properties of the pellet. Later at Fo ≥ 0.3, value of the Biot criterion remains practically constant. This proves establishment of regular heating conditions, at which distribution of temperatures over volume of the pellet does not depend upon initial conditions and is determined by conditions of heating and thermal physics properties of the pellet material.

Presented data also show that character of temperature distribution within the pellet volume is determined by the Biot criterion, i.e. conditions of external heat exchange, when intensity of internal heat exchange or internal heat resistance of the pellet does not change in the process of heating. As speed of the slag rotation increases, i.e. as intensity of the slag boiling gets higher, intensity of heat exchange between surface of the pellet and molten slag increases. So, when speed of the slag rotation increases from 0 to 0.04 m / s, the Biot criterion increases from 0.366 to 0.715 and coefficient of heat exchange from 73 to 143 J / (m^2·s·°C) (Figure 4).

As intensity of heat exchange in the pool increases, rate of the pellet heating gets higher (Table 5).

Data, presented in Table 5, prove that heating of a pellet in the rotating slag reduces time, necessary

Table 2. Value of absolute and dimensionless temperatures of pellet center and surface, and Fourier and Biot criteria in case of pellet heating in rotating slag (speed of rotation v_{sl} = 0.01 m / s)

τ, s	T_c, °Ñ	θ_c	Fo	Bi	θ_s	T_s, °Ñ
5	81	0.040	0.064	--	--	--
10	110	0.059	0.129	0.520	0.219	355
15	211	0.125	0.193	0.510	0.276	442
20	290	0.176	0.257	0.455	0.315	502
25	375	0.232	0.320	0.445	0.367	582
30	456	0.285	0.386	0.435	0.413	652
35	532	0.330	0.450	0.415	0.455	717
40	604	0.380	0.515	0.420	0.495	777
45	669	0.424	0.580	0.415	0.535	839
50	728	0.462	0.640	0.415	0.565	884
55	784	0.500	0.700	0.420	0.595	930
60	836	0.533	0.770	0.410	0.625	976
65	890	0.568	0.840	0.410	0.653	1019

Note. Here in all cases Bi_{av} = 0.425; α_{av} = 85 J / (m^2·s·°Ñ).

Table 3. Value of absolute and dimensionless temperatures of pellet center and surface, and Fourier and Biot criteria in case of pellet heating in rotating slag (speed of rotation v_{sl} = 0.02 m / s)

τ, s	T_c, °Ñ	θ_c	Fo	Bi	θ_s	T_s, °Ñ
5	81	0.040	0.064	--	--	--
10	133	0.074	0.129	0.655	0.250	402
15	226	0.140	0.193	0.565	0.315	502
20	327	0.207	0.257	0.545	0.375	594
25	427	0.266	0.320	0.515	0.425	670
30	519	0.326	0.386	0.500	0.470	739
35	604	0.380	0.450	0.500	0.515	808
40	688	0.436	0.515	0.510	0.555	869
45	762	0.485	0.580	0.510	0.593	927
50	828	0.528	0.640	0.505	0.625	976
55	884	0.565	0.700	0.510	0.655	1022
60	930	0.595	0.770	0.500	0.697	1086

Note. Here in all cases Bi_{av} = 0.51; α_{av} = 102 J / (m^2·s·°Ñ).

Table 4. Value of absolute and dimensionless temperatures of pellet center and surface, and Fourier and Biot criteria in case of pellet heating in rotating slag (speed of rotation v_{sl} = 0.04 m / s)

τ, s	T_c, °Ñ	θ_c	Fo	Bi	θ_s	T_s, °Ñ
5	75	0.036	0.064	--	--	--
10	169	0.097	0.129	0.870	0.321	511
15	298	0.180	0.193	0.725	0.402	635
20	430	0.268	0.257	0.760	0.483	759
25	550	0.346	0.320	0.750	0.548	858
30	650	0.410	0.386	0.695	0.583	912
35	741	0.470	0.450	0.685	0.630	984
40	825	0.526	0.515	0.685	0.670	1045
45	922	0.590	0.580	0.715	0.705	1099

Note. Here in all cases Bi_{av} = 0.715; α_{av} = 143 J / (m^2·s·°Ñ).

Table 5. Influence of slag rotation speed on rate of pellet heating

v_{sl}, m / s	Time of heating (s) at T in center of pellet, °C				
	500	600	700	800	900
0	36.5	45.0	53.0	61.5	70.5
0.01	33.0	40.0	47.5	56.5	66.0
0.02	29.0	35.0	41.0	47.5	56.5
0.04	23.0	27.5	33.0	38.5	44.0

for achievement of the preset temperature of the pellet center. So, at speed of the slag rotation 0.01 m / s time, necessary for achieving by center of the pellet of temperature 900 °C, reduces in comparison with immobile slag by 6.8 %, and if speed of the slag rotation increases up to 0.04 m / s it reduces by 60 %.

So, results of the investigations allowed establishing dependence of the heat-transfer coefficient upon intensity of the slag mixing.

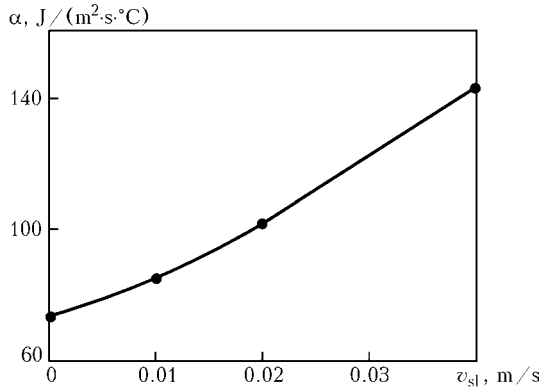

Figure 4. Influence of speed of slag rotation on intensity of heat exchange between slag and surface of pellet

1. Goldfarb, E.I., Sherstov, B.I. (1975) *Heat-mass-exchange processes in bath of steelmaking units*. Moscow: Metallurgiya.
2. Trakhimovich, V.I., Shalimov, A.G. (1982) *Use of direct-reduced iron in melting of steel*. Moscow: Metallurgiya.
3. Kachula, V.V., Fofanov, A.A., Antonova, S.M. (1978) About influence of natural properties of concentrates on strengthening of pellets and their behaviors during reduction. *Izvestiya Vuzov. Chyorn. Metallurgiya*, **8**, 25–28.
4. Kitaev, V.P., Yaroshenko, Yu.G., Suchkov, V.D. (1957) *Heat exchange in shaft furnaces*. Sverdlovsk: Metallurgizdat.
5. Kitaev, V.P., Yaroshenko, Yu.G., Lazarev, B.P. (1966) *Heat exchange in blast furnaces*. Moscow: Metallurgiya.

OUR CONGRATULATIONS

To 80th anniversary of academician Boris A. Movchan

Known scientist in the field of materials science and electron beam technology, academician of Academy of Sciences of UkrSSR Boris A. Movchan is 80 years of age.

Boris A. Movchan was born on 9th of January 1928 in village Makievka, Chernigov oblast. In 1944 he finished incomplete secondary school, in 1946 ---- two years of Kiev Ship Building Technical School, and in 1951 ---- physical faculty of the T.G. Shevchenko Kiev State University, where he specialized in «Physics of metals».

Since 1951 till nowadays B.A. Movchan has been working in the E.O. Paton Electric Welding Institute of the National Academy of Sciences of Ukraine, first as a research assistant of the Institute, and from 1960 till 1994 as Head of the department of electron beam technologies; since 1994 he has been the founder and director of International Center for Electron Beam Technologies of the E.O. Paton EWI (IC EBT). Beginning from 2003 till nowadays B.A. Movchan has been occupying position of chief research assistant of the Department of vapor-phase technologies of non-organic materials of the E.O. Paton EWI and research assistant-consultant of IC EBT.

In 1954 B.A. Movchan defended thesis for scientific degree of candidate of engineering sciences, and in 1961 became doctor of engineering sciences. In June 1964 he was elected a corresponding member of Academy of Sciences of UkrSSR, and since March 1978 ---- academician of Academy of Sciences of UkrSSR in the field of «Materials science and strength of materials».

Main direction of scientific activity of B.A. Movchan is structure and properties of non-organic materials, electron beam technologies, and new materials.

He may be rightfully called the founder of a new scientific school for producing new materials and multifunctional coatings by the method of electron beam technology of evaporation and condensation in vacuum. B.A. Movchan published more than 360 scientific works, 7 monographies and received more than 100 patents. He trained 56 candidates and 6 doctors of engineering sciences. He is member of the editorial boards of a number of scientific journals and scientific councils.

Scientific activity of B.A. Movchan is marked by a number of state awards. In 1974 he was awarded State prize of UkrSSR in the field of science and technology, in 1976 ---- Order of the Red Banner of Labor, in 1981 ---- second Order of the Red Banner of Labor, in 1984 ---- Lenin prize for work in the field of electron beam technology, in 1988 ---- order of Lenin, in 1989 ---- Evgeny Paton prize of the NAS of Ukraine, in 1998 ---- order «For Merits» of III degree. In 2004 Boris A. Movchan was awarded honorary title «Honoured Worker of Science and Technology of Ukraine». B.A. Movchan is marked by honorary diplomas of American Vacuum Society (1983, 1988) and Honorary diploma of Ministry of Aircraft Industry of China (1988).

Academician B.A. Movchan meets his 80th anniversary full of creative energy. We congratulate the hero of the anniversary, wish him good health, happiness, and further success for the welfare of our Ukraine.

E.O. Paton Electric Welding Institute of NASU
International Center
for Electron Beam Technologies
Editorial Board of journal
«Advances in Electrometallurgy»